In vivo imaging models for testing the inflammatory potential of implant materials and infection

Von der Fakultät für Lebenswissenschaften

der Technischen Universität Carolo-Wilhelmina zu Braunschweig

zur Erlangung des Grades

einer Doktorin der Naturwissenschaften

(Dr. rer. nat.)

genehmigte

D i s s e r t a t i o n

von Bushra Rais
aus Fatehpur, India

1. Referent: apl. Professor Dr. Peter Paul Müller
2. Referent: Professor Dr. Dieter Jahn

eingereicht am: 03.06.2015
mündliche Prüfung (Disputation) am: 21.07.2015

Druckjahr 2015

Vorveröffentlichungen der Dissertation

Teilergebnisse aus dieser Arbeit wurden mit Genehmigung der Fakultät für Lebenswissenschaften, vertreten durch den Mentor der Arbeit, in folgenden Beiträgen vorab veröffentlicht:

Publikationen

Rais B., Rahim M.I., Lienenklaus S., Weiss S., Tolle C., Seitz J.M., Menzel H., Hauser H. and Müller P.P. Animal Test Models for Implant-Associated Inflammation and Infections.Biomedical Technology.74: Springer International Publishing; (2015).

Rahim M.I., Eifler R., **Rais B.** and Müller, P.P. Alkalization is responsible for antibacterial effects of corroding magnesium. Journal of Biomedical Materials Research Part A. (2015).

Tagungsbeiträge

Rais B. and Müller P.P., Animal model for monitoring biomaterial associated inflammation or infection. **Talk**. Annual meeting of the Scandinavian Society for Biomaterials- Latvia. May 6–8th, 2015.

Rais B., Rahim M.I., Guledani A., and Müller P.P., Real time imaging of cells, tissue and bacteria. **Talk**. Annual Retreat – Helmholtz Centre for Infection Research- Goslar. May 20th-22nd, 2015

Rais B., and Müller P.P., In vivo imaging of biomaterial associated inflammation and infection. **Talk**. Progress Seminar – Helmholtz Centre for Infection Research- Braunschweig. March 20th, 2014

Rais B., Tolle C., Köster M., Hauser H. and Müller P.P., In vivo imaging of biomaterial associated inflammation or infection. **Poster**. BMT – 48th DGBMT Annual Conference – Hannover. October 8-10th, 2014.

Rais B. and Müller P.P., Quantification of biomaterial associated inflammation and infection. **Poster**. 7th International PhD symposium- Helmholtz Centre for Infection Research. December 11th , 2014

Rais B. and Müller P.P., Development of biological test systems to study interactions of novel implant materials with cells, tissues and bacteria. **Poster**. 6th International PhD symposium- Helmholtz Centre for Infection Research. December 12th, 2013.

Rais B., Rahim M.I. and Müller P.P., In vitro and in vivo biocompatibility testing of medical implants. **Poster**. International Conference on Biomedical technology - Hannover. November 20th-22nd, 2013.

Rais B. and Müller P.P., In vitro and in vivo evaluation of implant biocompatibility. **Poster**. Annual Retreat – Helmholtz Centre for Infection Research- Bad Bevensen. June 13th-14th, 2013

1. Abstract

Novel medical implant materials are in increasing demand. Conventional implants can fail due to lack of proper integration into host tissue or due to bacterial infections. Microbial implant infections are a significant clinical problem due to their resistance to conventional antibiotics. There is a need of dedicated implant materials with improved biological properties. Novel biomaterials or implant coatings need to be tested *in vivo* before going to clinics. Traditionally, histology was used to evaluate tissue interactions of implant materials but this method requires animal sacrifice and only a single time point can be analyzed. Here, we developed *in vivo* models that have the ability to distinguish inflammatory implant material responses from the wounding responses and from bacterial infections. Non-invasive imaging was used for visualization and quantification of biomaterial induced inflammation. Initially, reactive products of inflammation such as reactive oxygen species, proteases and inflammatory cell growth stimulatory molecules were visualized using fluorescent imaging. With these approaches, highly inflammatory materials could be differentiated from the biocompatible implants. However, the technique suffered from high background and from autofluorescence of tissue. For this reason, adoptively transferred bioluminescent immune cells were used to evaluate the inflammatory potential of implant materials. Immune cells were isolated from luciferase expressing murine bone marrow. The luminescence was controlled by a promoter with a high basal activity that was further stimulated by bacterial infections that enabled to visualize and quantify the luminescence of immune cells at the site of inflammation *in vivo*. Several materials of different inflammatory potential were tested. Inflammatory and infected biomaterials showed a clear difference in signal intensity when compared to biocompatible materials or injury. The highest signal was observed from infection. Polystyrene and the wound suture material poly lactic-co-glycolic acid (PLGA) implants acted inflammatory in this assay. The results were validated by using histology. Thus, bioluminescent immune cells provided a non-invasive, reliable and sensitive readout that correlated with the inflammatory potential of materials. This method may be used for evaluating the inflammatory potential of new implant materials or implant coatings and may be further developed as method for early detection of implant infections in the clinic.

2. Introduction

2.1 Biomaterials and their importance in health care

Biomaterials are part of medical devices or implants that are introduced into host tissue for replacing or enhancing natural function of damaged tissue or organ. Over fifty years, biomaterials have been a part of medicine and are employed in the fabrication of simpler implants such as intraocular lenses to more complex structures like biosensors, pacemakers and total artificial heart. These devices can not only extend the life span of patients but also improve the quality of life. The use of medical devices has increased over the last decade. In United States, the demand for medical devices increases by 7.7% every year [1]. The most commonly used are orthopedic and cardiovascular implants. The implanted biomaterial must be biocompatible and able to support replaced or enhanced function of tissue or organ for longer period of time. Therefore, the development of a suitable biomaterial involves integrated innovations in materials and biological sciences.

The primitive materials used for fabrication of implants were of natural origin such as tooth implants made of ivory and gold. Then, industrial materials were developed with improved mechanical and physiological properties. The desirable property of a material largely depends on its application in the host. For example, hip implants are subjected to high levels of mechanical stress and hence should be strong and rigid whereas vascular grafts should be flexible and less strong. For pacemakers, the important properties of the material are its electrical and thermal conductivity and light transmission [2]. In 1990s, due to the introduction of tissue engineering, the paradigm of material shifted to use of scaffolds. Scaffolds are artificial structures that can -support three dimensional growth of tissue. These structures provide suitable niche to cells by supporting their survival and proliferation in the host and after serving the purpose, scaffold has to degrade by hydrolysis or enzymatic digestion [3]. Another breakthrough in the field of biology was stem cell research in early 2000s, where the power lies in the human cells to regenerate the tissue and restore the function. This challenged the role of existing biomaterials and urged the need of novel materials that can perform signaling functions to instruct the local cellular processes [4].

Table 1: Examples of biomaterials and their medical applications [5]

Application	Biomaterials
Joint replacements	Stainless steel, titanium, polyethylene
Pacemakers	Titanium, polyurethanes
Intraocular lenses	Poly (methyl methacrylate)
Cochlear implants	Platinum, silicone
Artificial heart valves	Dacron, carbon, metal
Catheter	Silicone rubber
Dental implants	Titanium, Alumina, Hydroxyapatite
Breast implants	Silicone
Stents	Stainless steel
Artificial tendon or ligament	Polyester fibers
Sutures	Polylactic acid

2.1.1 Generation of biomaterials

To understand the evolution of biomaterials, the iterative process was categorized into three generations of materials. Biomaterials in each generation represent the evolution of requirements and properties of materials.

In the **first generation of biomaterials (ancient-1940),** the implants were prepared by using mostly available industrial materials such as metals and cobalt chrome alloys with the intended use of replacing damaged or diseased tissue with minimum immune responses in the host. Metallic implants were used by ancient Egyptian and Etruscan civilizations for fixing fractures or other skeletal injuries [6]. Some civilizations also used gold plates to fix broken bone which was evident from the skull found in Peru corresponding to 2000 BC [7]. In 1886, Hansmann was the first surgeon to introduce metallic plates and screws for the bone. He performed a surgery where he repaired the fracture by fixing the bone using metal plate and screws [8]. Early 20^{th} century saw an increased use of metals in orthopedic implants. Cobalt-based alloys were used in orthopedic surgery because of its low level of corrosion and these alloys still have their applications in orthopedics [9]. In 1940s, titanium was studied *in vivo* and was found to be biocompatible along with good integration in the bone. Since then, titanium was investigated in depth and was proposed to be used in dental implants [10]. Apart from metals, ceramics and polymers were also used as biomaterials. For example, the first artificial kidney was transplanted by using the hemodialyzer made of cellophane tubing [11]. The intraocular lens used for treatment of cataract was made of polymer, poly(methyl methacrylate) in 1948 [12]. The goal of biomaterials during this period was focused on inertness of the materials.

The **second generation of biomaterials (1980-2000)** was focused on development of materials that are not completely inert but able to induce a controlled specific response in the physiological environment. For example, the use of hydroxyapatite (HA), a natural mineral of the bone, supports

bone ingrowth and osseointegration while placed in bone tissue [13]. Synthetic hydroxyapatite was used as porous implants, powder or coatings on the maxillofacial and dental implants. These coatings provided a bioactive interface and promoted the osteoconduction process. Studies have shown that titanium implants with HA coatings had greater bone contact when compared to the uncoated implants [14]. Other most commonly used biomaterials were resorbable polymers that degrade in physiological environment in a controlled manner. For example, drug eluting stents were manufactured by resorbable polymers to avoid the problem of stenosis in the coronary arteries [15]. After reaching a saturation point in the first and second generation of biomaterials, it was realized that a shift towards more biological based methods was essential.

The third or present generation of biomaterials (2000-present) exposes novel materials and their applications in medicine but they are not meant to replace materials of the first generation. The biomaterials of third generation are tailored to stimulate cellular responses specific to their application. Resorbable scaffolds are designed to support proliferation and differentiation of embedded progenitor cells into desired tissue. This artificial system is implanted in the patient where tissue integrates in the host and scaffolds are resorbed. The development of artificial tissue to replace or enhance diseased tissue function is known as tissue engineering [3]. The other way to orchestrate such tissue growth is by using bioactive materials that release ions or embedded growth factors, thereby stimulating the cells in contact. Recent in vitro studies have shown that bioactive glasses genetically control the cellular responses of osteoblasts. A set of genes in the osteoblasts were upregulated upon exposure to bioactive glass. These genes express proteins involved in differentiation and proliferation of the cells [16].

The three generations represented an evolutionary picture of mechanical, chemical and biological properties of biomaterials. Coming years would expect a further increase alongside more sophisticated and greater reliable biomaterials.

In the coming chapters, the study has been divided into three major categories to develop a background. The first section gives an overview of biocompatibility of different materials and then moves to available biocompatibility testing methods. The second chapter highlights immune response to biomaterials explaining the signals induced by inflammatory cells and tissue cells in response to materials and also possible strategies to modulate inflammation. The third chapter gives an overview of infections on implants and mechanism of bacterial colonization in brief.

2.2 Biocompatibility

Biocompatibility is a general term extensively used for all biomaterials. In 1987, biocompatibility was defined as ‘‘the ability of a material to perform with an appropriate host response in a specific situation’’ [17]. Each biomaterial has its individual tissue interaction and the definition proposed seemed to be generalized. However, due to diversity in the materials and their host responses, a different paradigm of biocompatibility was evolved [18]. In addition to the characteristics of materials, there are several other parameters of biocompatibility such as the site of application of biomaterial, clinical intervention during implantation surgery, the recipient of implant (age, sex and general health), the design of biomaterial and its interaction with host, the presence of microbes on implants and the presence of endotoxins produced by microbes [19-21].

The biocompatibility essentials of a material used to design an implant depends upon their application. For instance, if the implant is intended for long term applications then the most desired properties to approve it as biocompatible would be 1) minimal production of wear particles 2) minimal tissue response 3) minimal disturbance of homeostasis [22, 23]. Similarly, other long term implants such as breast implants need additional biocompatible features like minimum fibrosis around the material to allow the development of glandular and fatty tissue. Silicone gel in combination with silicone elastomeric shells were used as breast implants providing the consistency, size and shape [24]. This shows customized list of biocompatibility features of implants depending on their application site. One should not forget the standards of biocompatibility for degradable implants where the pressure on the materials is not only to perform but also to degrade and eliminate from the body after its performance with minimum tissue reaction. The process of degradation leads to production of side products, which are capable of stimulating immune response, therefore, the material can be classified as biocompatible only if the response is clinically acceptable. Polyester sutures degrade within 3-12 weeks and the degradation products are physiologically acceptable [22, 25]. The other clinical use for biodegradable polymers is in drug delivery where they can be used in the form of microspheres or coatings on metallic implants. The tissue response to microspheres follow the sequence of inflammation from acute, sub-acute and chronic until the microspheres disappear from tissue either due to resorption or phagocytosis by macrophages [22, 26]. The biocompatibility of microspheres not only depends on the degradation rate and degradation products but also on the size of microspheres. The fundamental shift in the understanding of the biocompatibility was when tissue engineering was introduced in which regeneration ability of the cells was exploited. Cells can be stimulated to grow into tissue in a controlled fashion *ex vivo* or *in vivo*. Biomaterial is used either to impart the shape or to provide the mechanical stability to the cells, referred to as scaffold or matrix, which ideally should elicit an appropriate response [22, 27]. Hence, considering the variations or diversity in the materials and their applications biocompatibility was redefined by Williams as –

‘‘ Biocompatibility refers to the ability of a biomaterial to perform its desired function with respect to medical therapy, without eliciting any undesirable local or systemic effects in the recipient or beneficiary of that therapy, but generating the most beneficial cellular or tissue response in that specific situation, and optimizing the clinically relevant performance of that therapy [22].’’

2.2.1 Biocompatibility testing

Novel implant materials are tested for their biocompatibility before going into clinics. There are traditional standard in vitro and in vivo test systems to study interaction of implant materials with cells and tissue.

2.2.1.1 In vitro biocompatibility tests

The International Organization for Standardization (ISO) 10993-5 sets up standard *in vitro* testing protocols which should include positive and negative controls of the materials, the tests should be performed not only with the materials directly but also with material extracts. Appropriate cell lines and cell media should be used [28]. For instance, primary rat osteoblast cell culture is a standard to study the parameters supporting formation and mineralization of the extracellular bone matrix [29-31]. *In vitro* tests are cheaper, sensitive, reliable, convenient and reproducible compared to *in vivo* testing [32, 33]. Additional *in vitro* tests to evaluate the cytotoxicity, carcinogenesis/mutagenesis and cell functions are established [32-36]. For cytotoxicity testing, MTT (3-(4,5-dimethylthiazo-2-yl)-2,5-diphenyltetrazolium bromide) assay is used in which MTT compound is reduced by the mitochondrial enzyme of living cells and after reduction it converts into formazon, a colored water insoluble compound. The amount of produced formazon is recorded using a spectrophotometer which can be correlated to the living cells [28]. Another test is the Ames test, which evaluates the mutagenesis using bacterium *Salmonella typhimurium* with a mutated gene and this mutation disables the bacterium to generate amino acid histidine from culture medium. In presence of a mutagenic agent, this mutation can revert back to regain the ability to synthesize histidine. Mutagenicity is assessed by growing the bacterium in the presence of material extracts [28].

2.2.1.2 Animal test models to evaluate the biocompatibility of biomaterials

Animals used for the biocompatibility studies depend upon the type of implants such as cochlear implants in kittens [37], orthopedic implants in sheep or pigs [38] and dental implants in rats [39]. Larger animals are used to monitor the functionality and biocompatibility of biomaterials. One of the limitations of using larger animals in the study is need for bigger storage space and their breeding in pathogen free conditions. Secondly, with the development of novel biomaterials, there is a need of a reliable screening system to evaluate their biocompatibility with minimum usage of animals. For this,

the study shifted to mouse or rat models due to its 1) similarity to humans [40] 2) convenient in house breeding under pathogen free conditions 3) minimum storage space.

Conventionally, the cage implant model in rats was established to monitor inflammatory reactions in response to glucose sensors [41]. The biomaterial is placed inside the cage of stainless steel and is then implanted in rats; the exudate can be collected from cage without sacrificing the animal [42-44]. Glucose sensors were tested in this model and antibodies in response to the biomaterial were checked to characterize immune response [41]. However, the cage model does not involve direct interaction of the tissue and only exudates can be examined.

Numerous other mouse models have been established to evaluate the biocompatibility of implants using in vivo imaging techniques. Recent publications have demonstrated the development of fluorescent or luminescent reporter molecules that can detect inflammatory reactive oxygen species, nitric oxide, proteases and hydrogen peroxide *in vivo*. Implant related inflammation was imaged non-invasively using near infra-red fluorescent hydrocyanines that can image reactive oxygen species [45]. Hydrocyanines are the reduced form of commercially available cyanines which becomes fluorescent when encounter reactive oxygen species [45]. Other, fluorescent reporter molecules such as diaminocyanine sulfate specific to nitric oxide were generated to detect implant associated inflammation [46]. Recently, luminol (5-amino-2,3-dihydro-1,4-phthalazinedione) and its analog L-012 were used to detect oxygen radicals in response to inflammatory materials [47, 48]. L-012 and luminol are chemiluminescent probes, whereby L-012 was found to be more sensitive and specific for oxygen radicals [49-51]. Several other strategies were followed to monitor the device associated inflammation such as peroxalate nanoparticles used to detect hydrogen peroxide [52, 53]. The other method to monitor inflammatory response is to target the proteolytic enzymes such as cathepsins, secreted by neutrophils and macrophages as part of immune reaction in response to the implants. For this, a commercially available fluorophore by Perkin Elmers, Prosense 680 targeted the produced cathepsins in response to inflammatory implants [54]. However, these inflammatory reporter molecules are not used as standards to evaluate biocompatibility of implant materials.

The immune response to implants is studied extensively but still there is no standard mouse model that can be used for evaluation of implant-tissue interactions. The immune response to implant materials is a dynamic process that involves complex signaling between immune cells and tissue cells. The next chapter will provide step-wise explanation of immune response to implant materials.

2.3 Wound healing and inflammatory response to biomaterials

Immune reaction in response to implanted biomaterial is a series of sequential events starting from the injury caused due to implantation procedure. Soon after implantation, proteins from the blood and interstitial fluid are adsorbed on the surface of biomaterial. The layered protein surface on the materials serves as provisional matrix for inflammatory cells. Injury also plays a role in attracting and activating the immune cells. The first cells to arrive at the implantation site are the circulating polymorphonuclear leukocytes that release granular enzymes. The inflammatory response can become chronic. Macrophages can adhere to the biomaterial surface and then fuse to form a foreign body giant cell. These giant cells secrete large quantities of degradative enzymes impairing wound healing process and leading to failure of implanted device. As a part of wound healing, macrophages and endothelial cells also secrete pro-fibrotic factors promoting the formation of a fibrous capsule surrounding implant. The thickness of the fibrous tissue surrounding the implant depends upon the immunogenicity of biomaterial. Excessive fibrosis can lead to loss of functionality of implant, for example, fibrosis on coronary stents block the blood flow of arteries and then the device needs to be removed from the patient [55-58].

To make the mechanism understandable, the immune response will be discussed at each step. First step is the formation of protein layer on implant surface. These proteins have a major influence on the inflammatory response to biomaterials.

2.3.1 Adsorption of proteins

As soon as the implant comes in contact with the host tissue, proteins from blood and interstitial fluids are adsorbed on the surface of implants. The acquisition of a protein layer occurs in nanoseconds (Fig. 1). This affects the interaction of implant with tissue. Adsorbed protein layer provides a provisional adhesion matrix to inflammatory cells or other cell types [59]. For example, osteoblastic cells are found to be dependent on the adsorbed fibronectin or vitronectin for adhesion and proliferation on polystyrene cell culture plates, titanium, stainless steel and hydroxyapatite *in vitro* [60-62]. The surface properties of the materials also decide the type, concentration and orientation of the proteins. A difference has been observed in the adsorption rates of proteins on hydrophobic and hydrophilic surfaces. Hydrophilic materials such as titanium and hydroxyapatite exhibited superior abilities to integrate in the bone [63-66]. However, the surface charge of the material also showed different degrees of adsorptions of proteins but the effect was not as profound as in case of hydrophilic surfaces. In the absence of cellular interactions, adsorbed proteins can be replaced by proteins exhibiting higher affinity to the material surface, this phenomenon is known as Vroman effect [67]. Moreover, fibronectin and vitronectin adhesion protein could support macrophage adherence and formation of foreign body giant cells *in vitro* [68, 69]. This means that adsorbed proteins on the biomaterial surface

may influence the wound healing or inflammatory response [70]. The differential protein-mediated biomaterial cell interactions can be intervened therapeutically to enhance the integration of biomaterial into tissue.

2.3.1.1 Role of coagulation and complement proteins

Injury or mechanical damage to cells is associated with the implantation procedure. Injured blood vessels activate intrinsic and extrinsic coagulation pathways by producing initiators of the coagulation system; Factor XII (FXII) and tissue factor respectively [71]. Studies have shown that FXII gets activated by contact with the negatively charged surface of biomaterials that activates a cascade of proteins eventually releasing thrombin. The released thrombin is not sufficient to produce clots but activates platelets. Activated platelets release mediators of the coagulation cascade. Eventually, proteins of the extrinsic pathway become activated by accumulating on the activated platelets [72]. Thrombin is generated in large amounts that cleave the fibrinogen to fibrin. Deposited fibrin forms a primary mesh or clot around the biomaterial which is in turn is sensed by phagocytes, thus initiating inflammatory response (Fig. 1) [73, 74]. As a result, blood coagulation on biomaterials is a combined effect of contact activation and platelet activation [70, 75-78].

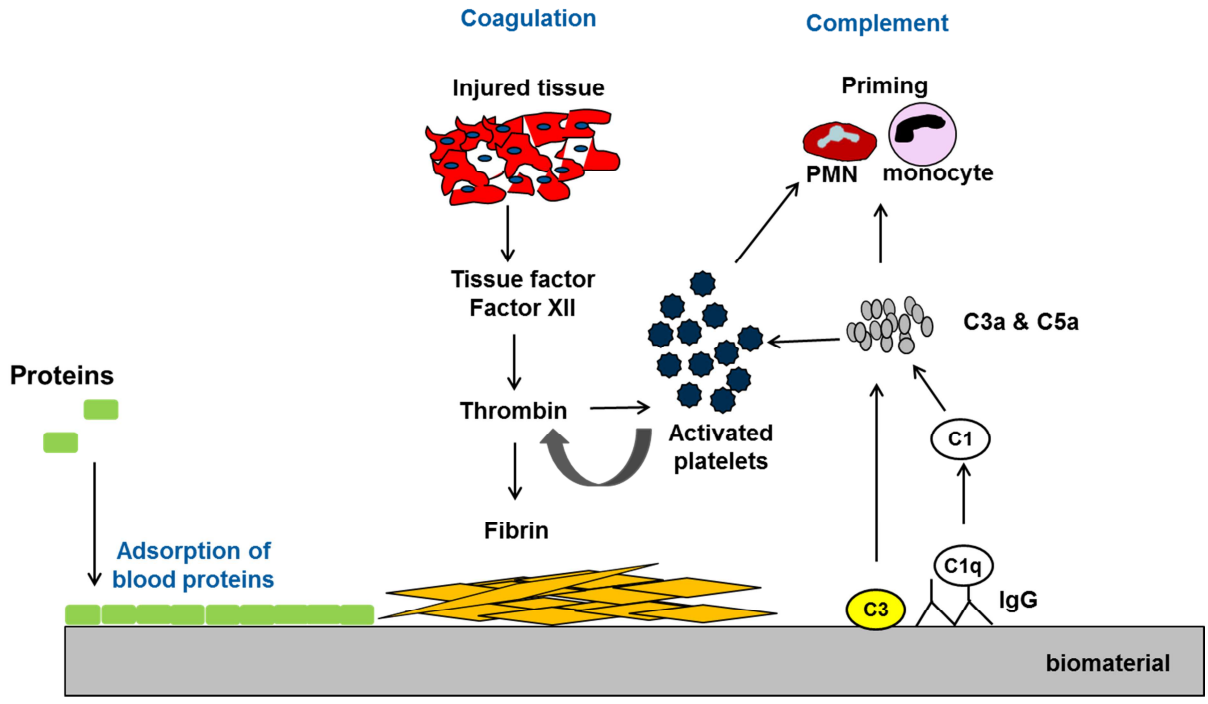

Figure 1 : Priming of immune cells: Proteins from blood adsorb on the surface of biomaterials preparing adhesion matrix for cells. In parallel, injury stimulates coagulation pathway that activates platelets and eventually fibrin is formed that forms a mesh surrounding the biomaterial. Activated platelets also prime inflammatory cells. Complement proteins produce toxins (C3a and C5a) through classical and alternative pathway that leads to priming of immune cells. C stands for complement proteins and PMNS are polymorphonuclear leukocytes. Modified from [70]

The complement system is a part of innate immunity. It constitutes small proteins present in blood in inactive state. The complement system gets activated by foreign surfaces by three different pathways, the classical, the alternative and the lectin pathway. All the pathways produce C3 convertase enzyme that leads to the release of toxins C5a and C3a. Biomaterial-associated complement activation largely depends on the classical and the alternative pathways [70, 79-81]. Adsorbed proteins on the implant includes IgG molecules that engages C1q (complement protein) and forms the C1 protein complex which is the first enzyme of the classical pathway [82]. Moreover, C3 protein can directly adsorb on the surface of biomaterial and activate the alternative pathway [83]. As a result, the initiating C3 convertase enzyme is generated which further amplifies the loop by producing more mediators. Once sufficient enzyme is produced, it promotes the release of pore forming toxins C3a and C5a. These toxins have multiple functions such as priming granulocytes and monocytes, inducing the release of reactive oxygen species by granulocytes, triggering mast cell degranulation and increasing vascular permeability of the cells (Fig. 1) [84].

The coagulation and complement pathway function synergistically on the biomaterial surface to promote the inflammatory responses [85]. Fibrinogen, factor X, iC3b, fibronectin and vitronectin were shown to be adsorbed on the biomaterial surface [86]. These proteins are known as the ligands for receptors of the inflammatory cells. The receptor ligand binding promotes the adherence of the inflammatory cells to the surface and subsequently activates them.

2.3.2 Danger signals recognized by polymorphonuclear leukocytes (PMNs)

Alternatively, injury due to implantation surgery can also activate the inflammatory cells. Injured tissue releases danger molecules or alarmins which are recognized by a set of receptors of the polymorphonuclear leukocytes leading to their activation (Fig. 2). Apart from the pathogens, trauma is one of the causative agents of cell and tissue damage. Alarmins are endogenous molecules released by dying cells. Inflammatory cells recognize these molecules through special receptors and promote the innate and adaptive immune responses [87]. The most common example of alarmins is HMGB1 (High mobility group box 1) which is a nuclear protein with a DNA binding domain [88]. During non-programmed cell death, this protein is passively released [89, 90]. Recent studies have shown that those macrophages engulfing apoptotic cells also secrete HMGB1 [91]. It also acts as signaling protein and helps in migration of monocytes, macrophages, dendritic cells and neutrophils [92-94]. There are some calcium binding proteins that behave as alarmins during inflammation like S100 proteins, these proteins are expressed by phagocytes [95]. Heat shock proteins (HSPs) are secreted by necrotic cells and they mediate the release of inflammatory signaling molecules by binding to cells of the innate immune system [96]. Alarmins evoke immune response by binding to receptors of immune cells. This receptor-ligand binding activates signaling pathways of innate immunity.

Table 2: Examples of alarmins and their functions [87]

Alarmins	Origin	Physiological function	Target receptors	Extracellular function
HMGB1	All cell types	Transcription regulator	RAGE TLR2 TLR4	- Pro-inflammatory cytokines - Activation of platelets - Chemotactic activity
S100A8/A9/A12	Phagocytes Epithelial cells	Calcium homeostasis	RAGE	- Pro-inflammatory immune response - Release of neutrophils from bone marrow - Increases vascular permeability
Heat shock proteins, HSP60 and HSP70	All cell types	Assist protein folding	TLR2/TLR4	- Release of pro-inflammatory cytokines - Imuunostimulation of natural killer cells

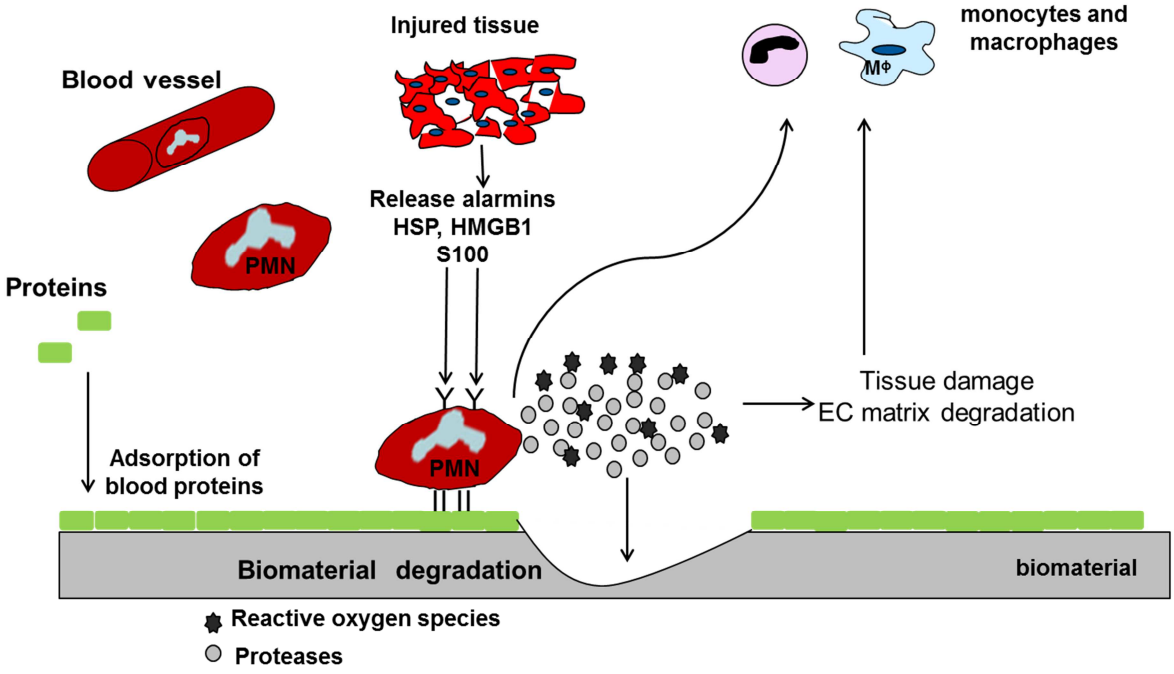

Figure 2: Immune response to implants: Sequential events triggering the immune response after implantation, proteins from the blood and the interstitial space are adsorbed on the surface of the implants. PMNs reach to the site of implantation and get activated by recognizing alarmins released from the injured tissue through receptors and initiate the secretion of reactive oxygen species and proteases. Prolonged activation of PMNs leads to the release of signal proteins that recruit monocytes and macrophages to the inflammation site. Modified from [70]

Polymorphonuclear leukocytes (PMNs) form the first line of defense and are the first cells to arrive at the site of inflammation. Following injury and protein adsorption, PMNs migrate from blood to the

implantation site rapidly. They sense injury because of alarmins released by injured tissue, activated platelets and endothelial cells. PMNs recognize protein coated implant surface and bind to the bound proteins by engaging their transmembrane receptors that promote cell-cell interactions or cell-extracellular matrix interactions. The adherent cells sense damage by their receptors. This recognition triggers phagocytic activity of the cells [70, 97, 98]. The cells start to release certain proteases and reactive oxygen species to promote pathogen killing. Excessive production of oxygen radicals or proteases can corrode biomaterial surface, for example, polyurethane [99]. The production of destructive agents by PMNs also hinders integration of biomaterial into tissue by damaging the tissue and prolonging the inflammatory response. PMNs release molecules that signal to attract more inflammatory cells to the site of inflammation [100]. Within two days after implantation, PMNs disappear from the implantation site [86] (Fig. 2).

2.3.3 Role of macrophages in wound healing and in biomaterial associated inflammation

Monocytes and macrophages are guided to the implantation site in response to signal molecules released by granulocytes [70, 101]. Monocytes undergo phenotypic change and become macrophages in the tissue (Fig. 3). Macrophages are phagocytic cells that engulf cellular debris and foreign particles. They secrete cell signaling proteins called as cytokines in inflammation or wound healing that affects the behavior of immune cells. Based on function of macrophages, they are generally classified as classically and alternatively activated [102, 103]. Classically activated macrophages are inflammatory cells that induce production of inflammatory cytokines such IL-12, IL-6 and IL-1 and perform microbicidal activity by producing reactive oxygen species [70, 102, 103]. However, the alternatively activated macrophages are further subdivided into regulatory and wound healing macrophages [103]. Wound healing macrophages down regulate the inflammatory cytokines and promote tissue resolution by inducing the production of extracellular matrix or activation of fibroblasts [103, 104]. Regulatory macrophages can dampen inflammation by excessive production of IL-10 which is a very strong immunosuppressive cytokine [70, 103]. The early phase of inflammation involves phagocytic and microbicidal activity of classical activated macrophages. Later, the wound healing macrophages become active and play crucial role in tissue resolution. It is still unclear that the macrophages already at the site of inflammation change their phenotype from one type to the other or they emigrate from the site [70]. The plasticity of macrophages makes them a potential target in immunomodulation therapy.

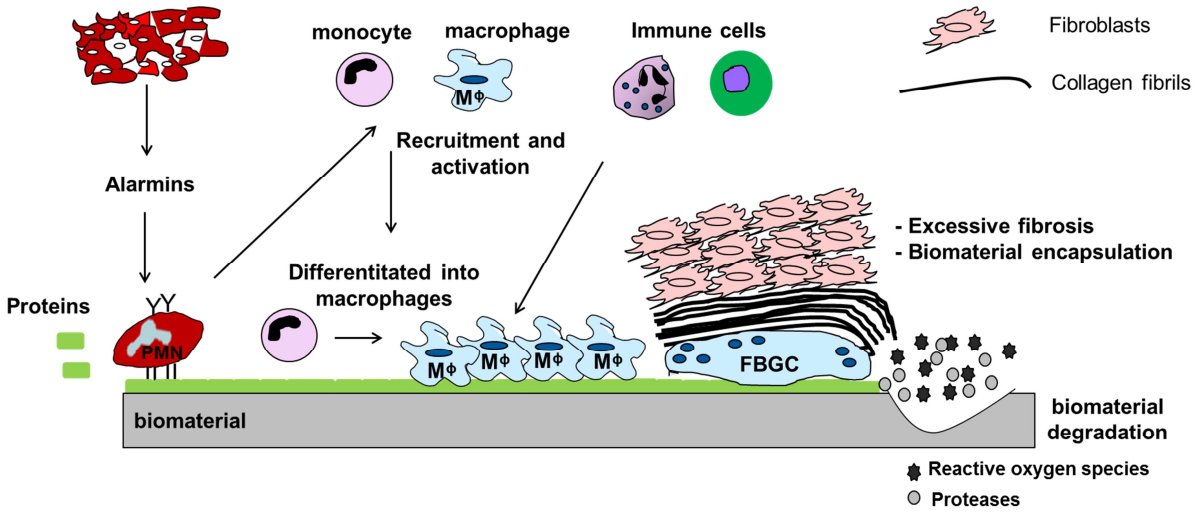

Figure 3: Formation of giant cells and fibrosis: Monocytes and macrophages are recruited in response to the signaling proteins released by PMNs. The recruited macrophages start fusing with each other in response to stimuli from other immune cells and they form multinucleated foreign body giant cell (FBGC). Giant cells produce proteases and oxygen radicals, eventually corroding the biomedical polymers. Fibroblasts proliferate and synthesize type 1 collagen which when produced in excess amounts can encapsulate the biomaterial. Modified from [70]

2.3.4 Formation of foreign body giant cells and device failure

Macrophages adherent to the biomaterial surface are classically activated and exhibit the pro-inflammatory response by secreting reactive oxygen species, degradative enzymes and cytokines. They start phagocytosing particles up to size of 5 μm and upon encountering the particles bigger than this size (>10μm), macrophages fuse with each other to form foreign body giant cells (Fig. 3) [105]. Other immune cells signal the fusion of macrophages by secreting signaling proteins [106-108]. Fused cells are phenotypically closer to alternatively activated macrophages [103]. However, fused cells also start the frustrated phagocytosis phenomenon, according to which, fused macrophages have reduced phagocytic ability than adherent macrophages but their capacity to secrete degradative enzymes such as reactive oxygen species and protons is enhanced (Fig. 3) [109-111]. These giant cells can stay at the site of implant for longer period of time, but it is unclear whether they become inactive or persistently produce degradative enzymes. As a result, the degradative chemical environment at biomaterial-tissue interface may result in the degradation of biomaterials depending upon their surface properties of materials. Polymers are susceptible to degradation such as polyethylene used in artificial joints can be oxidized by the reactive oxygen radicals. Moreover, a device can also fail by cracking due to stress by adherent macrophages and foreign body giant cells, for instance, lead insulation of the pacemaker made up of polyether polyurethane cracked due to the environmental stress [112, 113].

2.3.5 Fibrosis

Fibrosis is the last phase of wound healing process [114]. Foreign body giant cells release the destructive agents in the tissue material interface, impairing the wound healing response [57, 115]. Macrophages, endothelial cells, lymphocytes and fibroblasts themselves, produce profibrotic factors which triggers the continuous proliferation of fibroblasts and production of connective tissue, resulting in fibrosis. Other profibrotic factors such as macrophage derived growth factors and fibroblast activating factors (FAFs) also upregulate the synthesis of type I and type II collagen which are extracellular matrix proteins [116]. The continuous proliferation of fibroblasts and production of collagen fibrils may encapsulate the biomaterial surface and the functionality of the device may fail (Fig. 3).

2.4 Strategies to improve the interaction of biomaterial with tissue and modulation of inflammatory responses

To improve the implant tissue interaction, specific cell responses can be promoted by modifying the surface of biomaterials [117]. For instance, titanium is an inert material with several biological applications as implants. The properties of titanium can be improved by modifying the surface in a way that allows migration, and adhesion of bone forming cells, hence enhancing the osseointegration [118]. Several strategies have been employed either by changing the physiochemical properties of the biomaterials or incorporating molecules or matrices to the surface of biomaterials influencing function of cells.

2.4.1 Surface modifications of biomaterials

The type and orientation of proteins adsorbed on biomaterial surface depend on the surface chemistry of material. The protein layer may enhance adhesion of immune cells by providing ligands to their receptors [59]. Modulating this protein layer on the surface of biomaterial could trigger desired functions of macrophages and PMNs. This strategy is categorized as passive modulation of immune responses to biomaterials. Proteomic analysis of macrophages cultured on different surface chemistries of polymers, hydrophilic, hydrophobic or anionic, revealed differential protein expression profiles [119, 120]. The amendments in the surface chemistry and topography of biomaterial also showed changes in macrophage responses. Natural extracellular matrix components imprinted at micron or nano scale on the surface of materials have the ability to direct cellular responses, increasing the adhesion, spreading, migration and proliferation of target cells [121, 122]. Parallel gratings were imprinted on different polymers and it was observed that independent of the surface chemistry of material, these induced topographic changes affected macrophage morphology and function *in vitro* and adhesion of macrophages to the surface *in vivo* [123].

2.4.2 Biological functionalization of implant materials by using bioactive molecules

The performance of material could be improved by optimizing biological properties at the surface of implant material to improve interaction with the host tissue. The material - tissue interactions can be augmented by local and long long-lasting delivery of biological agents that can be either therapeutic or can enhance adhesion of only desired cells to the surface. Bioactive molecules are pharmacologically active agents that are either derived from natural sources or chemically synthesized. Immobilizing bioactive agents such as integrin adhesion sites, growth factors or anti-inflammatory drugs on the surface of biomaterials directs desired cellular responses. Short oligopeptide sequences of receptor binding domains for immune cells were synthesized and immobilized on the biomaterials, enhancing adhesion of specific cells [124, 125]. The domains of fibronectin RGD (arginine-glycine-aspartate) and PHSRN (proline-histidine-serine-arginine-asparagine) attached on the biomaterial regulated macrophage functions *in vitro* and *in vivo* [126, 127].

Alternatively, anti-inflammatory drugs could be incorporated on the surface of biomaterials. For instance, glucocorticoids are potent immunosuppressive agents that trigger the downregulation of inflammatory signaling proteins, proteases and reactive oxygen species while up regulating anti-inflammatory mediators to promote tissue resolution [128]. Another most commonly used anti-inflammatory drug is dexamethasone that reduces the number of PMNs at the site of implantation in the initial phase of inflammation. At the chronic stage, presence of dexamethasone reduces macrophage number and fibrous capsule formation. Dexamethasone may also delay wound healing process [129, 130]. Biomaterials are required to supply dexamethasone throughout its survival time as the reduced effect will lead to infiltration of inflammatory cells thus increasing the immune response [131].

Growth factors may primarily affect tissue cells but are capable of modulating immune response. A tight cross talk between the inflammatory cells and tissue cells has been observed during wound healing and inflammation [132]. Fibroblasts regulate the production of inflammatory or anti-inflammatory signaling proteins to maintain the homeostatic balance [133]. In tissue remodeling the mutual interaction of monocytes and fibroblasts has been observed [134]. Some growth factors can directly modulate the migration of macrophages during wound healing process. Therefore, immobilizing growth factors may directly or indirectly modulate the activity of monocytes or macrophages, hence improving the integration of biomaterial into tissue.

2.4.3 Artificial extracellular matrix design

Alternatively, researchers designed artificial matrices that can be used alone or as coating on the biomaterial surface to support specific cellular processes. These matrices could very well extrapolate

in vivo situation at the implant – tissue interface due to their high similarity to natural extracellular matrix. As we know, there is an extracellular space in the human tissues in which cells release biomolecules. These molecules help provide mechanical support to cells, in organization of the cells into tissues and controls the functions of cells to some extent [135]. Extracellular matrix (ECM) constitutes proteins and glycans. There are two classes of proteins present in the extracellular space, structural proteins such as collagen, elastin and proteins promoting cell adhesion, fibronectin or laminin [135, 136]. The most abundant protein is collagen that provides the tensile strength while elastin imparts elasticity to the ECM [137]. Glycans are negatively charged, polysaccharide-rich substances filled in the spaces between the cells, for example, glycosaminoglycans (GAGs) and proteoglycans (PGs). They prevent the breakdown of tissue by filling aqueous spaces between protein fibrils in swollen state [135, 136, 138].

Tissue engineering matrices are currently designed to simulate the natural extracellular matrix that can provide several bioactive factors, essential for cell adhesion, spreading, proliferation and migration. Hydrogels are scaffolds used in tissue engineering due to high water content and its properties resemble soft tissues [139]. They are available as natural or synthetic hydrogels. Natural hydrogels are made of natural protein polymers such as collagen, fibrin or polysaccharides polymers (alginate, chitosan, hyaluronic acid and dextran) while synthetic hydrogels are synthesized using polymers such as poly (acrylic acid) (PAA), poly (ethylene glycol) (PEG), poly poly (vinyl alcohol) (PVA) or other polypeptides. Moreover, biomimetic hydrogels can be produced by grafting them with several bio-functions such as decorating them with protein derived cell adhesive peptides to foster the cell adhesion process, incorporating growth factors to promote tissue regeneration and modulating its sensitivity to enzymatic degradation [139]. Although, hydrogels produced are known to be bio inert, but comparative studies demonstrated their immunogenic behavior depending upon their origin (natural or synthetic), handling methods or sterilization procedures, which limited their use [140].

Artificial extracellular matrix can also be generated by coating implants with proteins (eg. collagen) of extracellular matrix. Collagen coatings on titanium have shown to improve initial attachment of the bone cells [141]. Studies also demonstrated up-regulation of bone matrix proteins leading to bone remodeling around the collagen coated titanium implants [142]. Although collagen facilitated the initial attachment and spreading of bone cells it did not promote proliferation or differentiation of bone progenitor cells [143]. To this end, collagen matrices were prepared along with glycans GAGs and PGs, to mimic properties of natural ECMs. Proteoglycans (PGs) not only enhance the attachment of osteoblasts but also serves as mediators between the matrix and endogenous growth factors [144]. Sulfate groups in GAGs are identified as growth factor binding site in the natural ECM, hence artificially increasing the frequency of sulfate groups on GAGs may promote the tissue regeneration process. Chondroitin sulfate increases the sulfate groups on GAGs and the combination of collagen

with chondroitin sulfate improved the osteoconductive properties of titanium implants [145, 146]. Sulfated GAGs also modulate the immune response by promoting the binding of IL-10, a strong anti-inflammatory cytokine, to monocytes or macrophages eventually enhancing the anti-inflammatory immune response [147, 148]. Therefore, the glycan of ECM acts passively or actively in modulation of the immune response and improving the tissue regeneration.

Implant-related inflammation limits the function of implanted medical device. Therefore, it is essential that biomaterial integrates into tissue. Several approaches have been employed to modulate the inflammatory response by modification of the physiochemical properties or local delivery of bioactive agents to elicit the desired cellular response. The most promising approach is the design of the artificial extracellular matrices and due to their higher similarity to natural matrices they can regulate the immune response in a more specified and desirable manner.

2.5 Implant – related infection

Permanent or temporary implants usually face two challenges; inappropriate tissue integration and microbial colonization [149]. Implant surface is an attractive substrate for attachment and growth of microbes. When implants are introduced into a mammalian host, the tissue integration process competes with microbial colonization for the same surface, referred to “race for the surface” [149]. The rapid integration of biomaterial into tissue minimizes the chances of bacterial colonization. This indicates that the implant should be highly biocompatible to promote wound healing process. However, in case of inferior bio-compatibility the immune system becomes compromised leading to delayed wound healing and bacteria can easily escape the immune reaction and may colonize the implant surface [149]. Studies have shown colonization of *Staphylococcus epidermidis* and *Staphylococcus aureus* on biomaterials [149-151]. Numerous other bacteria such as *Pseudomonas aeruginosa*, *Proteus mirabilis*, *Escherichia coli* and beta hemolytic streptococci also colonize medical implants [149, 150]. *Pseudomonas aeruginosa* caused bacterial keratitis by colonizing the used contact lens [152]. The mechanism of microbial colonization on medical implants has been delineated into several categories to make the process understandable [149].

2.5.1 Biofilm formation on medical implants

These steps closely represent *in vitro* mechanisms of bacterial biofilms formation, but very little is known about *in vivo* situation. The first step involves initial attachment of the bacteria on implant which depends upon the physicochemical properties of material. The planktonic bacterium moves towards the implant surface due to the effect of physical forces such as Van der Waals forces [153]. When the bacterium reaches a distance of 1 nm to the surface it adheres to the surface by ionic, hydrogen or covalent bonding [149]. After initial attachment, adhesion proteins on the bacterial

fimbriae support the bacterial adherence on the biomaterial [150]. Studies have shown that some specific proteins of bacteria also mediate their adherence to the surface; for instance, autolysins are the adhesion proteins that bind to the surface by hydrophobic or ionic interactions [154, 155]. The initial attachment or adhesion of the microbes to the surface of biomaterials is not sufficient for accumulation of bacteria on biomaterial surface. Subsequent to the initial attachment, bacteria change their phenotype and start secreting extracellular polymeric substances (EPS) that promote cell to cell aggregation process and forms microcolonies [149, 156]. Microcolonies are the basic units of a mature biofilm and upon encountering appropriate environmental conditions bacterial cells proliferate in the EPS matrix. Extracellular matrix includes the polysaccharides, proteins, nucleic acids and lipids that promotes the cell to cell binding, provides mechanical stability and protects bacteria from dehydration and antimicrobial agents [157, 158]. Role of extracellular DNA in the biofilm formation was investigated for *Bacillus cereus*, *S. aureus* and *L. monocytogenes* [159-161]. Under adverse conditions, bacterial cells sense the environmental changes and communicate with each other to regulate the gene expression in accordance to maintain the existence of the entire community; such communication system is referred as Quorum sensing [162, 163]. This cell to cell signaling is cell density dependent as only bacteria in mature biofilm are able to perform the quorum sensing [164]. Several functions can be regulated through communication system such as release of virulence factors to increase attachment to the host cells, motility, secretion of defensive factors to fight against the host cells, DNA exchange and formation of three dimensional structures [163, 165, 166]. When mature biofilm structure reaches its maximum size, cells from the periphery detach due to nutrient depletion and migrate to a new potential site for biofilm formation [163]. The dissemination process also involves the movement of bacteria from the highly populated area to the periphery due to lack of nutrients. These cells have the ability to relocate and restart the biofilm formation processes [167].

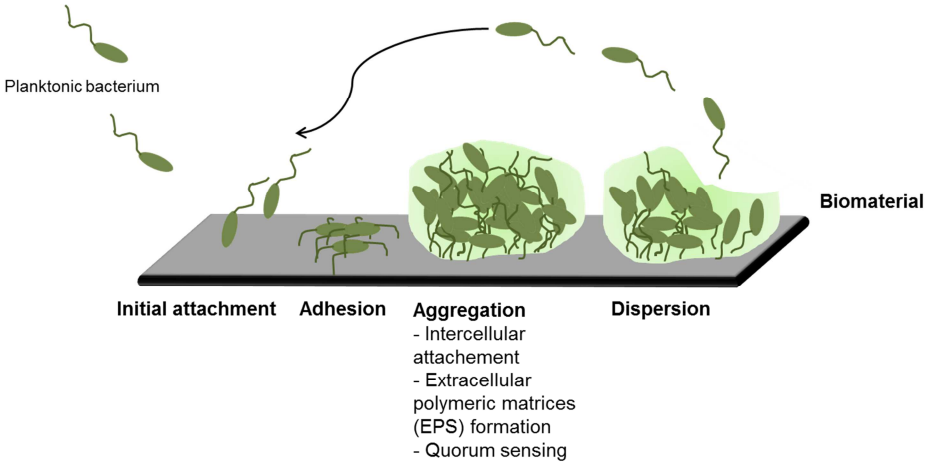

Figure 4 : Overview of the phases of bacterial biofilm formation on an implant surface [168].

Bacterial infection not only leads to the loss of functionality of the implant but also damages surrounding tissue. These infections are mostly resistant to conventional antibiotics because bacteria propagate in self-produced matrix, which cannot be easily penetrated using conventional antibiotic therapy. The solution to problem is revision of implant surgery but risk of relapse of infection is high. For example, in primary replacements of hip and knee, the frequency of peri-prosthetic infection is between 1.5-2.5% and this rises to 5-40% after revision surgery [169]. Another example is penile prosthesis in which primary incidence is 2-5% but in revision patients it increases to 10% [170].

2.5.2 Preventing biofilm infections

Medical implants such as urinary catheters, vascular grafts, prosthetic joints, pacemakers, endotracheal tubes, breast implants and contact lens are prone to infection [171]. Biofilm formation on these implants imposes a serious concern to health. The hazardous consequences of biofilms on medical implants include tissue destruction, systemic infection and loss of implant functionality eventually leading to serious illness of patients. These infections are not only resistant to immune defense mechanisms but also to conventional antibiotic therapy. The only way is to prevent biofilm formation by controlling the behavior of bacteria and medical devices, for which numerous novel strategies are being followed: 1. Disabling quorum sensing by using biomolecules [172-174] 2. Biomaterials coated with nanoparticles loaded with antimicrobial agents 3. Immunotherapy includes blocking of receptors, responsible for bacterial cell adhesion to the surface or inhibiting the intercellular adhesion 4. Disrupting the extracellular polymeric matrices by using matrix targeting enzymes such as DNaseI or Proteinase K [175]. Taken together, the bactericidal coatings on implants or coatings preventing bacterial adhesion to the surface appears to be the most promising strategy because it provides the local and slow release of antimicrobial agents that can prevent infection for an extended period. There are several anti-biofilm agents disrupting quorum sensing and matrix of the biofilms but their therapeutic efficacy is still a question. Besides, these agents are also immunogenic or allergic in some cases.

3. Aims

Existing implant materials are not optimal materials because they are taken over from technical developments. There is a great need for implant materials designed for specific applications. Novel implant materials or coatings on standard materials need to be tested *in vivo* before introducing into clinics. So far, there are no methods that allow quantification of inflammatory potential of different implant materials *in vivo*. There are known implant materials of varying inflammatory potential that are clinically used. Glass and titanium implants are non-inflammatory but degradable polymers have different effect according to histology results [176]. Moreover, wear particulates of hip or knee implant materials cause inflammation [177]. To this end, there is a need of sensitive, accurate and reliable animal model to evaluate inflammatory potential of different implant materials. Therefore the aim of this study was:

1. To characterize the inflammatory potential of various implant materials of different size and textures.
2. Additionally, to establish a system that enables to continuously monitor implant-related inflammation
3. To distinguish inflammatory potential of several implants in one mouse that will improve comparability between materials by eliminating animal to animal variability and will reduce animal usage.
4. To differentiate inflammation due to injury, implant and infections
5. To compare and evaluate sensitivity and reliability of different detection strategies.
6. To establish a sensitive detection system to monitor bacterial infections that respond solely to infections and not to material induced inflammation or injury related surgery.

4. Outline of the study

To distinguish inflammatory potential of implant materials, several approaches were used. To this end, the study is divided into three major parts in which the initial strategy was to target inflammatory reactive products by fluorescent imaging. The second approach was to visualize immune cells of inflammation by bioluminescent imaging. Finally, to detect implant infections a new compound has been synthesized which was tested *in vivo* in this study.

4.1 Visualizing reactive inflammatory molecules by fluorescent imaging

Reactive oxygen species generated by PMNs were monitored using hydrocyanines, a chemical sensor which when oxidized converts to fluorescent cyanines. Cyanines can be visualized by in vivo imaging after excitation in the near infra-red [45]. Second strategy is to image inflammatory proteases like cathepsins produced by PMNs and macrophages. A commercially available protease activated fluorophore can be used that is hydrolyzed in the presence of cathepsins [178]. The third approach involves the visualization of autotaxin activity. Autotaxin is an inflammatory enzyme that produces a lipid signaling molecule, eventually stimulating cell proliferation, migration and survival [179]. For imaging, a fluorophore linked to the quencher by the autotaxin sensitive substrate can be used. Autotaxin separates the quencher from the fluorophore that can then be visualized in the in vivo imaging system (Fig. 5).

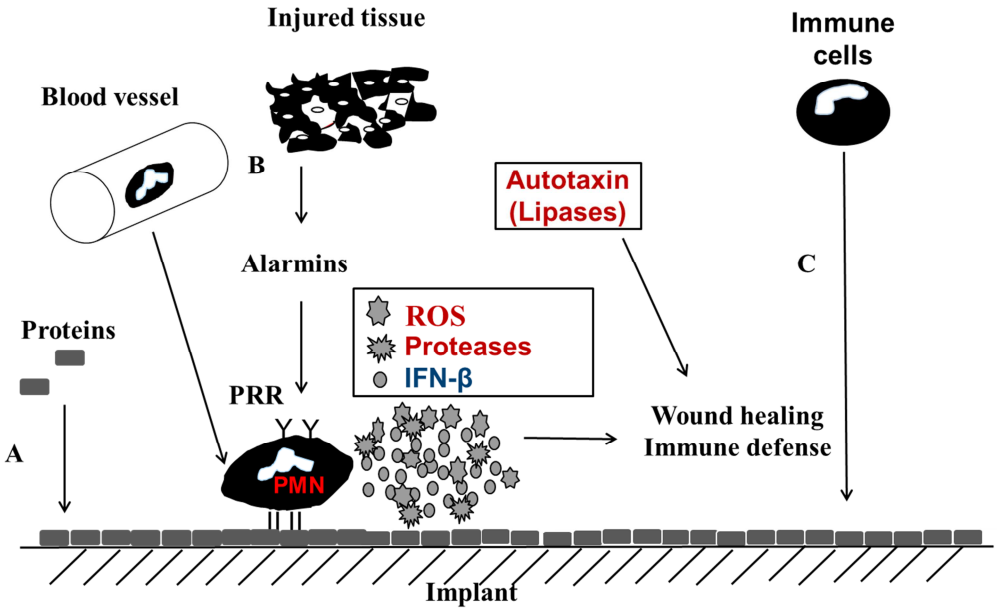

Figure 5:Inflammatory products imaged in the study : Following the implantation, proteins adsorb on the implant surfaces (A), PMNs from the blood vessels reach the site of implantation (B) and upon activation release

reactive oxygen species (ROS), proteases , lipases and IFN-β (in case of bacterial infection). The immune response is amplified by further recruitment of the immune cells (C). (Picture was modified from [70])

4.2 Imaging inflammation using immune cells

To detect implant induced inflammation in real time, inflammatory cells were isolated from the bone marrow of mice with substantial constitutive expression of luciferase under the transcriptional control of Mx-2 gene promoter [180]. Mx-2 promoter responds to type 1 interferons during bacterial infection in the host [181-183]. These bone marrow derived immune cells were adoptively transferred to the implanted mouse model. Different cell types like neutrophils, monocytes or total bone marrow cells were used to visualize and quantify inflammation (Fig. 6). The biocompatibility of several implant materials of different size and texture was tested such as polymer poly lactic – co – glycolic acid (PLGA), titanium and magnesium discs and microspheres of different polymers.

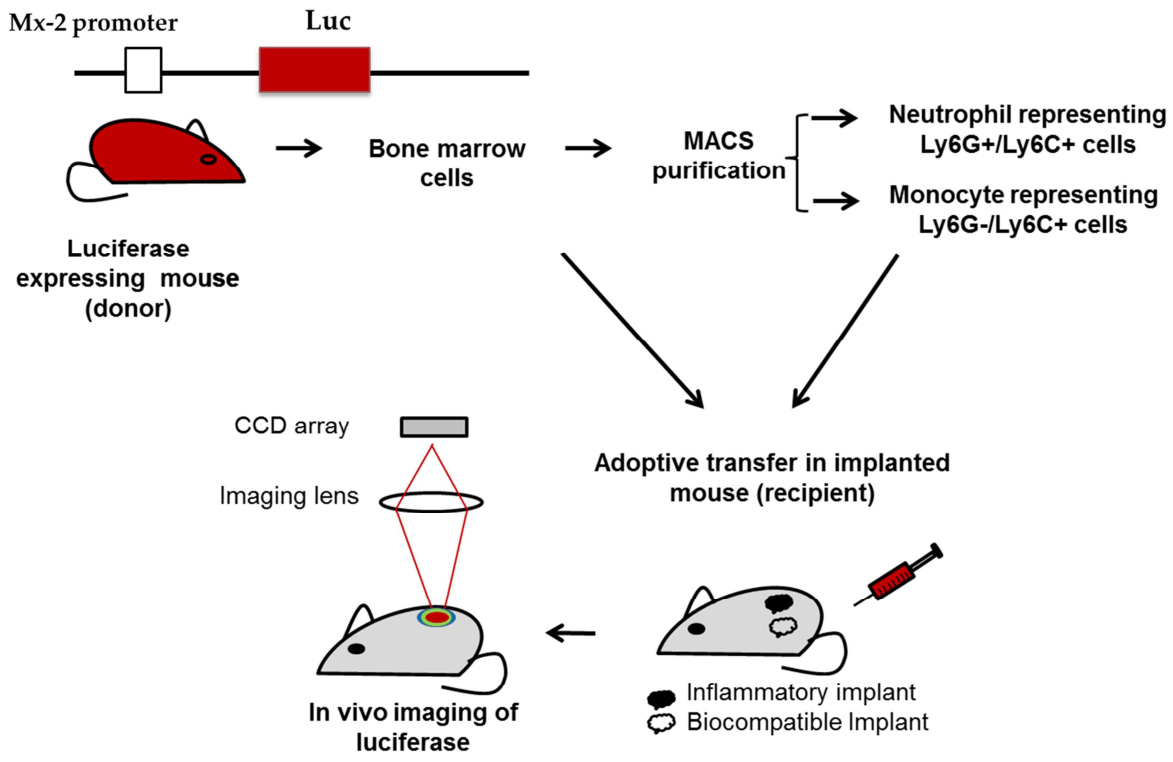

Figure 6: Flow scheme for monitoring inflammatory response to implant materials: Bone marrow cells were isolated from transgenic donor having substantial luciferase expression under the influence of Mx-2 promoter. Neutrophil and monocyte representing cells were purified and adoptively transferred in the implanted mouse model and luciferase reporter expression was exploited to visualize the cells at the site of implantation.

4.3 Visualizing infection related cytokine and bacteria

The incidence of implant related infection is higher in the early stages of implantation. Immune cells activated by the bacterial infection secrete cell signaling proteins like Interferon-β [184, 185]. Bacterial infections can be visualized using transgenic mice in which one allele of IFN-β gene is deleted by luciferase reporter gene for imaging [186].

Alternatively, bacterial infection can be monitored by labelling bacteria *in vivo*. For this, bacterial iron acquisition system was used to label the bacteria. An agent based on 1,4,7,10-tetraazacyclododecane-1,4,7,10-tetraacetic acid amide (DOTAM) derivatives comprising siderophores was synthesized (Fig. 7). Siderophores are iron chelators that are synthesized by bacteria and exported in the extracellular environment to capture iron under nutrient limiting conditions. Here in this study, IFN-β reporter mice were used to visualize the immune response to bacteria (*Pseudomonas aeruginosa*) by bioluminescent imaging and fluorescence of the compound was visualized by the linked near infra-red Cy5.5 fluorophore in same mice.

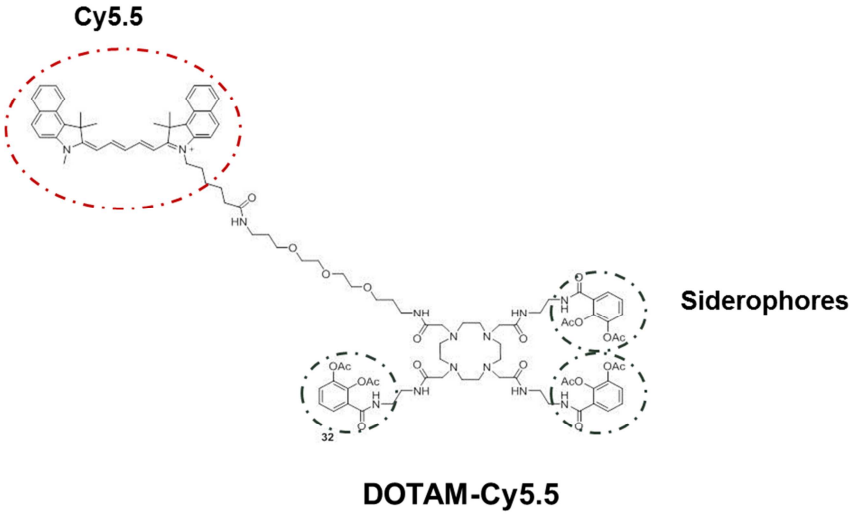

Figure 7: Chemical structure of DOTAM-Cy5.5: Red circle represent near infra-red fluorophore Cy5.5 and circles in green represent siderophore catecholates. The middle ring is DOTA with amide groups to which siderophores are linked (chemical structure drawn and kindly given by Dr. Haiyu Hu)

.

5. Materials and Methods

5.1 Materials

Table 3 : List of equipments used

Equipment	Manufacturer	Model
Autoclave	Belimed Dampf Sterilisator	6-6-6 HS1,FD
Biological stirrer	Techne	MCS-104S
Cell counter	Beckman Coulter	Z2-AF263
Cell separator	MACS Miltenyi	
Centrifuges	Heraeus Sorvall	Multifuge X3 FR RC 5B Plus
CO2 incubators	Labotect	C200
Confocal microscope	Zeiss	LSM 510 Meta
Deionized water	Milli Q	
Electric Shaver	Aesculap	
Flow cytometer	BD Biosciences	FACS Calibur BD™ARIA cell sorter
Freezer	- 20°C:Liebherr - 80°C: Thermo Forma	
Fridge	Liebherr	
Hot plate	IKAMAG® RET	
In vivo imaging machine	Xenogen IVIS system, Caliper	IVIS 200
Light microscopes	Nikon Olympus	TMS CKX41
Mini centrifuge	Heraeus Christ Minifuge GL Biofuge fresco	
Micropipettes	Gilson	
Nitrogen tank	HarscoK Series	
pH meter	Beckmann	M340
Photometer	Nanodrop	ND-1000
Pipettor	Pipetboy IBS Integra Biciences	
Plate reader	Tristar 2 Berthold technologies	
Precision weighing scale	Sartorius	
Rotary shaker	Certomat ®	
Spectrophotometer	Eppendorf / Biophotometer	
Sterile work benches	Baker/ BDK/ Heraeus	SG 400 E / HSP 18
Thermomixer	Eppendorf	5437
Vortex	Scientific Industries	Vortex- Genie 2
Water bath	GFL	

Table 4 : List of consumables

Articles	Company
Cell culture plates (96 well)	Nunc, Corning
Cell strainer (100 µm) Nylon	BD Falcon
Falcon tubes (15, 50 ml)	Greiner BioOne
Flow cytometry tubes	Sarstedt
Injections (1 ml)	Omnican ® F

Needles 26 G	Sterican
Pipette tips	Star lab
Polyglactin filaments Number 6-0	Ethicon
Surgical kit	Fine Science tools

Table 5 : List of reagents

Reagents	Company	Catalogue code
Acetic acid	Sigma	
Acetone	Sigma	
Agarose	Biozym	840004
Formaldehyde solution	Roth	P087.3
Hematoxylin-solution	Sigma-Aldrich	HHS16-500ML
Interferon -β	Cell culture supernatant of BHK-21 cells	
Isofluran	Allbrecht GmbH	A29951,0025
Indocyanine green	Sigma	I2633
Ketamine-xylazine	Animal facility- HZI	
Luciferin	Synchem	BC219
Luciferase firefly juice	P.J.K GmbH	102511
Methanol	J.T. Baker®	
Mouse GM-CSF recombinant protein	ebiosciences	14-8331-62
Sodium borohydride	Sigma	

Table 6 : List of kits and fluorophores used

Kits / Fluorophore	Company	Catalogue code
ATX Red fluorophore	Echelon Biosciences	L2010
BD cytofix/cytoperm kit	BD Biosciences	554714
Live dead viability cytotoxicity kit	Molecular Probes	L-3224
Monocyte isolation kit mouse	MACS Militenyi	130 – 100 – 629
Neutrophil isolation kit mouse	MACS Militenyi	130-097-658
Prosense 680	Perkin Elmers	P/N NEV10724

Table 7: List of softwares used in the study

Software	Manufacturer
Adobe design standard CS5	Adobe Systems Inc.
Axio vision 4.9	Zeiss
FlowJo 10	Tree Star
GraphPad prism	
ImageJ	rsbweb.nih.gov/ij/
Living image software version 4.3.1	Caliper life sciences
Microsoft office 2007/2008	Microsoft Incorporation

5.2 Methods

5.2.1 Sterilization

Glassware was sterilized at 180°C for 4 hours. The surgical kit and plastic materials such as eppendorf tubes, pipette tips and solutions for cell culture were autoclaved at 121°C for 25 minutes. Temperature sensitive solutions were filtered through 0.22 μm size filter.

5.2.2 Cell culture

Cell culture work was carried out in a sterile workbench (Herasafe, Heraeus). The working surface was disinfected with 70% ethanol before and after use. In addition, disposable consumables or autoclaved or sterile-filtered solutions or media were used. Before starting work, all solutions and media were preheated in a 37°C water bath.

Roswell Park Memorial Institute medium, RPMI powder

100 ml HEPES (1 M), 1.68 g/l NaHCO3, pH 7-7.4, add H_20 10 l

100 x Pen / Strep

6.06 mg / ml ampicillin (10,000U/ml), 10 mg/l streptomycin, pH 7.4, stored at -20°C

100 x Glutamine

29.23 mg/ml glutamine, sterile filtered, stored at -20°C

Phosphate buffer saline (PBS)

140 mM NaCl, 27 mM KCl, 7.2 mM Na_2HPO_4, 14.7 mM KH_2PO_4, pH 6.8-7.0

TEP (trypsin EDTA)

6 mM EDTA, 0.1% trypsin (Gibco) in PBS

ACK lysis buffer

150 mM NH_4Cl, 10 mM $KHCO_3$, 0.1 μM EDTA, pH 7.2-7.4

5.2.3 Bacterial culture

Staphylococcus aureus (wild type) and *Pseudomonas aeruginosa* (PA01) wild type were kindly given by Dr. Siegfried Weiss (Molecular Immunology, HZI) and Dr. Susanne Haussler (Head of molecular bacteriology department, HZI) and grown in Lysogeny Broth medium.

LB-Medium (Bacterial growth)

10 g/l Bacto Trypton, 5 g/l Yeast extract, 10 g/l NaCl

LB Agarose plates

500 ml LB, 7.5 g Agarose

5.2.4 Preparation of hydrocyanine

2 mg of indocyanine green was dissolved in 4 ml of methanol. 3 mg of sodium borohydride was added to carry out reduction reaction. The solution was stirred continuously for 5 minutes in absence of oxygen. Solvent was evaporated in the presence of vacuum using rotary evaporators. The dried powder was stored at -20°C overnight. Before injection, the reduced hydrocyanine powder was dissolved in 2 ml of deionized water making up the final concentration to 1 mg/ml [45].

5.2.5 Heat inactivation of *Staphylococcus aureus*

Heat inactivated *Staphylococcus aureus* suspensions were prepared by streaking the bacteria on a lysogeny broth medium (LB) agarose plate and incubated over night at 37°C. Single colonies were picked with a sterile needle and used to inoculate a liquid LB culture that was incubated on a rotary shaker at 180 rpm at 37°C. When the density of the culture reached an OD_{600} of 0.2, 1 ml of the bacterial culture was centrifuged at maximum speed in a centrifuge for 5 minutes at room temperature. The supernatant was discarded and the pellet was suspended in 1 ml of phosphate buffered saline (PBS), pH 7.0. For inactivation, the bacteria were heated to 75°C for 15 minutes and then stored on ice until use.

5.2.6 Implant preparation

Beads were implanted with and without heat inactivated *S.aureus*. Poly-(lactic-co-glycolic acid) was coated on plain titanium discs by dissolving 50 mg of PLGA powder in 1 ml of acetone and small volumes ~ 10 µl of the dissolved PLGA was added drop-wise on a titanium disc kept on hot plate, set at temperature of 60°C until the volume of 1 ml was finished. Coated discs were dried at room temperature for overnight. Injectable chitosan suspensions were prepared by dissolving 50 mg of chitosan in 50 ml of 0.1% acetic acid.

Table 8: List of implants used in the study

Implant type	Dimensions	Company
Chitosan from shrimp shells		Sigma
Magnesium discs	5 mm diameter - 2 mm thickness	Institute of material science, Leibniz Universität, Hannover
Titanium discs	7 mm diameter - 1 mm thickness	TU Braunschweig, Germany
PLGA powder		Sigma Aldrich

PLGA microspheres	1 µm	Phosphorex, USA
Porous glass beads	Round – 4 mm , Pore size- 60 µm	VitraPOR
Polystyrene microspheres	1 µm	Phosphorex, USA
Poly-L-lactic acid beads	5 mm diameter	GoodFellow, England

5.2.7 Subcutaneous implantations in mice

C57BL/6 mice were housed under specific pathogen free conditions. Anesthesia was induced by the intraperitoneal injection of ketamine (10 mg/kg) and xylazine (4 mg/kg) in PBS in mice. The dorsal side of the mice was shaved using an electric shaver and wiped with tissue dipped in 70% ethanol to remove remains of hair after shaving. A small incision of 1 cm was made in the dorsal skin using micro dissecting scissors. A pouch under the skin was created for implants. Incisions were closed by interrupted suturing using polyglactin filaments Number 6-0 (Ethicon, Germany). For mock implantations involved the entire surgical procedure without any inserted implant material. For injectable biomaterials, 50 µl of suspension was injected using 1 ml syringe on the shaved back of the mice. All animal experiments were done in accordance with the regulations and with the approval from the local authorities Lower Saxony State Office for Consumer Protection and Food Safety (LAVES), permission number 33.42502/07-10.5.

Table 9 : List of mice used in the study

Genotype	Background	Reference
Wild type	C57BL/6	Harlan Laboratories
Wild type	Balb/c	Harlan Laboratories
IFN-β+/Δβ-luc	Balb/c - albino C57BL/6	[186]
Mx-2 Luc	C57BL/6	[180]

5.2.8 In vivo imaging of the oxidation potential using hydrocyanines

After anesthesia 30 µg of hydrocyanine solution was injected subcutaneously at the site of implantation. After 30 minutes, fluorescent imaging was done in the near infrared spectrum using an in vivo imaging system (IVIS200). The excitation wavelength of hydrocyanines was 750 nm and the emission wavelength was 840 nm. Acquired images were corrected for the background using image math tool of living image software. In order to correct for the background, a region of interest was selected from a mouse without implants after addition of the fluorophore. The background value was calculated and automatically subtracted from the images by the software.

5.2.9 Monitoring inflammatory protease activity

The protease activity dependent fluorescent sensor, Prosense 680 was used according to the manufacturer's recommendations. A dose of 2 nmol was injected intravenously into the mouse tail. Fluorescent imaging of the tissue with implants was done after a period of 30 minutes with an excitation and emission wavelength of 680 and 700 nm, respectively, using in vivo imaging system (IVIS 200). Similarly, the background of fluorescent images was subtracted using image math tool of living image software as described above.

5.2.10 Visualization of cell growth signaling

Lipase activity in the mouse tissue was monitored using ATX Red. 10 µg of ATX Red fluorophore was injected intravenously into the mouse tail. Whole animal imaging was done in the near infrared spectrum at an excitation and emission wavelength of 775 and 800 nm, respectively, 30 minutes after injection of ATX Red. Images were processed in the same way as explained above.

5.2.11 Isolation of bone marrow cells from Mx-2 luc mice

C57BL/6 mice that ubiquitously expressed luciferase from a Mx-2 luc construct were used for isolating the cells from the bone marrow [180]. Mice were euthanized by asphyxiation using CO_2 in a chamber. Hind legs (femur and tibia) were removed and were cleaned from adhering tissues. These bones were kept in a petri plate filled with ice cold RPMI medium supplemented with 1% Penicillin/Streptomycin and 1% Glutamine. The bones were soaked in 70% ethanol for 1 minute and then transferred to fresh ice-cold RPMI media with supplements. Using veterinary scissors, joints of the bones were cut off. Bone marrow was flushed using a 26G syringe with filled ice cold RPMI medium and collected in a 50 ml falcon tube. The collected bone marrow was centrifuged at 1500 rpm for 5 minutes. The supernatant was discarded and the pellet was suspended in erythrocyte lysis buffer; ACK lysis buffer (1ml per mouse) followed by an incubation at room temperature for 1.5 minutes to remove erythrocytes. 10 ml of RPMI medium was added to neutralize the ACK lysis buffer and was centrifuged again at 1500 rpm for 5 minutes. The supernatant was discarded and cells were suspended in 10 ml of fresh RPMI media. Cells were filtered through 100 µm mesh and were counted using an automated cell counter.

5.2.12 Purification of cell populations from isolated bone marrow cells

Neutrophils and monocytes were purified from bone marrow cells by MACS (Magnetic Activated Cell Sorting) using Neutrophil isolation kit mouse and Monocyte isolation kit mouse (Miltenyi Biotech, Germany) respectively using a QuadroMACS™ magnetic separator. After isolation, cells were treated with Fc blocking antibody for 20 minutes and then stained using anti-mouse Ly6G and anti-mouse Ly6C in FACS buffer (PBS + 2% fetal calf serum (FCS, Biovest, Germany)) for 30 minutes. Stained

cells were washed twice using PBS and were fixed following instructions of BD cytofix/cytoperm™ kit (BD Biosciences, Germany). Purified cell suspensions were acquired using BD LSR II flow cytometer (BD Biosciences, Germany) and analyzed using FlowJo software (TreeStar, Germany).

5.2.13 Monitoring luminescence per cell

Isolated neutrophils, monocytes and total bone marrow cells were cultured in 96 well plates in RPMI medium supplemented with 10% heat inactivated FCS, 1% Penicillin/Streptomycin, 1% Glutamine and mouse GM-CSF recombinant protein at concentration 5 ng/µl. The cell number of neutrophils, monocytes and total bone marrow cells per well was 10^3. 5 µl of heat inactivated *S.aureus* in PBS was added to the culture and as control 5 µl of PBS without bacteria was added to individual wells. To measure the luminescence of the cells, cultured neutrophils, monocytes and total bone marrow cells in 96 well plates were centrifuged at 1500 rpm for 5 minutes to settle down the suspended cells. The supernatant was carefully removed and discarded and 100 µl of luciferase firefly juice was added to the pellet and mixed. The luminosity was read in plate reader (Tristar^2, Berthold Technologies). To determine the cell number, cells were stained using 2 µM of Calcein AM (Life Science Technologies, Germany) in PBS added to centrifuged pellet of cells (as described above) and kept at 37°C for 30 minutes. Cells were washed gently using 100 µl of pre-warmed PBS and re-suspended in 100 µl of PBS. The relative fluorescence was measured in a plate reader at excitation and emission wavelength of 485nm and 535 nm.

5.2.14 Adoptive transfer of cells and imaging

Immediately after implantation, (~ 1 million) luciferase labelled cells were suspended in 150 µl of PBS and adoptively transferred through tail vein of C57BL/6 mice carrying implants. For in vivo visualization of the transferred cells, 150 µl of (30 mg/ml) luciferin was injected intraperitoneally. After 15 minutes, luminescent imaging was performed using an in vivo imaging system. Data were analyzed by Living image software® 4.3.1. To monitor the effect of type I interferon, in vivo imaging was performed of IFN-luciferase expressing mice before and after local injection of 1000 units of Interferon-β (IFN-β). Mouse IFN-β was recombinantly produced in stably expressing BHK-21 cells and was harvested from cell culture supernatant.

5.2.15 Histology

Mice were subcutaneously injected with 50 µl of PLGA and polystyrene microspheres of 1 µm in size and 50 µl of PBS. Mice were adoptively transferred with total bone marrow cells isolated from luciferase expressing mice and were sacrificed at day 2, day 5 and day 8. Tissue sections with local injection of microspheres and PBS were excised and transferred to tissue embedding cassettes. These tissue sections were fixed in 4% formaldehyde solution for not more than 48 hours and were then transferred to 70% ethanol solution. Histological slides of approx. 3 µm thickness were prepared from

formalin fixed, paraffin embedded tissue. The sections were stained with Hematoxylin/Eosin (H&E) staining according to standard laboratory procedures. After heat mediated antigen retrieval, immunohistochemistry was done. Tissue sections were treated with anti-Myeloperoxidase and anti-IBA-1. Anti-myeloperoxidase stains myeloperoxidase protein expressed by neutrophils. Anti-IBA-1 is ionized calcium binding adaptor molecule-1 expressed specifically by macrophages.

Table 10 : List of antibodies

Antibody	Company	Dilution
Anti-mouse Ly6G – V450	BD Biosciences	1:400
Anti-mouse Ly6C - APC	BD Biosciences	1:200
Fc blocking antibody	Group of Molecular Immunology - HZI	1:500
Anti-myeloperoxidase (rabbit polyclonal)	Thermo Scientific	1:200
Anti-IBA-1 (rabbit polyclonal)	Synaptic systems	1:800

5.2.16 Imaging interferon-β induction in transgenic reporter mice

Transgenic female BALB/c mice with a luciferase gene replacing IFN-β coding sequence on one allele were used for non-invasive in vivo imaging of the IFN-β induction [186]. 150 µl of (30 mg/ml) luciferin was injected intraperitoneally. After 15 minutes, luminescent imaging was performed using an in vivo imaging system (IVIS 200).

5.2.17 Imaging bacterial infection using a siderophore containing compound

Wild type *P.aeruginosa* (PA01) were streaked on LB agarose plates and incubated at 37°C overnight. Single colonies were picked and inoculated in LB media. Inoculated cultures were incubated on shakers at 180 rpm at 37°C until the optical density of the culture reached OD_{600} 0.1. IFN-β reporter mice were used to visualize the immune response to infection. The dorsal side of the mice was shaved and 5 µl of bacterial culture was injected subcutaneously. Siderophore containing compounds were synthesized in the Helmholtz Centre for Infection Research, Braunschweig by Dr. Haiyu Hu. After infection, the Cy5.5 conjugated siderophore compound (20 µg/kg of mouse body weight) and as a control Cy5.5 without siderophore were injected intravenously in mice through the tail vein. Fluorescent imaging was performed at excitation and emission wavelengths of 675 and 694 nm, respectively. For visualizing the immune response, 150 µl of (30 mg/kg) luciferin injected in the same mice after 5 hours of infection and bioluminescent imaging was performed. Mice were sacrificed and organs such as liver, spleen, kidneys, intestine and heart were extracted and fluorescent imaging was done at excitation and emission wavelengths of 675 and 694 nm, respectively. Fluorescent images

were processed by subtracting the autofluorescence of tissue using image math tool of Living image software.

5.2.18 Neutrophil culture

Neutrophil representing cells were isolated from bone marrow of luciferase expressing mice using MACS isolation kit and were sorted again using BD FACSAria™ III to separate side population of $Ly6C^{hi}$ monocytes and get pure neutrophils ($Ly6G^{+}/Ly6C^{int}$). 10^5 purified neutrophil cells were cultured in RPMI media with 10% heat inactivated FCS, 1% Penicillin/Streptomycin, 1% Glutamine and in presence and absence of growth factor mouse GM-CSF recombinant protein at concentration of 5 ng/µl in 96 well plates. Half of the media with or without GM-CSF was replaced every second day of culture. Luminosity from the cells was measured using plate reader. For live dead assays, pure neutrophils and contaminating $Ly6C^{hi}$ monocytes were cultured at cell density of 2×10^3 cells in each well of 96 well plates with or without 5 ng/µl of GM-CSF. Live dead staining was performed by following the instructions of the kit (Live dead viability cytotoxicity, Molecular Probes). Images were acquired using fluorescence confocal microscopy.

5.2.19 Phenotype of sorted and purified neutrophils in presence of GM-CSF

Purified neutrophil cell culture after sorting was analyzed by FACS as follows. Cells were incubated in 50 µl of trypsin for 3 minutes and then 100 µl of RPMI medium was added to neutralize trypsin. Cells were then transferred to fresh 96 well plates and centrifuged at 1500 rpm for 5 minutes. The supernatant was discarded and the cell pellet was suspended in Fc blocking antibody for 15 minutes. The plate was centrifuged and the supernatants were discarded. Cell pellets were suspended in a mix of Ly6G and Ly6C antibodies as described above and incubated for 30 minutes at 4°C. Cells were washed twice using PBS and then fixed using BD cytofix/cytoperm™ kit (BD Biosciences). Fixed cells were acquired using BD LSR II flow cytometer and analyzed using BD FACSDIVA software as described above.

6. Results

6.1 Fluorescent inflammation reporter molecules

6.1.1 Monitoring reactive oxygen species produced in response to inflammatory implants using a chemical sensor

To visualize the inflammatory potential of implants over the time, biocompatible and immune stimulatory materials were implanted subcutaneously in mice. During inflammatory conditions, neutrophils and macrophages are known to produce reactive oxygen products which can be detected after subcutaneous administration of hydrocyanines [45, 70]. Cyanine was reduced to hydrocyanine. This reduced dye becomes fluorescent after an oxidation reaction with oxygen radicals. To investigate this detection method, highly inflammatory porous glass beads loaded with heat-inactivated bacteria were used to stimulate the immune response. In vivo imaging revealed increases in fluorescence intensity during first two days (Fig. 8 A). The site with the bacteria appeared brighter fluorescent when compared to bare glass implants. These results showed that oxidation sensitive dyes could be used to differentiate inflammatory and biocompatible implants. However, the response to a sterile implant and surgical injury in absence of implants showed similar fluorescence intensities and could not be differentiated by this method (Fig. 8 B). The difference observed in the relative fluorescence intensities at the site of sterile and bacterial coated implants was around 1.5 fold (Fig. 8 B). This showed the low sensitivity of the detection system. Moreover, after systemic administration of hydrocyanine fluorescence was not detected at the site of inflammation or implantation. Instead, the signal was detected from the organs of the mouse, locations corresponding to liver and lungs (Fig. 8 C).

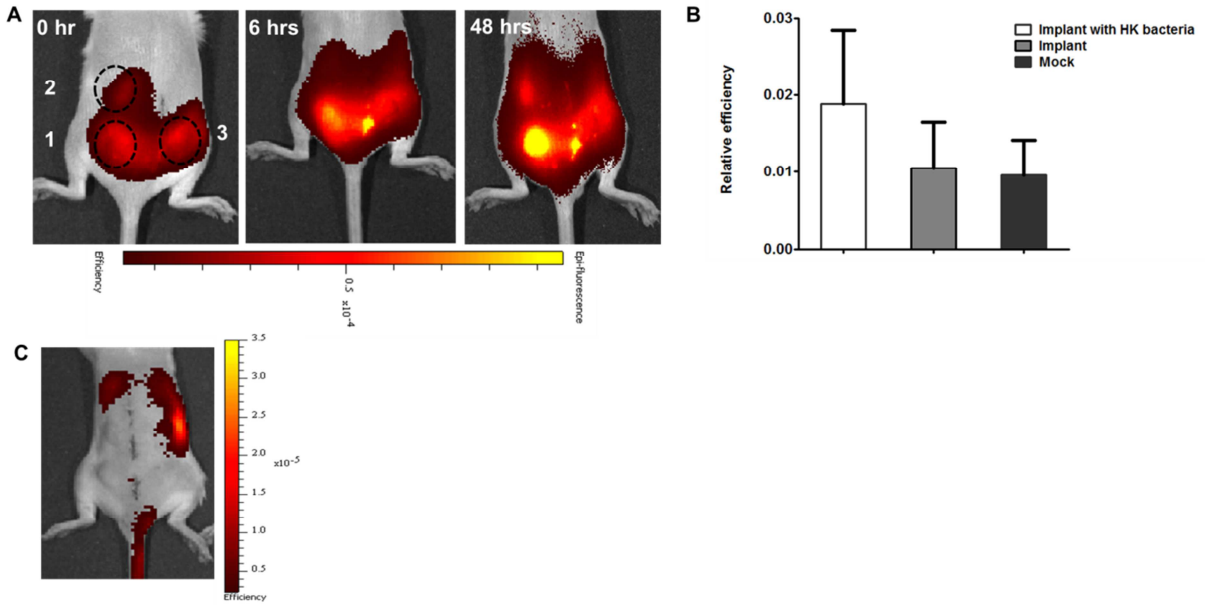

Figure 8: Enhanced oxidizing potential in response to inflammatory implants visualized by a fluorescent probe: Biocompatible glass implants and glass implants coated with inflammation-inducing heat inactivated *S.*

aureus were subcutaneously implanted into Balb/c mice. Hydrocyanine solutions were injected at the site of implantation as oxidation-sensitive dye precursor molecules. Fluorescence intensity was determined at 0 h, 6 h and 48 h after dye injection (A). The fluorescence efficiency was quantified at 24 hours and normalized to initial time point (B). The following implants were used: 1. Glass bead coated with inactivated bacteria; 2. Glass bead implant; 3. Surgery without implant. Dashed circles represent the site of implantation.

6.1.2 Visualization of inflammation specific proteases

Immune cells recruited during inflammation secrete some enzymes such as proteases which is essential to allow migration of cells through the tissue. To observe if cathepsin protease activity could be used to distinguish inflammatory from non-inflammatory implants, different implant materials were subcutaneously implanted in mice. A commercially available cathepsin-activatable fluorophore was injected intravenously in mice and whole body imaging was performed. The results showed an overall increase in fluorescence intensity with time (Fig. 9 A). The fluorescence appeared to be delocalized and could not be assigned to individual implants. Furthermore, opaque implants quenched even the background fluorescence. This phenomenon could be used to precisely localize the position of the implants (Fig. 9 A; implant 3 at 6 hours and 48 hours). At 48 hours, the implant with bacteria showed a brighter fluorescence compared to the biocompatible glass implants (Fig. 9 A; 48 hours). The relative fluorescence associated with implants (Fig. 9 A; implant 1, 2 and 6 at 48 hours) was calculated and small differences between implants with and without bacteria were observed (Fig. 9 B). However, the signal intensities from the implant and injury alone were similar, indicating that only highly inflammatory bacterial products could be differentially recognized by this approach (Fig. 9 B).

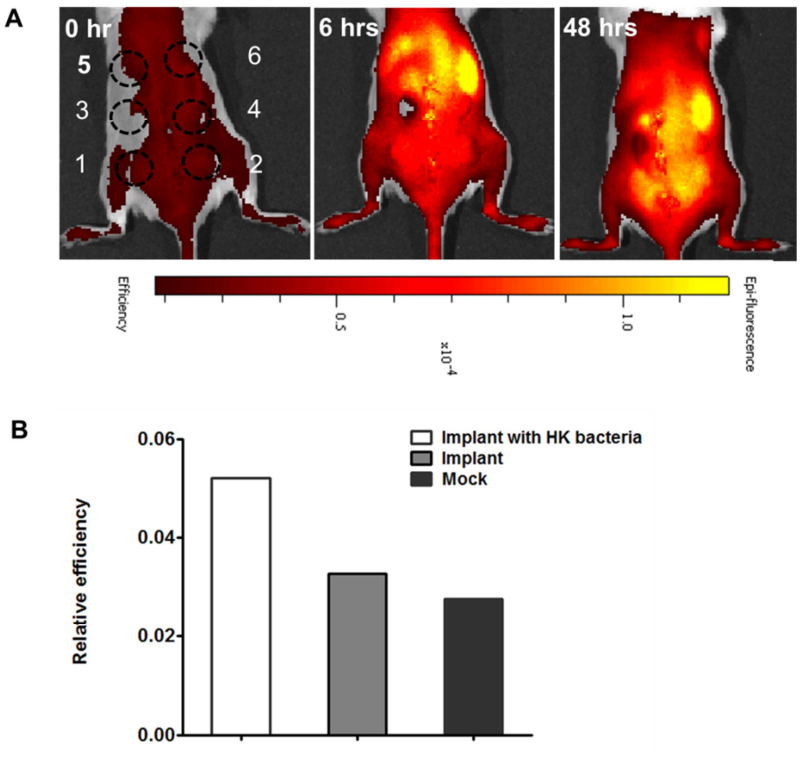

Figure 9: Delocalized protease activity in response to pro-inflammatory implants over the time period: Fluorescent images were taken at 0 hr, 6 hrs and 48 hrs (A). Relative fluorescence intensity related to implant 1, 2 and 6 was calculated at 48 hrs (B). The format of implantation was following- 1. Porous glass implant soaked in dead bacteria 2. Porous glass implants 3. Magnesium 4. Poly-L-lactic acid 5. Heat killed bacteria & 6. Surgery without implantation. Dashed circles represent the site of implantation. Fluorescence was quantified after 48 hours and normalized to values of 0 hr to calculate relative fluorescence efficiency (B).

6.1.3 Monitoring inflammatory cell growth signals

Injury stimulates cell growth and tissue repair processes [114]. Cell growth, survival and migration can be stimulated by lipase signaling [187]. Autotaxin is an inflammation specific lipase that activates a lipid mediator essential for cell motility and growth signaling, it has been shown to be produced in lung inflammation [179, 187]. ATX Red is a near infra-red fluorescent precursor molecule and analogue of the substrate for autotaxin lipase. This enzyme substrate reaction generates a fluorescent product that can be detected by in vivo imaging. Various biocompatible and inflammatory implant materials were implanted in mice to evaluate this method. After implantation, mice were injected intravenously with ATX red (Fig. 10; 0 hour). To monitor the basal levels of autotaxin, one mouse without implants was included (Fig. 10). Enhanced signals were observed from the implants with bacteria as compared to biocompatible glass implant (Fig. 10; implant 2, 48 hours). A signal peak was obtained 48 hours after the dye injection at a site where there was no implant and which may correspond to the location of the spleen (Fig. 10, 48 hours, yellow spot on the left side of each animal). However, the autotaxin activity appeared to be delocalized and there was a high background signal, making it difficult to determine the response to individual implants. Quenching of the fluorescence signal was also observed at the site of opaque implants (Fig. 10; implant 4, 6 and 48 hours).

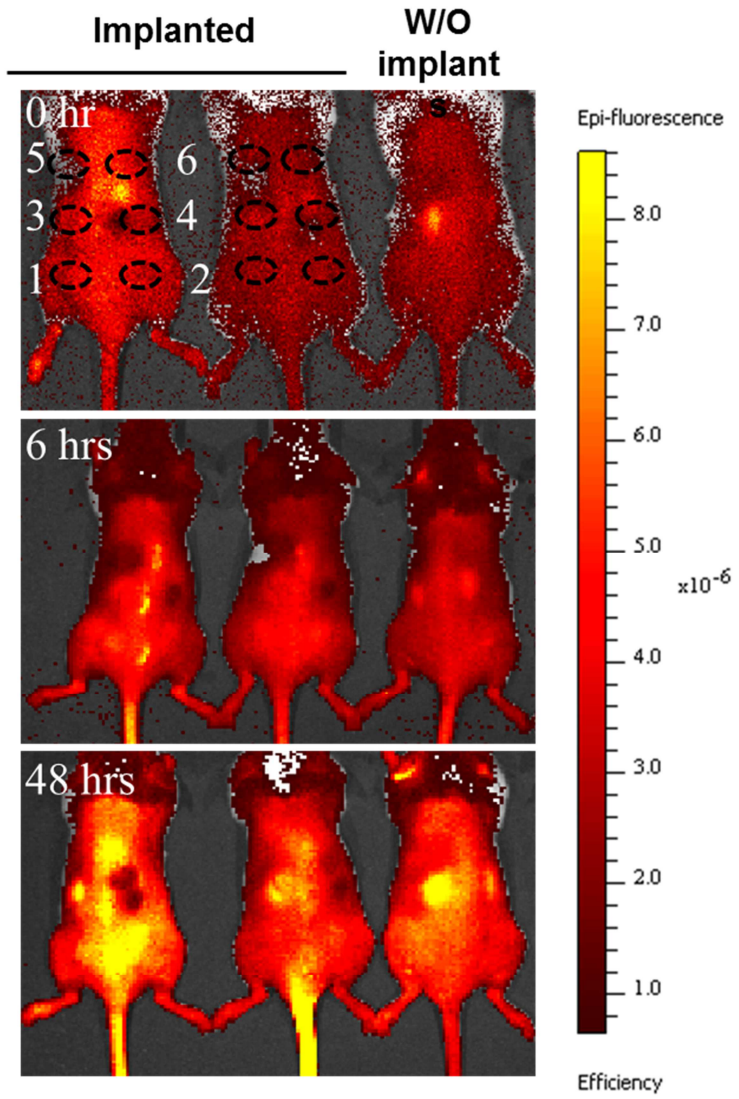

Figure 10: Imaging of increased but delocalized inflammatory cell proliferation signals: Mice were implanted with various inflammatory and non-inflammatory materials. ATX-red was applied and fluorescent images of the following time points: 0hr, 6hrs and 48hrs. The first two mice from the left were with implants and the third mouse is without implants and surgery. Implants were as follows: 1. Porous glass implant 2. Porous glass implant with dead bacteria 3. Poly-L-lactic acid 4. Magnesium 5. Mock and 6. Titanium. Dashed circles represent the site of implantation.

6.2 Imaging implant induced inflammation using bioluminescent immune cells

6.2.1 Purified luminescent labelled cells could be visualized and quantified after local injection *in vivo*

To evaluate the inflammatory potential of implant materials, luciferase labelled immune cells were employed. These cells were isolated from mice with substantial ubiquitous luciferase expression under

the influence of Mx-2 promoter sequences. Neutrophils and monocytes were purified from the bone marrow of luciferase expressing mice and were analyzed using Ly6G and Ly6C surface markers which are known to differentiate neutrophils from monocytes [188-190]. Approximately 85% population was positive for both markers (Ly6G and Ly6C) representing neutrophil population and 14% of the side population were $Ly6G^{-}$ and $Ly6C^{hi}$ (Ly6C high) monocytes (Fig. 11 A). Similarly, isolated monocytes were Ly6C positive cells (~ 91%) with minimal double positive cells (Fig. 11 B).

To visualize the luminescence of cells *in vivo*, same number of total bone marrow cells and purified neutrophils and monocytes were locally injected in the mice with or without heat inactivated bacteria. Luminescence of neutrophils, monocytes and total bone marrow cells was detectable at 0 hour. The signals of total bone marrow cells, neutrophils and monocytes gradually increased and peaked on day 1. Increase in luminosity of cells was irrespective of presence or absence of bacteria. Therefore, this temporal increase of luminescence might be due to cell proliferation (Fig. 11 C). The radiance from the monocytes in presence or absence of heat inactivated bacteria was higher than neutrophils or total bone marrow cells till day 2 (Fig. 11 D & E). Moreover, a 5-fold difference was observed in the luminosity of the monocytes in the presence versus absence of dead bacteria on day 2 reflecting the effect of bacterial extract on Mx-2 promoter dependent luciferase activity (Fig. 11 D & E). These results indicated that basal luminescence of monocytes was higher than neutrophils or total bone marrow cells. Moreover, the luminescence of monocytes was enhanced in presence of bacteria which could be due to induced promoter.

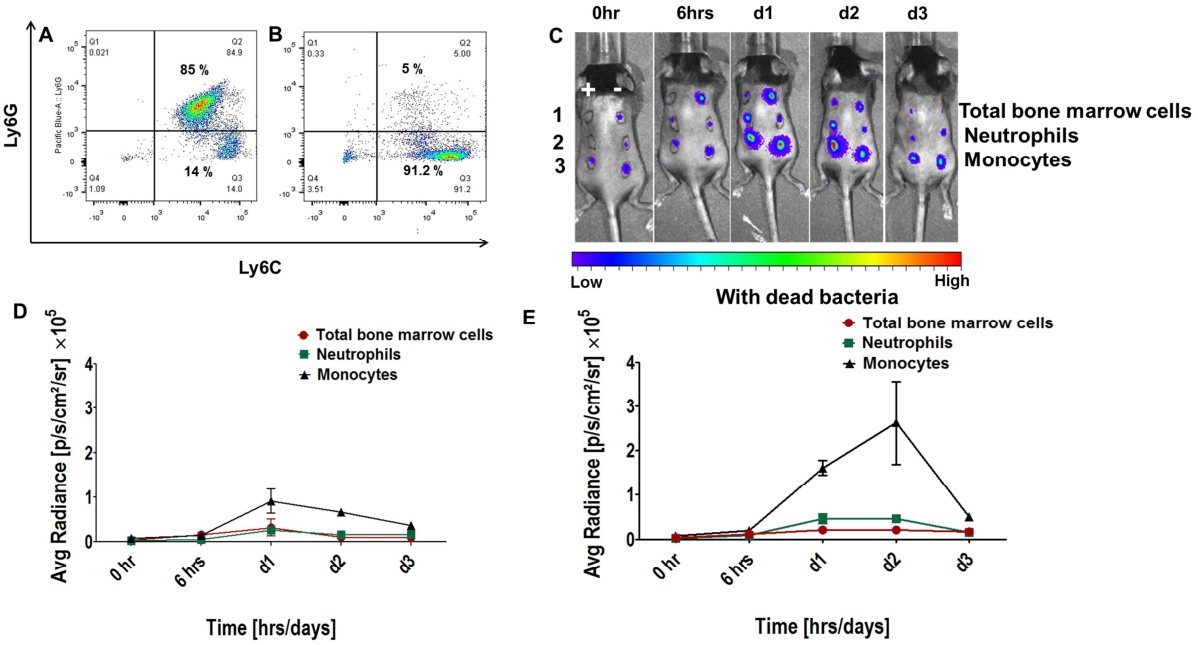

Figure 11: Luminescence quantification from the locally injected inflammatory cells in vivo: Neutrophils (A) and monocytes (B) were purified from the bone marrow of luciferase expressing mice using MACS purification kit. Purified cell populations were stained for Ly6G and Ly6C surface marker and analyzed using

FACS (A & B). Heat inactivated bacterial suspension were subcutaneously injected in the mice. Then, an equal number (10^5 cells) of total bone marrow cells, neutrophils and monocytes were added locally at the site of bacterial infection in the mice and bioluminescent imaging was performed by injecting luciferin substrate (C). The numbers indicate: 1. Total bone marrow cells 2. Neutrophils 3. Monocytes (C). '+' reflects the presence of heat inactivated *S.aureus* and '–' indicates its absence (C). The average radiance values were calculated for bone marrow cells, neutrophils and monocytes in the absence and presence of heat inactivated bacteria (D and E).

6.2.2 Luminescence of single cells

To determine relation between luminescence and cell proliferation, an in vitro experiment was set up in which the neutrophils and monocytes were isolated from the total bone marrow cells of luciferase expressing mice and cultured with or without heat inactivated bacteria. The luminosity of the luciferase labelled immune cells was read using a plate reader and represented as relative luminescence units (RLU). To determine the cell viability and proliferation, cultured cells were stained with a cell permeant calcein stain and fluorescence of the dye was read as relative fluorescence units (RFU) in a plate reader. In this case, manual counting of cell number was difficult because the culture contained both adherent cells and cells in suspension. So, the cells can be lost during handling. Moreover, calcein is known to be more sensitive than trypan blue exclusion. The fluorescent dye stains live cells by reacting to intracellular esterases while dead cells lack active esterases. The background of the calcein is very low because it must interact with esterases of live cells to become fluorescent. Therefore, the fluorescence intensity is directly proportional to cell number.

The total bone marrow cells showed similar luminescence intensity (RLU) when cultured with or without dead bacteria indicating minimum effect of bacterial components on Mx-2 promoter dependent luciferase expression (Fig. 12 A). However, the viability of cultured bone marrow cells was checked using a cell permeant fluorescent dye and a small increase in fluorescence intensity (RFU) of total bone marrow cells in presence or absence of dead bacteria was observed which could be due to increase in cell number (Fig. 12 A). Neutrophils cultured with or without dead bacteria showed almost identical changes in luminosity and fluorescence intensity when compared to total bone marrow cells (Fig. 12 A & B).

In contrast, monocytes were found to be 4-fold higher luminescent than neutrophils and total bone marrow cells at 6 hours. However, the fluorescence intensity of the monocytes at the initial time point (6 hours) was comparable to neutrophils and total bone marrow cells which were in accordance with the equal number of cells in the inoculum. This showed that monocytes had higher basal luciferase expression than neutrophils and total bone marrow cells (Fig. 12 C). In addition, the differential promoter activity of monocytes could be seen after 24 hours where luminosity of monocytes was higher in presence than in absence of dead bacteria (Fig. 12 C; RLU). Moreover, the fluorescence

intensity of monocytes was increasing after 24 hours of culture that indicated rapid proliferation of monocytes (Fig. 12 C; RFU). Interestingly, on comparing fluorescence intensity of monocytes in presence versus absence of bacteria after 48 hours and 72 hours, it was observed that number of monocytes decreased in presence of dead bacteria. This could be due to apoptosis of monocytes after phagocytosis of bacterial components. Such process is known as phagocytosis induced cell death (PICD) [191] (Fig. 12 C; RFU). However, the luminosity of monocytes in presence of dead bacteria after 48 and 72 hours was comparable to the luminescence in absence of bacteria that could be due to induction of promoter by bacterial components (Fig. 12 C; RLU).

These results suggested that monocytes were highly luminescent when compared to neutrophils or total bone marrow cells and the increase in cell number of monocytes *in vitro* was in agreement with *in vivo* studies (Fig. 12 C & 11 D). So far, we assumed that monocytes could be an optimal cell population for distinguishing inflammatory responses to implant materials due to observed higher basal luciferase activity than total bone marrow cells and neutrophils, differential promoter activity in presence of stimulus and rapid proliferation when compared to total bone marrow cells and neutrophils.

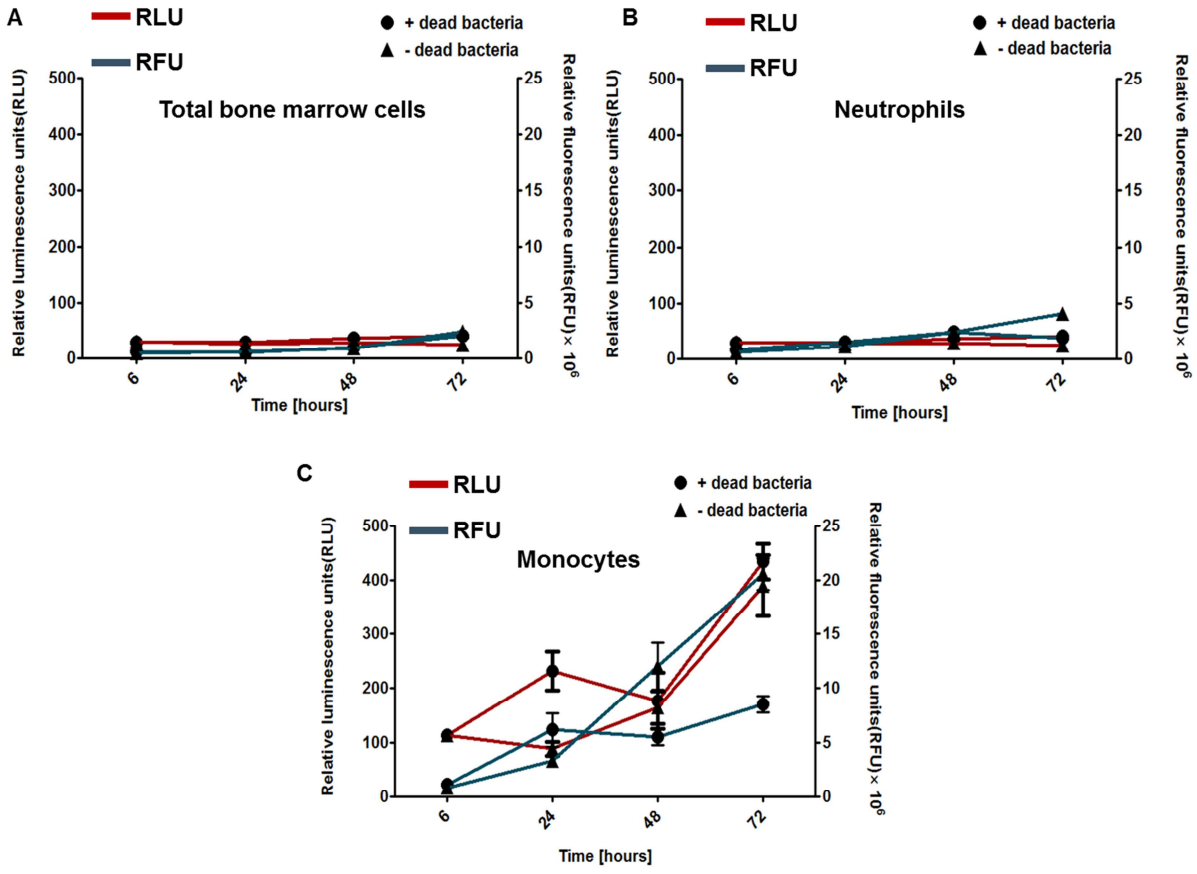

Figure 12: Luminescence per cell in inflammatory or non-inflammatory conditions: Luminescent labelled total bone marrow cells (A), neutrophils ($Ly6G^{+}/Ly6C^{int}$) (B) and monocytes ($Ly6G^{-}/Ly6C^{hi}$) (C) isolated from

bone marrow of luciferase expressing mice were cultured separately. Heat inactivated bacterial suspensions were added to the cell cultures. Luminosity was measured after adding luciferin to the cells and relative luminescence units (RLU) were calculated in a plate reader. For quantification of live cells, cells were stained using the fluorescent dye for live cells and the fluorescence (RFU) was measured in plate reader with excitation and emission filter of 485 nm and 535 nm, respectively.

6.2.3 The ability of neutrophils to accumulate at the site of inflammation is rapidly lost

There were two aims of this experiment, one was to find out the distribution of intravenously transferred cells in the mouse and second was to observe migration of cells in case of delayed or no inflammation. To achieve the goal, we needed a constant cell number throughout the experimental study. Therefore, neutrophils were used due to their non-dividing ability. Firstly, to determine distribution of intravenously injected cells, implants were inserted and neutrophils were adoptively transferred. Mice were sacrificed and bioluminescent imaging of organs was performed. After 6 hours of adoptive transfer, higher luminescence was observed in the spleen which was diminished at later time points indicating a probable role of spleen for homing of neutrophils (Fig. 13 A).

Secondly, to visualize the inflammation specific cell migration, neutrophils were adoptively transferred in the mice and inflammation by implantation procedure was stimulated at later time points post adoptive transfer of cells (Fig. 13 B). The luminosity decreased gradually in the case of delayed implantations or injury. The average radiance from the inflammation site progressively decreased with the increased delay in inducing an inflammatory insult and no signal was observed in absence of inflammation on day 5 (Fig. 13 B). This indicated that the ability of neutrophils to reach to the site of inflammation was lost after 24 hours. Therefore, adoptive transfer of the cells and insertion of implants must be at the same time. Secondly, if there is no inflammation, transferred neutrophils disappeared from the circulation after 24 hours. There could be two possibilities, either neutrophils were undergoing apoptosis in absence of inflammation or cells were present but were unable to reach the inflammation site.

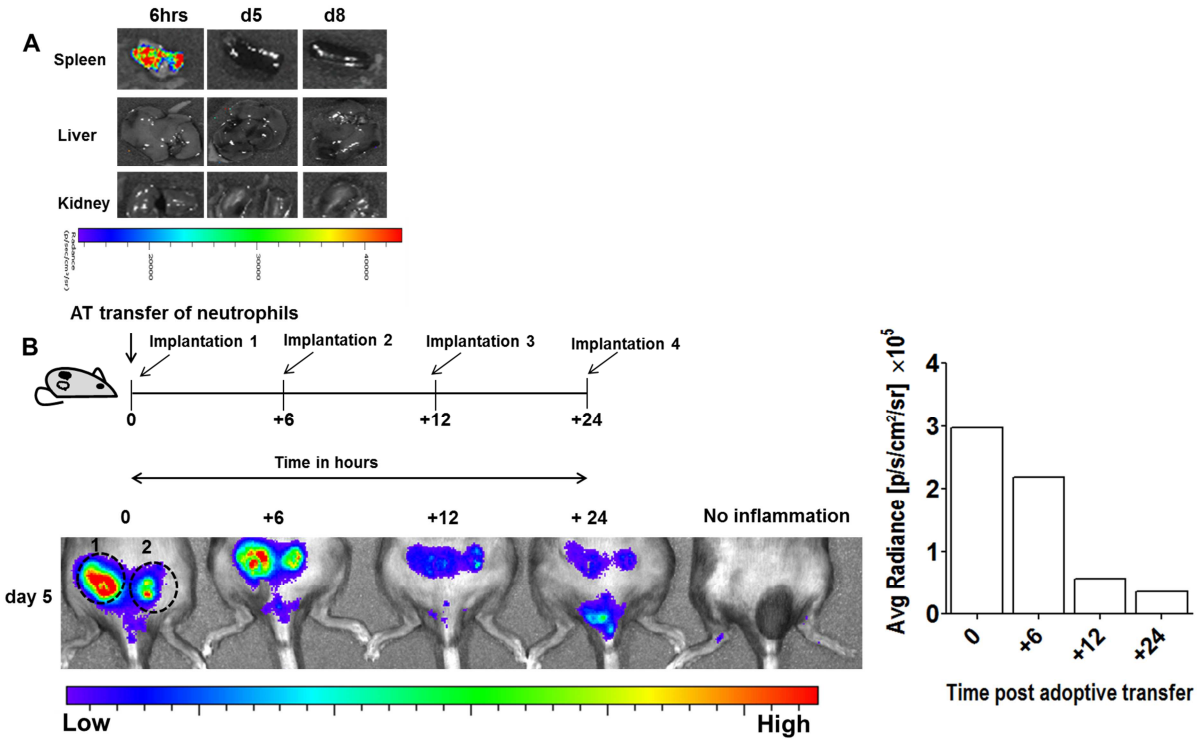

Figure 13 : One day time window for adoptively transferred neutrophils to migrate to the site of inflammation. Bioluminescent imaging of spleen, liver and kidney of the mouse with inflammation and adoptively transferred neutrophils (A). Mice were implanted 0, 6 hrs, 12 hrs and 24 hrs post adoptive transfer of purified neutrophils from bone marrow of luciferase expressing mice. Bioluminescent image at day 5 was produced and quantified. The implants are as follows: 1. Porous glass bead 2. Incision injury without implant. The dashed circle represents the site of implants (B).

6.2.4 Effect of IFN-β on the luminescence of neutrophils

Neutrophils are considered to be non-dividing cells; therefore the luminosity of cells could not depend upon the cell number. We needed a constant cell number to visualize signals only in response to the induced promoter. Interferon-β (IFN-β) is a potent inducer of Mx-2 promoter activity [180]. The recombinant Mx-2 promoter-luciferase construct has detectable activity even in the absence of interferon-β. To quantify the effect of IFN-β on Mx-2 promoter dependent luciferase expression neutrophils were isolated from the bone marrow of mice with expression of luciferase under the influence of Mx-2 promoter and were adoptively transferred in mice with implants. Interferon-β was locally injected on the top of implant and imaging was done before and after 6 hours of treatment each day (Fig. 14 A). The luminescence before and post IFN-β addition was found to be almost identical up to 6 days (Fig. 14 B). Local additions of IFN-β did not improve the luminescence of the neutrophils at the inflammation site suggesting the saturation of promoter activity due to endogenously produced IFN-β in response to sterile injury. Injury associated with implantation procedure involves necrotic cell death. These cell remnants can be internalized by macrophages and transferred to lysosomes. In

absence of DNase II alpha in lysosomes, DNA is not degraded and can stimulate the production of type I interferons through STING signaling [192]. Therefore, the basal promoter activity appeared to be very high with a minimal influence of IFN-β on the luminosity of neutrophils.

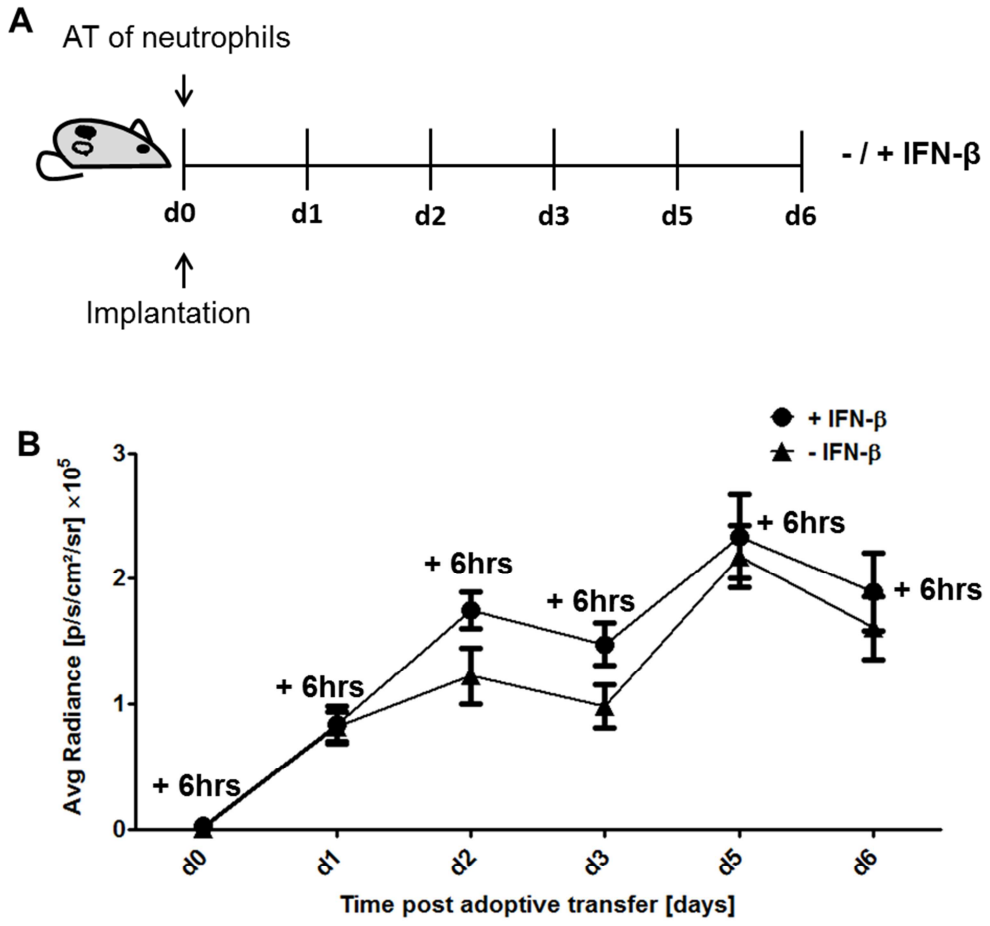

Figure 14: Minor effects of local additions of IFN-β on the luminescence of adoptively transferred neutrophils: Neutrophils were isolated from the bone marrow of luciferase expressing mice and adoptively transferred into mice with porous glass bead implants. Imaging was performed before treatment and after 6 hrs post injection of IFN-β each day (A). The luminosity was quantified before and post 6 hours of subcutaneous application of IFN-β each day, starting from d0 (B).

6.2.5 Sensitive detection of labelled bone marrow cells accumulated at the site of implantation and unexpected longevity of neutrophil population

The aim of present work was to visualize labelled immune cells at the site of implantation after intravenous adoptive transfers. To this end, inflammatory and non-inflammatory materials were implanted and purified labelled total bone marrow cells, neutrophils and monocytes were adoptively transferred. Total bone marrow cells, neutrophils and monocytes could be detected at the site of inflammation 24 hours post adoptive transfer (Fig. 15 A, B & C). The brightness increased at the site

of inflammatory implant surface 3 days after adoptive transfer of total bone marrow cells and neutrophils (Fig. 15 A & B; d3). The signal intensity of total bone marrow cells and neutrophils reached their maximum on day 5 and then a gradual decrease was observed and eventually signal disappeared after 19 days (Fig. 15 A & B). However, neutrophils are short living cells with half-life of few hours in circulation but surprisingly; we observed their prolonged survival in tissue which was unexpected. For monocytes, the luminescence at site of implants remained constant after day 2 and the signal intensity was not different for implant with or without dead bacteria (Fig. 15 C). Although, luminosity of monocytes could be distinguished at the incision site between the two implants on day 2 which might be due to inappropriate closure of wound (Fig. 15 C). The luminescence of monocytes disappeared after 9 days of adoptive transfer which is much earlier than total bone marrow cells and neutrophils (Fig. 15 C).

Results from this experiment indicated that bioluminescent labelled immune cells were detectable at the inflammation site and signals were localized to the site of implants or injury. As a part of side finding, we also observed prolonged neutrophil survival in tissue which was unexpected due to their short half-life in circulation.

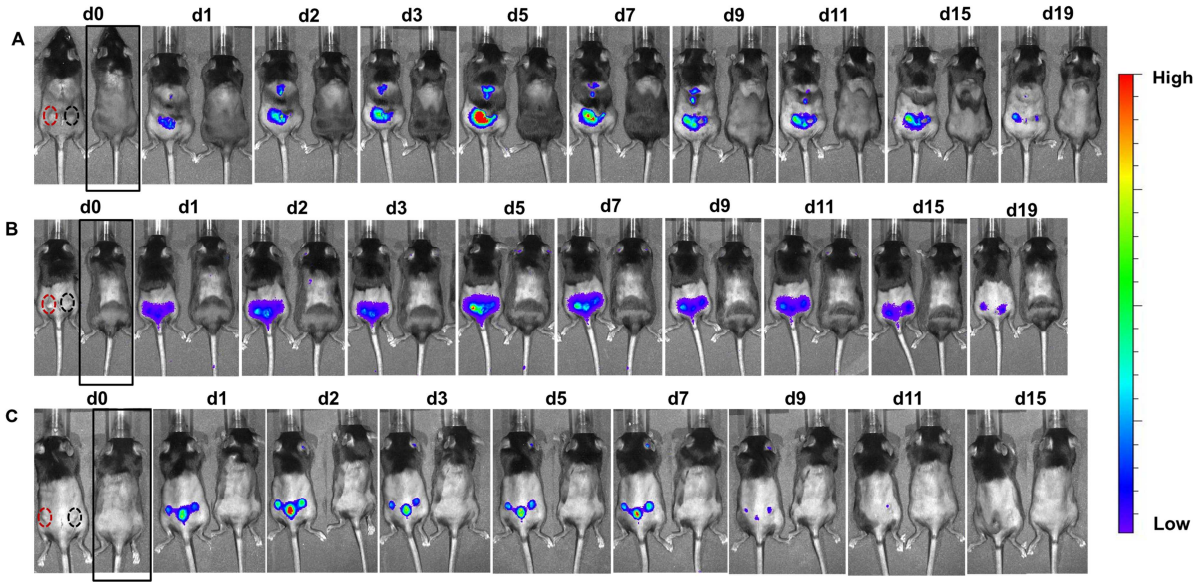

Figure 15: Detectable and localized signals from labelled immune cells accumulated at the site of implantation: Mice were implanted with porous glass beads subcutaneously with or without heat inactivated bacteria. Dashed circles in red represent the site of implant with heat inactivated bacteria and black colored circles represent the site of sterile implant. The same number of total bone marrow cells (A), neutrophils (B) and monocytes (C), isolated from the bone marrow of luciferase expressing mice, were adoptively transferred in the mice with the implantations. Bioluminescent imaging was performed by injecting luciferin substrate in an IVIS 200 imager. Black boxed mice indicate the control animals with transferred cells but without implantations.

6.2.6 Bioluminescent bone marrow cells could differentiate infected and sterile implants

To identify optimal cell population for evaluation of inflammatory responses to implant materials, the luminescence of neutrophils, monocytes and total bone marrow cells accumulated at the site of inflammation was quantified and intensity was compared. Signals were localized because of which quantification was possible. On day 1 post adoptive transfer of labelled immune cells, total bone marrow cells, neutrophils and monocytes could be detected at the site of implantation but luminescence of cells were close to background (Fig. 16 A, B & C). Moreover, the luminosity of total bone marrow cells, neutrophils and monocytes increased at the site of implants after 2 days of adoptive transfer (Fig. 16 A, B & C). There were differences in the signal intensities from the site of infected implant and sterile implant in case of each cell type (Fig. 16 A, B & C). However, this difference was highest ~ 3.5 fold in mice transferred with total bone marrow cells on day 5 which becomes lesser at later time points (Fig. 16 A). This means that transferred total bone marrow cells showed clear difference between infected and sterile implants which was restricted to one time point. In contrast, infected implants could not be differentiated from sterile implants using neutrophils and monocytes due to small differences in signal intensity (Fig. 16 B & C). However, the luminescence of total bone marrow cells, neutrophils and monocytes recruited at the site of sterile implant appeared similar (Fig. 16 A, B & C).

Results revealed that total bone marrow cells recruited at the inflammation site were able to distinguish the infected and sterile implant materials. Bioluminescent bone marrow cells were found to be optimal cells that can be used to screen the biocompatibility of different implant materials. This method fulfilled our all expectations. Signals were localized and clearly detectable. Moreover, the difference between inflammatory or non-inflammatory implant materials could be clearly observed.

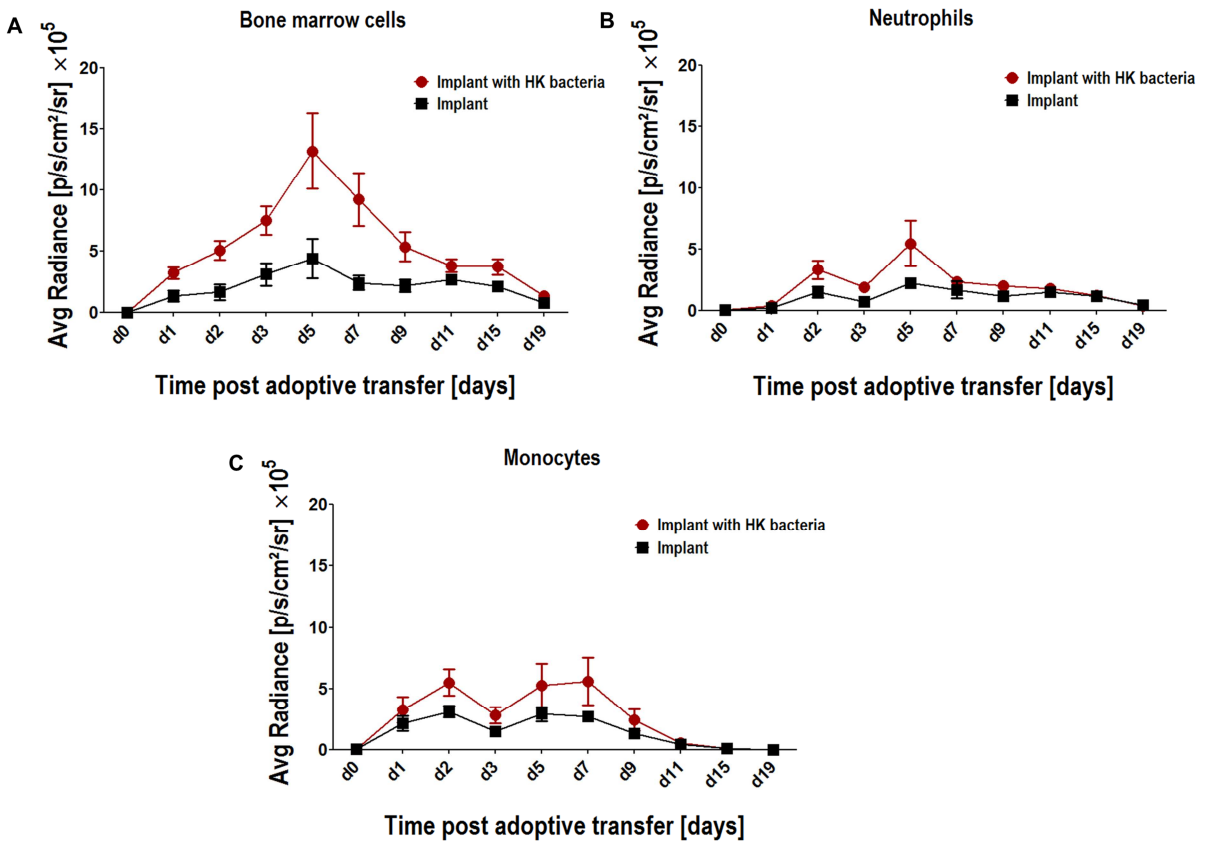

Figure 16 : Differential signal intensities at the site of infected and sterile implants: Total bone marrow cells (A), neutrophils (B) and monocytes (C) isolated from luciferase expressing mice were adoptively transferred through tail vein to the mice (n=5) carrying implantations of glass beads with or without heat killed (HK) bacteria. Images were acquired using IVIS 200 and quantified to show the luminosity appearing at the site of implantations.

6.2.7 Differential response to surgical injury and injection associated injury

Injury due to surgery induces inflammation even in the absence of implants [114]. To evaluate the tissue reaction in response to injury, luciferase labelled total bone marrow cells were adoptively transferred to the mice with injury but without implants. As a control, PBS was subcutaneously injected without surgical wounds in mice and the radiance values were compared to the injury due to incision (Fig. 17). Signal intensity at the site of buffer injection was close to the basal values and larger relative difference was observed from injury (Fig. 17). This assay showed that implantation associated injury was a potent stimulant of inflammation and bone marrow cells were accumulated at the inflammation site. The luminosity at the site of surgical incision was similar when compared to sterile implants which indicated that signals from sterile implants were due to injury and not due to implant (Fig. 17 & 16 A).

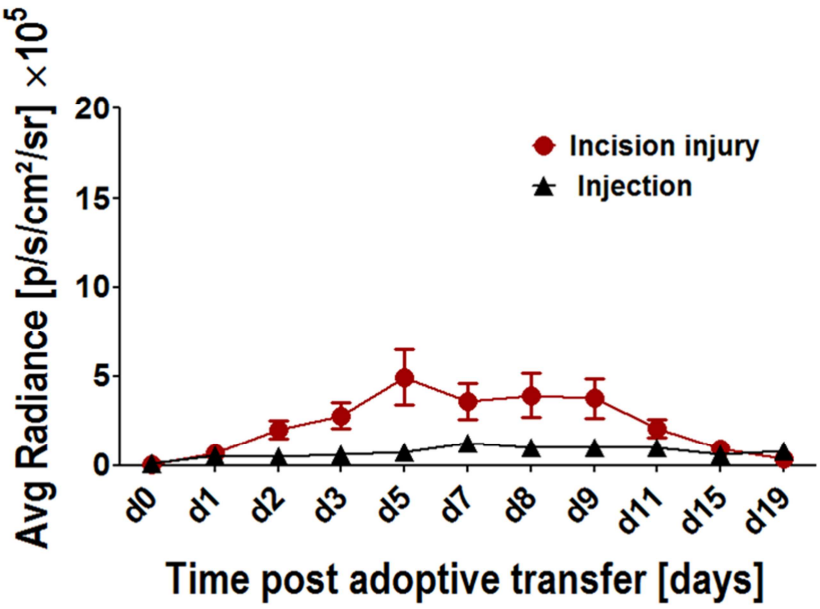

Figure 17: Inflammatory insults induced luminescence signal from adoptively transferred cells: Total bone marrow cells were adoptively transferred in two groups of mice, one group was treated with surgical injury (n=4) and other group of mice was treated with subcutaneous saline buffer injections (n=4). Bioluminescent imaging was done and images were quantified using Living image software.

6.2.8 Differentiating inflammatory potential of implant materials using bioluminescent immune cells

To rank inflammatory potential of clinically established materials, several implant materials were tested. Implant of biodegradable polymer, poly-lactic-co-glycolic acid (PLGA) was chosen as an inflammatory material because of production of acidic degradation products that induces immune response [193]. Titanium (Ti) and magnesium (Mg) discs were used as biocompatible controls. Inflammatory and biocompatible implants were implanted in mice and luciferase labelled total bone marrow cells were adoptively transferred in mice with implants. Luminescence of total bone marrow cells was detectable at the site of implantation on day 1 (Fig. 18 A). Amongst the three biomaterials used for testing, luminescence at the site of implanted PLGA discs increased gradually with a peak on day 3, day 4 and day 5 (Fig. 18 A; implant 1). In contrast, the signals were comparatively weaker at the site of titanium and magnesium implants (Fig. 18 A; implant 2 & 3). After quantification, signals from PLGA implant were significantly higher when compared to titanium and magnesium implants after 3 days of adoptive transfer (Fig. 18 B). A weak signal was observed at the site of magnesium implants on day 4 which could be injury related (Fig. 18 A; implant 3).

We observed localized inflammatory response to PLGA implants. Moreover, the signal was clearly detectable above background due to bioluminescent imaging. In addition, inflammatory materials were

clearly differentiated from known biocompatible implants. This indicated that the system was sensitive and could reliably distinguish inflammatory potential of implant materials.

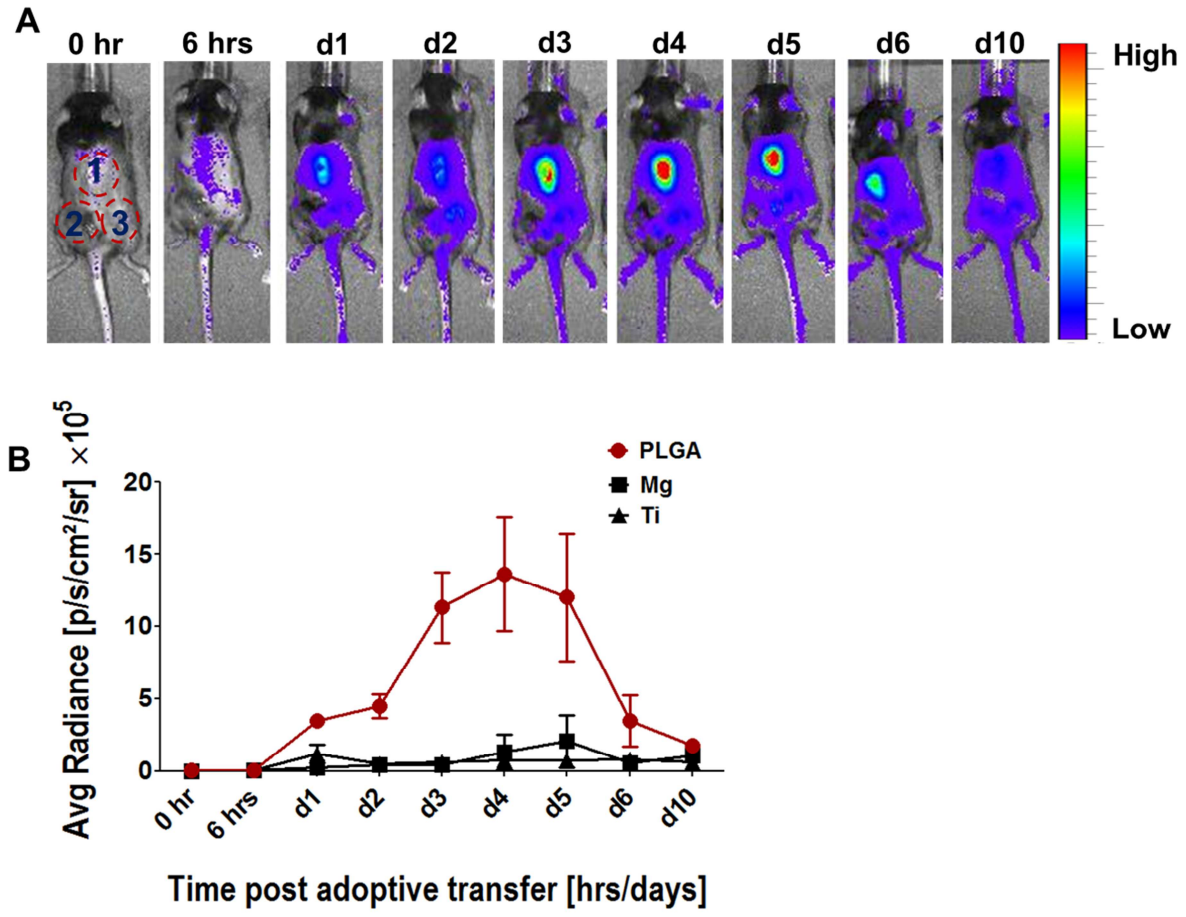

Figure 18: Ranking inflammatory potential of different biomaterials: PLGA material coated on titanium implant, plain titanium and magnesium implants were implanted in mice and luminescent bone marrow cells were transferred through tail vein. Bioluminescent images were produced using IVIS 200 (A) and quantified (B). The following implants were used: 1. PLGA coated titanium (7mm diameter and 0.1 mm thickness) 2. Titanium (Ti) (7mm diameter and 0.1 mm thickness) 3. Magnesium (Mg) (3mm diameter and 2 mm thickness). The dashed circles in red represent the site of implants.

6.2.9 Separating material induced inflammation from injury

Injury and material interactions both contribute to the resulting implant induced inflammation [70]. However, injections induce minimum tissue injury. Therefore, to separate the response to surgical insults from material induced inflammation, injectable biomaterials were used. Microspheres are the ideal injectable materials used for diagnostics or drug delivery purposes [194]. In this case, two types but similar sizes (1 μm) of microspheres were used, one of them was PLGA which is known to be biodegradable with the production of acidic by products and the other type was polystyrene, a non-degradable polymer that has the property to stay in the recipient for longer times. Polystyrene and

PLGA micro particles have already been characterized as inflammatory in animal test models [45, 47, 54]. Chitosan, one of the naturally occurring polysaccharides which have its application in wound dressing and drug delivery was another type of injectable material used [195, 196].

All the materials were applied subcutaneously in mice and luciferases expressing total bone marrow cells were adoptively transferred. Transferred immune cells were detectable at the site of implants 2 days after adoptive transfer (Fig. 19 A). Radiance of cells at the site of saline buffer injections was close to background which indicated minimum injury due to injection (Fig. 19 A; implant 2). Signals increased gradually in response to all implant materials (Fig. 19 A). The luminosity of cells recruited at the injection site of PLGA microspheres increased till day 5 and then disappeared which could be either due to resolution of material induced inflammation or resorption of the implant (Fig. 19 A; implant 3). Immune cells accumulated at site of chitosan injection showed saturated signals from day 3 till day 8 which then decreased afterwards (Fig. 19 A & B; implant 1). Luminescence of cells at the site of polystyrene implants was increasing gradually and peaked on day 5 with a gradual decrease with time (Fig. 19 A; implant 2). However, luminescence at the site of polystyrene implants persisted for more than 13 days when compared to PLGA and chitosan implants which indicated chronicity of the inflammatory response due to its non-degradable behavior (Fig. 19 A; implant 2). On comparing signal intensities, signal from location of polystyrene was significantly higher than from chitosan and PLGA implants on day 5 and day 6 post adoptive transfers of cells (Fig. 19 B).

This showed the uppermost inflammatory potential of polystyrene implants when compared to chitosan and PLGA implants as expected. Therefore, we were able to detect and quantify material induced inflammation by using injectable materials. The model could detect localized inflammation in response to materials and eventually could rank the inflammatory potential of implant materials.

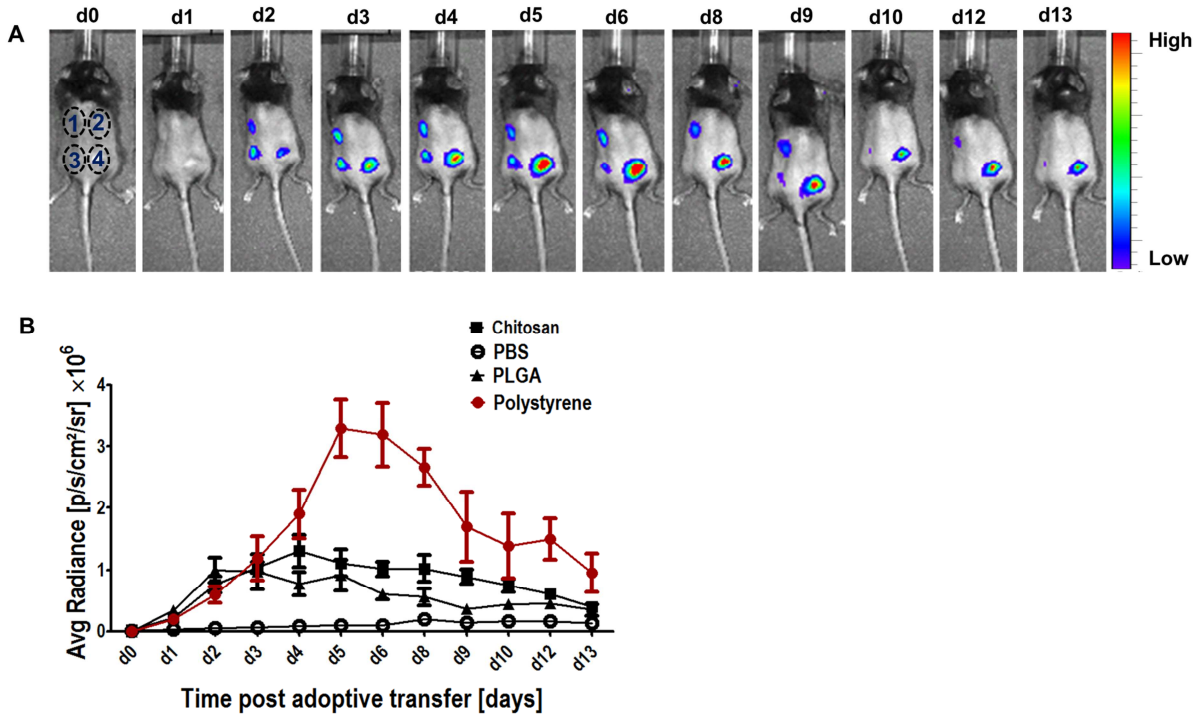

Figure 19: Higher luminescence induced by polystyrene microspheres compared to degradable implants: To eliminate injury from the inflammation model, injectable biomaterials were employed. PLGA and polystyrene microspheres of 1 µm and chitosan in 0.1% acetic acid were injected locally in the mice as indicated. Luminescent bone marrow cells were adoptively transferred and the extent of inflammatory potential of each biomaterial was monitored using IVIS200 (A) and quantified using Living Image software (B) 1. Chitosan 2. PBS 3. PLGA microspheres (1µm) 4. Polystyrene microspheres (1µm). The dashed black circles represent the site of injection.

6.2.10 Validation of the inflammatory reactions to the materials

To confirm results from in vivo imaging of luminescent immune cells, histological examination was done. Mice were injected with PLGA microspheres, polystyrene microspheres and PBS subcutaneously and total bone marrow cells were transferred. Skin sections were excised after sacrificing the mice. The mouse skin tissue sections were evaluated using hematoxylin and eosin, anti-IBA-1 and anti-myeloperoxidase. Hematoxylin and eosin stains nucleus and cytoplasm of the cells, thereby representing cells infiltrated in the tissue. On the other hand, IBA-1 is calcium binding protein-1 that is expressed specifically in macrophages [197]. We also checked myeloperoxidase activity in response to implants. Myeloperoxidase is an enzyme which is most abundantly expressed in neutrophil azurophilic granules.

Saline buffer treated tissue did not reveal infiltration of inflammatory cells. However, the brown staining in muscular layer and epidermis of PBS treated tissue appears to be background associated with anti-IBA-1 and anti-myeloperoxidase staining (Fig. 20 A). The implantation of PLGA and

polystyrene implants caused extravasation of lymphocytes and neutrophils into the dermis (Fig. 20 B & C; H and E staining). Furthermore, PLGA implant could not be found after day 5 (Fig. 20 B; H and E staining). High myeloperoxidase activity was observed in response to PLGA implants on day 2 which decreased with time due to implant resorption. Myeloperoxidase was present inside and in surroundings of the implant (Fig. 20 B; Myeloperoxidase). However, macrophages could be seen surrounding the PLGA implant on day 2 and persisted till day 8 even after resorption of PLGA implant (Fig. 20 B; IBA-1). This might be anti-inflammatory activity of macrophages where they clear the debris of implant and apoptotic inflammatory cells to resolve the inflammation. In contrast, polystyrene implants are non-degradable and could be seen up to 8 days (Fig. 20 C; H and E). Myeloperoxidase and macrophages were present in response to polystyrene implants up to 8 days. This demonstrated the chronic inflammatory response to polystyrene implants (Fig. 20 C). Interestingly, a fibrous capsule was observed around the implant which thickened temporally, again indicating the severity and chronicity of the inflammation (Fig. 20 C; H and E; blue arrows). Polystyrene microspheres induced a chronic inflammatory response which is in accordance to *in vivo* imaging data (Fig. 20 C & 19 A). The resolution of PLGA induced inflammation was observed to be dependent on the resorption of implant material. Therefore, PLGA implants induced acute inflammatory response (Fig. 20 B & 19 A).

Histological analysis was in agreement with results from in vivo imaging of bioluminescent immune cells. We observed higher inflammatory potential of polystyrene implants compared to PLGA implants which was already shown *in vivo* using bioluminescent immune cells. This evidenced the potential of test system to rank inflammatory potential of implant materials reliably and accurately.

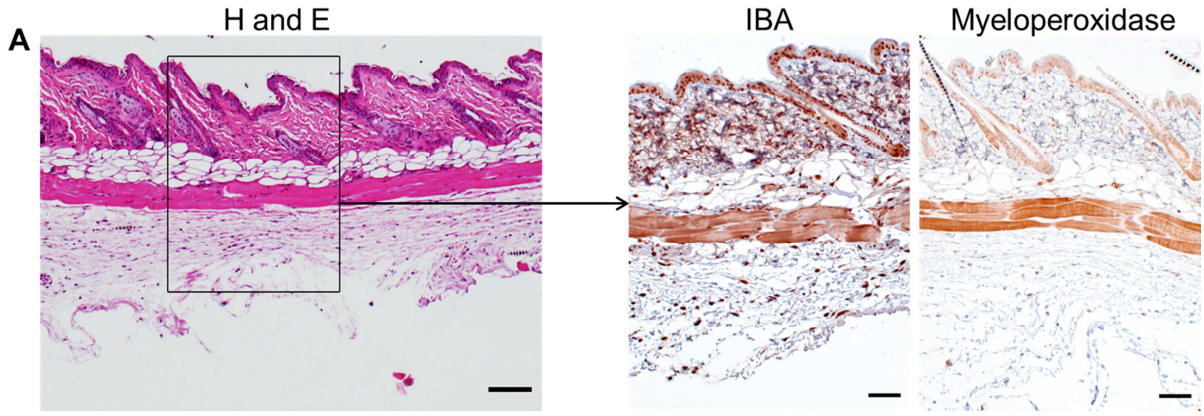

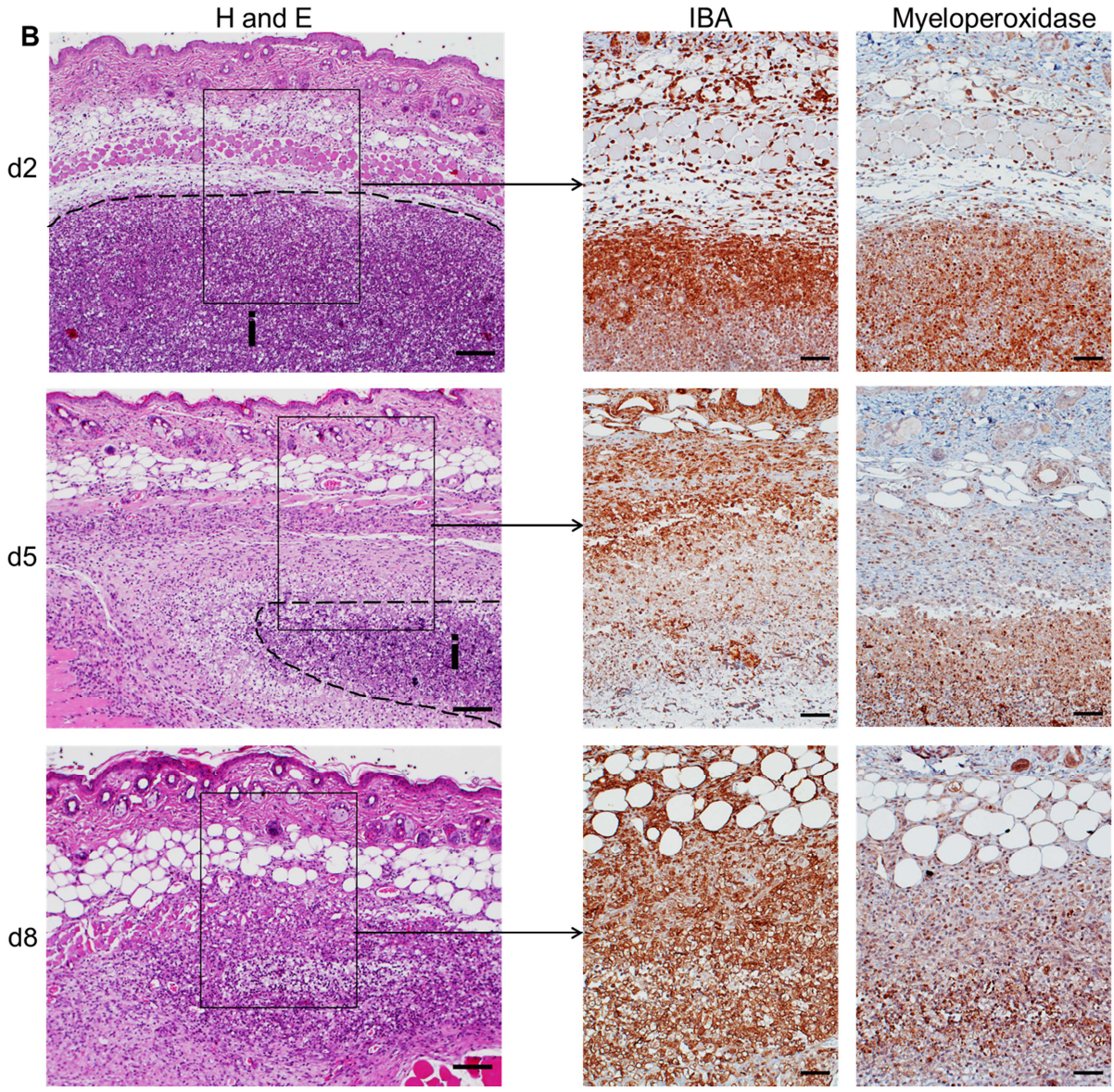
B
H and E
IBA
Myeloperoxidase
d2
d5
d8
i
i

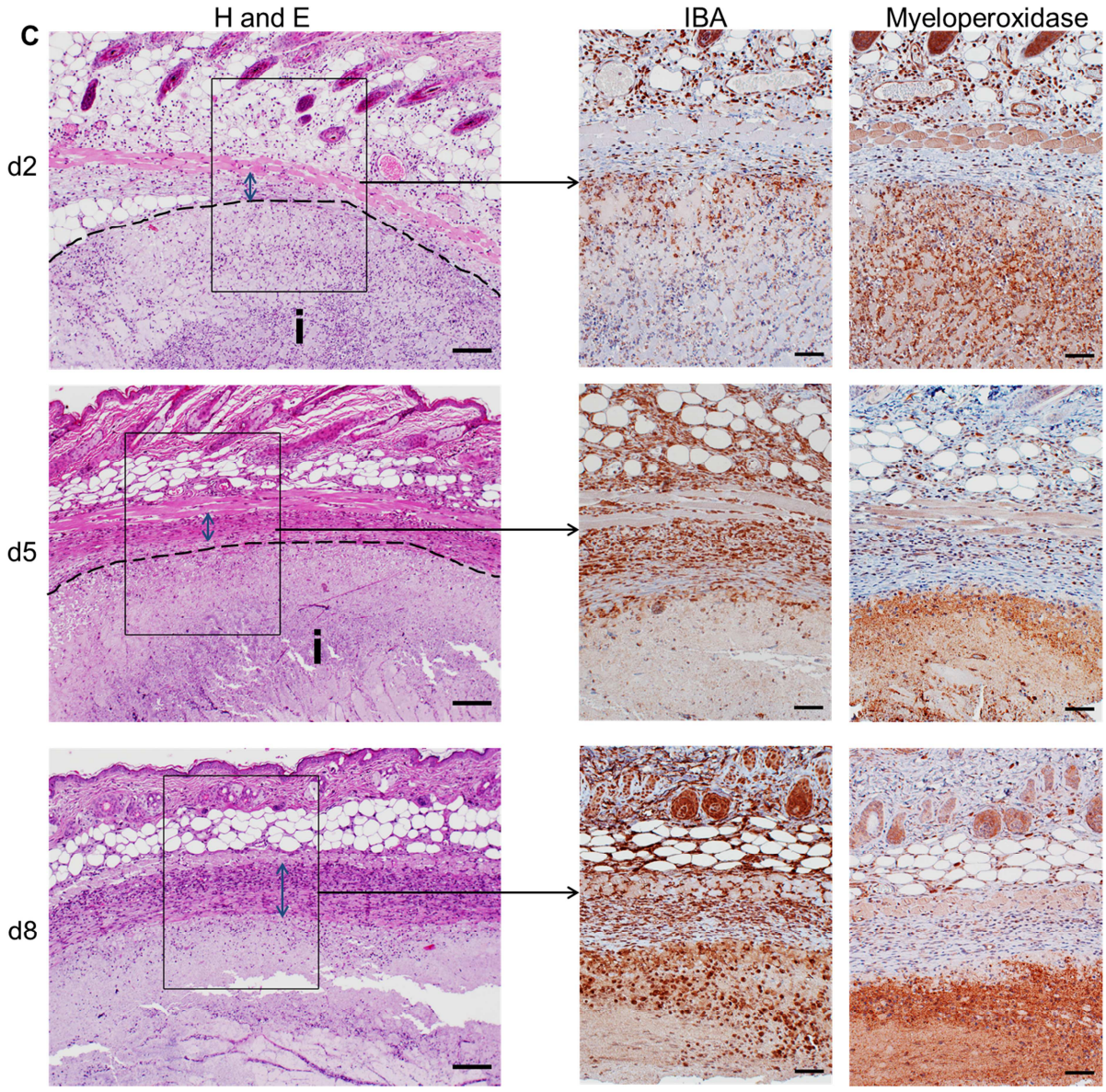

Figure 20: Increased inflammatory burden in response to polystyrene implants. Mouse skin tissues with injected PBS (A) PLGA (B) and polystyrene (C) microspheres were excised at days 2, 5 and 8 and stained using hematoxylin and eosin stain, anti IBA-1 and anti-myeloperoxidase antibody. Hematoxylin and eosin stained images are 10X where as IBA-1 and myeloperoxidase stained images are of 20X magnification. '**i'** represents the implant, blue arrow in H & E images (C) represents the fibrosis layer.

6.3 Monitoring Infection

6.3.1 Detection of innate immune responses to bacterial infections on implants

Implant infections are a serious concern in health care [198]. Microbial infections on implants are extremely difficult to treat. Early detection is essential for better treatment. Therefore, a reliable and sensitive detection method of high value was required. To this end, a transgenic reporter mouse was used. The genetic design of the animal involves the replacement of one allele of interferon-β (IFN-β) gene by luciferase gene [186]. The interferon-β gene can be activated by various infectious pathogens such as bacteria [184, 185]. To induce an inflammatory response titanium implants were coated with heat inactivated bacteria. IFN-β production was detected in response to bacterial extracts on the implant after a short delay of 6 hours and remained detectable for more than 24 hours (Fig. 21 A). Signals induced by bacteria were 10-fold higher when compared to the bare titanium implant (Fig. 21 B). Therefore, with this assay we could clearly and reproducibly detect and localize bacteria while uninfected control implants did not give a detetcable signal (Fig. 21 A). Inducers of IFN-β are infection related molecules such as DNA, bacterial lipopolysachcharides (LPS) or RNA of microorganisms which makes the detection system specific for infections whereas various sterile implant materials did not activate interferon-β [184, 185]. Reports also suggest that mammalian DNA or RNA which could be released from dead cells can also induce interferons [199] but here the injury alone was not detected suggesting that this was a minor inflammatory pathway during implantation.

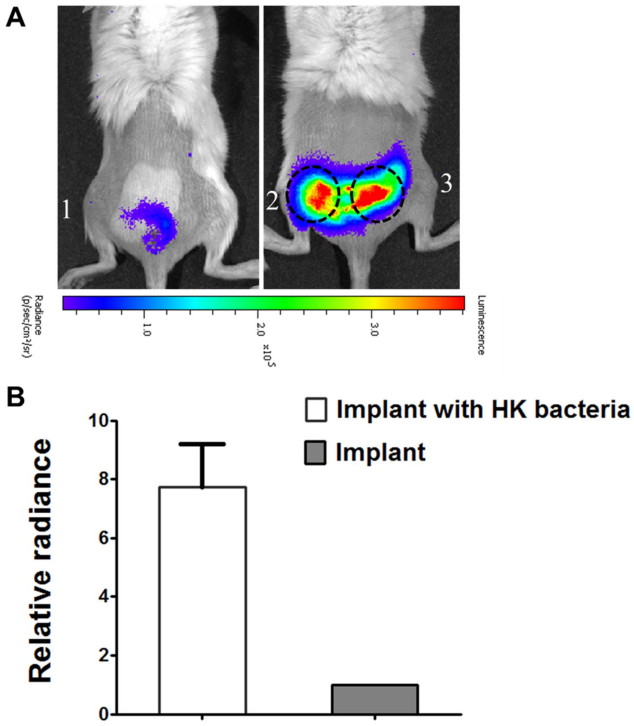

Figure 21: Sensitive detection of bacterial infections on implants: Interferon-β reporter mice were implanted with sterile and infected implants. Bioluminescent imaging was done after implantation and luciferin injection

(A). Implants are as follows: 1. Titanium implant 2 and 3. Titanium implant coated with heat killed (HK) bacteria. The relative radiance was calculated and the radiance of the control implant was arbitrarily set to 1 (B).

6.3.2 In vivo labelling of bacteria to monitor infections

To develop a sensitive detection system that responds solely to infections, it was essential to target bacteria *in vivo*. For this, a compound was needed that could specifically label bacteria *in vivo*. This method will be useful for imaging and treatment of bacterial infections in clinics. To this end, a novel compound was synthesized which is a 1,4,7,10 -tetraazacyclododecane-1,4,7,10-tetraacetic acid amide (DOTAM) derivative. This compound was linked to siderophores, iron complexing molecules. Bacteria need iron as limiting factor for bacteremia. *Pseudomonas aeruginosa* recognizes a diverse set of siderophores and can utilize these compounds for iron acquisition. Interferon-β luciferase reporter mice were infected subcutaneously using *pseudomonas aeruginosa*. Siderophore containing agents were linked to Cy5.5 molecules, so we will call them DOTAM-Cy5.5. This compound was injected in mice with or without bacteria and monitored for 24 hours (Fig. 22 A). The fluorescence intensity of the DOTAM-Cy5.5 was the highest at the site of bacterial injection till 3 hours and the intensity decreased gradually (Fig. 22 A). Moreover, the compound without siderophores (DOTA-Cy5.5) was also visible at the site of bacteria but with weaker intensity than siderophore linked compound (Fig. 22 B). To co-localize the immune response to bacteria and the DOTAM-Cy5.5 compound, bioluminescent imaging was performed in the same mice by visualizing IFN-β production in response to bacterial infection. Mice injected with the DOTAM-Cy5.5 and DOTA-Cy5.5 showed luminescent signals at the bacterial injection site (Fig. 22 C and D). The organ imaging of mice revealed that DOTAM-Cy5.5 was accumulated in liver and kidneys of the mouse and in spleen to some extent after 24 hours which showed lower specificity of the compound (Fig. 23 B). No accumulation of DOTA-Cy5.5 was observed in any of the organs after one day (Fig. 23 C).

Nevertheless, the siderophore linked compounds were able to label bacteria *in vivo* that was evidenced from co-localized signals of compound and immune responses to bacteria. This indicates that siderophore agents can target bacteria and can be used as therapeutic carrier to eliminate infections.

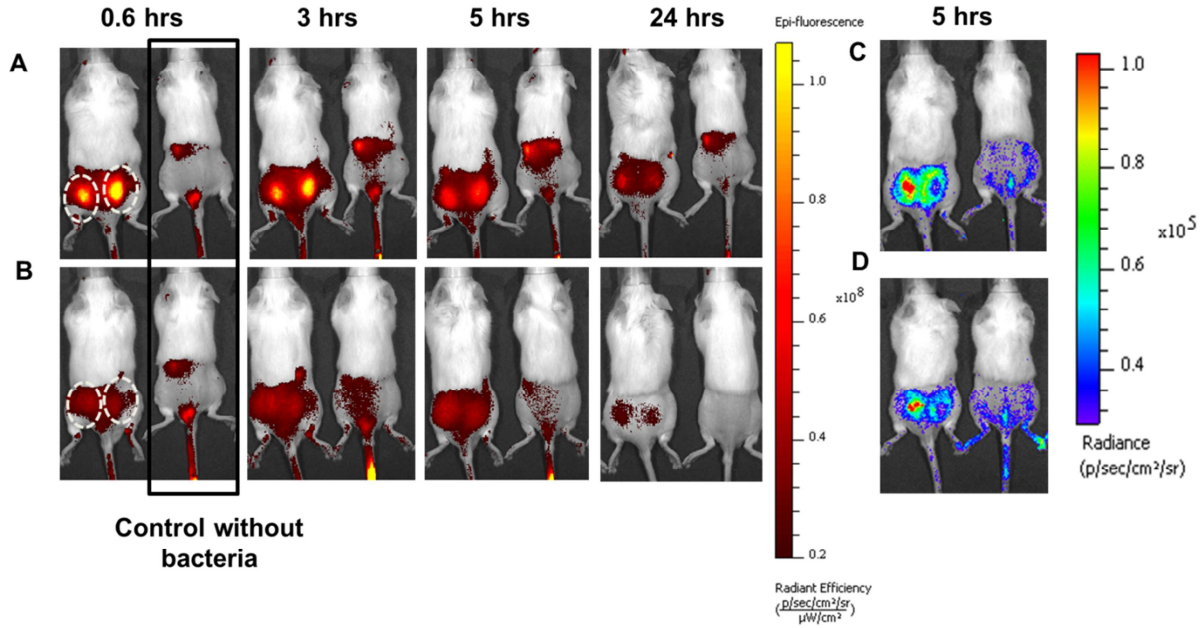

Figure 22: Real time monitoring of bacteria using fluorescent siderophore agents: *P.aeruginosa* (PA01 WT) was subcutaneously injected at the back of interferon-β luciferase reporter mouse. Control mice without bacterial infection were included. Mice were injected intravenously with Cy5.5 conjugated compound containing siderophore (DOTAM-Cy5.5) (A) and control group was injected with compound without siderophores DOTA-Cy5.5 only (B). Fluorescent imaging was performed and monitored for a day (A and B). Bioluminescent imaging of mice was done after 5 hours by injecting luciferin; mice with DOTAM-Cy5.5 (C) and DOTA-Cy5.5 alone (D). Dashed circles in white represent the site of bacterial infection.

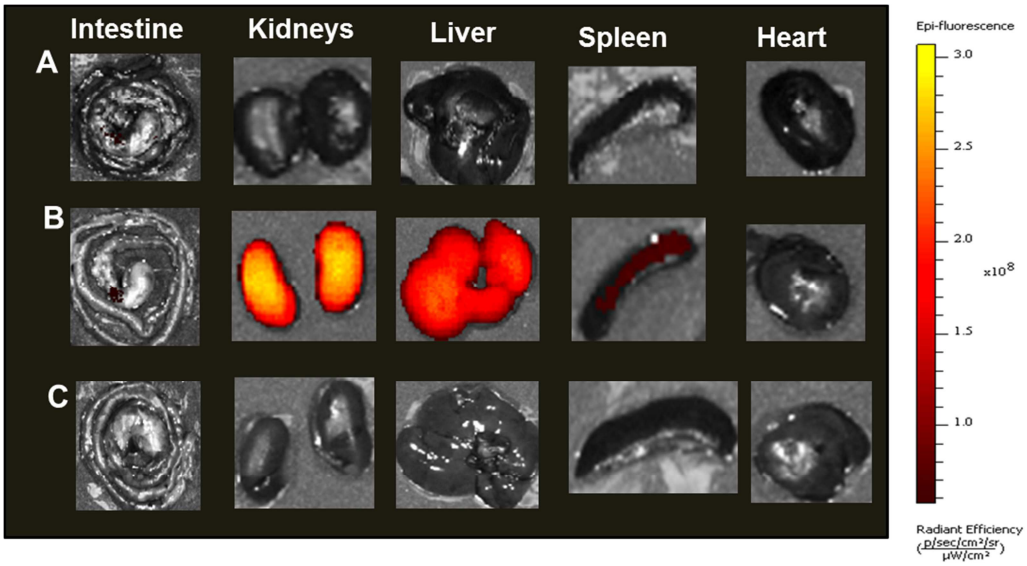

Figure 23: Accumulation of DOTAM-Cy5.5 in liver and kidneys: Control mice without bacterial infection but injected with DOTAM-Cy5.5 and DOTA-Cy5.5 as a non-specific control were sacrificed after 24 hours and organs were imaged to detect fluorescence. Organs from the mouse without any compound injection or infection was used as reference mouse to subtract the auto fluorescence from the organs (A). Organs of mice with

DOTAM-Cy5.5 compound (B) and DOTA-Cy5.5 alone (C) were imaged to detect siderophore associated fluorescence.

6.4 Unexpected longevity of neutrophils

This is a preliminary study related to our surprising finding about the bone marrow derived neutrophils. Neutrophils are the main cells of the innate immune system with a short half-life of few hours in circulation [200]. Here, we purified neutrophils from bone marrow of luciferase expressing mice using neutrophil isolation kit. Purified cells were mainly $Ly6G^{+}/Ly6C^{int}$ which represents neutrophil markers so we called them neutrophils. However, upon adoptive transfer of these cells in inflammation mouse model, we observed their survival for 19 days which is unexpected longevity of neutrophils. One possibility is the presence of monocytes as side population which is $Ly6G^{-}/Ly6C^{hi}$ cells. To confirm the possibility, we did a pre-characterization of neutrophil representing cells.

6.4.1 Growth factor mediated prolonged survival of neutrophils in vitro

In order to understand the behavior of isolated labelled neutrophil like population, it was essential to get pure neutrophil cells. Specific surface markers Ly6G and Ly6C were used to stain the MACS purified neutrophils from bone marrow of luciferase expressing mice and the two populations were observed; $Ly6G^{+}/Ly6C^{int}$ and $Ly6G^{-}/Ly6C^{hi}$ (possibly monocytes) which were then separated using cell sorter on Ly6G and Ly6C basis (Fig. 24 A). Purified neutrophil cells $Ly6G^{+}/Ly6C^{int}$ were cultured in presence and absence of granulocyte macrophage colony stimulating factor (GM-CSF). This growth factor is highly expressed during inflammation and is known to prolong the survival of granulocytes and helps in differentiation of the precursor cells [201]. Cell viability was measured using the luciferase expression of neutrophils. In the presence of GM-CSF, luminescence from neutrophils could be measured for 5 days while unstimulated cells underwent apoptosis within 2 days (Fig. 24 B). Life span of pure neutrophils in presence of a stimulus was improved. The growth factor mediated longevity of neutrophils was previously shown but in this study luminescent labelled neutrophils facilitated the study for extended period of time. Here, we speculate that the prolonged survival of neutrophils *in vivo* could be due to growth factors secreted during inflammation.

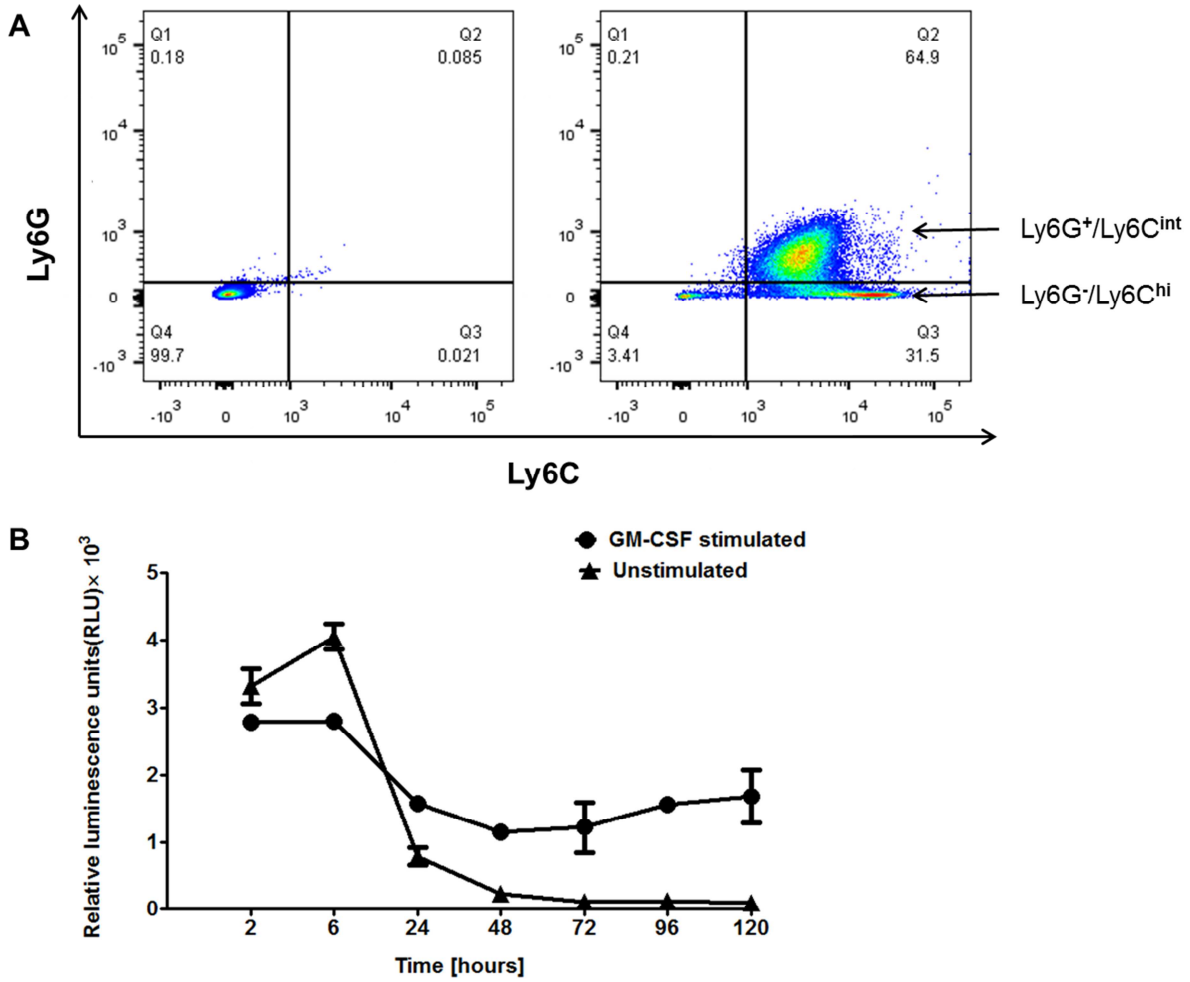

Figure 24: Growth factor induced prolonged survival of neutrophils: MACS purified neutrophils from the bone marrow of luciferase expressing mice were stained for surface markers, Ly6G and Ly6C. Two populations; $Ly6G^{+}/Ly6C^{int}$ and $Ly6G^{-}/Ly6C^{hi}$ were separated using cell sorter (A). $Ly6G^{+}/Ly6C^{int}$ population was cultured in presence and absence of GM-CSF. Relative luminescence units were measured by adding substrate for luciferase and values were obtained in plate reader (B).

6.4.2 Confirmation of longevity of neutrophils in presence of GM-CSF

The aim of present work was to confirm our observation about growth factor induced prolonged survival of neutrophils by visualizing viability of cells in inflammatory or non-inflammatory conditions. To this end, sorted neutrophil representing cells $Ly6G^{+}/Ly6C^{int}$ and side monocyte population $Ly6G^{-}/Ly6C^{hi}$ were cultured in presence or absence of GM-CSF and live dead staining was performed. Neutrophil representing cells appeared to survive for 8 days in presence of growth factor as compared to the unstimulated population (Fig. 25 A). In presence of GM-CSF, there was a decrease in neutrophil number with time but still viable cells could be seen on day 8 which showed their prolonged survival (Fig. 25 A; +GM-CSF; day 8). However, unstimulated neutrophils were mostly

dead and washed after 2 days which was expected (Fig 25 A; -GM-CSF; day 4). Side population of monocytes when cultured in presence of GM-CSF seemed to behave as macrophages because the cells appeared larger in size at later time points (Fig 25 B; day 6 and day 8). Numerous dead monocytes were observed in absence of stimulus and the culture was lost after two days (Fig. 25 B; -GM-CSF; d1 and d2). These results showed a clear difference in the survival time of neutrophils in presence versus absence of growth factor. From these results, we also ruled out possible effect of contaminating monocytes in purified neutrophils. This confirms that growth factors are inducing some changes in neutrophils that were responsible for their prolonged survival. However, the reason for prolonged survival in inflamed tissue is still unclear which needs more investigation.

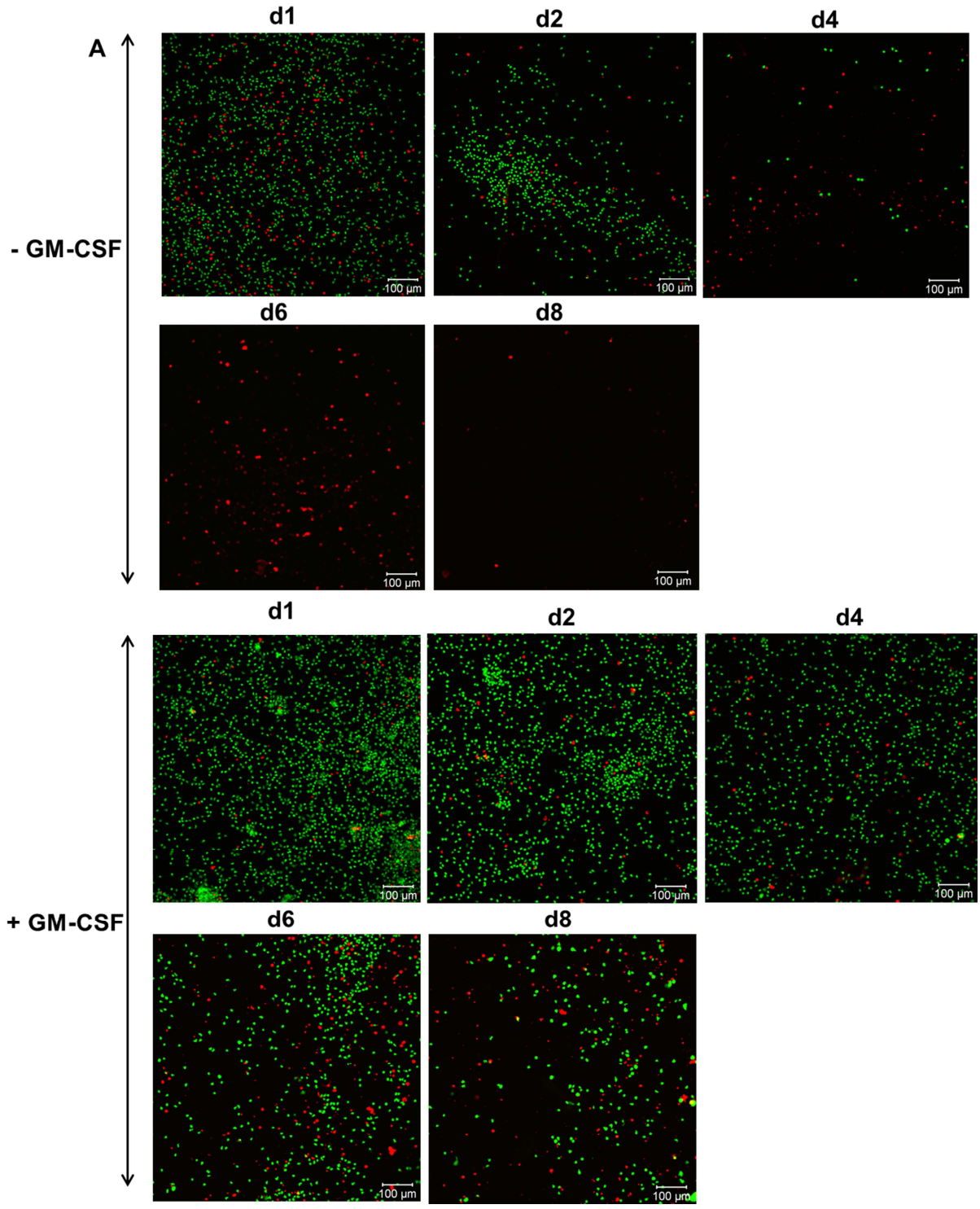
A
- GM-CSF
d1
d2
d4
d6
d8
100 µm
+ GM-CSF
d1
d2
d4
d6
d8
100 µm

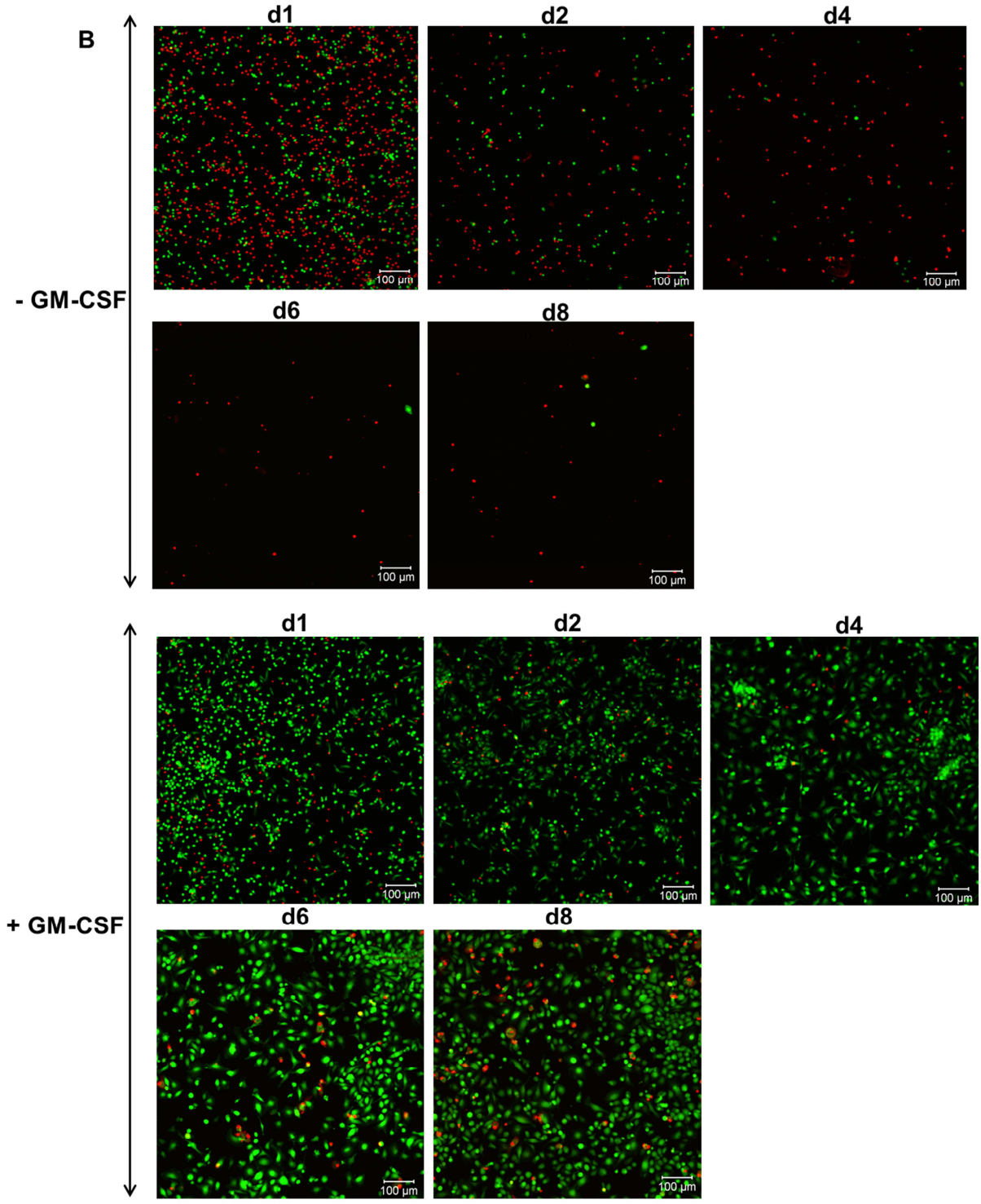

Figure 25: GM-CSF mediated prolonged survival of neutrophils and monocytes in cell culture: Neutrophils or $Ly6G^{+}/Ly6C^{int}$ cells (A) and side population of monocytes in the neutrophil population; $Ly6G^{-}/Ly6C^{hi}$ (B) were sorted and cultured in absence (-GM-CSF) and presence (+GM-CSF) of growth factor. Live dead staining was performed indicating, green cells to be the live cells and red dots are the dead cells. The magnification of images is 100X.

6.4.3 Change in phenotype of bone marrow derived neutrophils induced by GM-CSF

To understand the unusual longevity of neutrophils, it was essential to check phenotype of the cells in presence or absence of stimulus. To this end, bone marrow derived neutrophils from luciferase expressing mice were checked for their typical surface markers after culturing them in GM-CSF. The purified neutrophil population was $Ly6G^{+}/Ly6C^{int}$ population on day 0. The results showed that neutrophils gradually lose their typical phenotypic markers. Cultured neutrophils in the presence of GM-CSF started losing Ly6C surface marker (Fig. 26; d6) and then by day 8 a small percentage of cells are double negative (Fig. 26). Studies have shown that neutrophils altered their phenotype more oriented towards macrophage like cells in presence of growth factors or cytokines [202, 203]. These results also indicated the possible transformation of $Ly6G^{+}/Ly6C^{int}$ to some other cell type but the phenotypic and functional characterization of transformed cells needs further investigation.

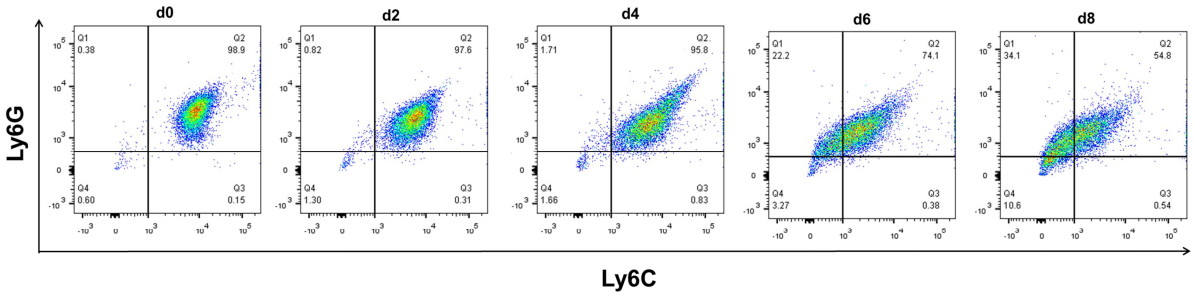

Figure 26: Gradual loss of typical surface markers of neutrophils cultured in the presence of GM-CSF: $Ly6G^{+}/Ly6C^{int}$ population was sorted to achieve high purity of neutrophils. These cells were cultured in presence of GM-CSF for 8 days and were stained for Ly6G and Ly6C surface markers and FACS analysis was done.

7. Discussion

The focus of the study was to establish a detection method that can distinguish inflammatory potential of biomaterials. This detection method will allow evaluating biocompatibility of novel materials and will help in development of optimal materials. The strategy was to detect inflammatory products in tissue by non-invasive imaging. Inflammatory products were targeted using fluorescent reporter molecules and with this strategy inflammatory implants could be differentiated from biocompatible materials. However, the signal was delocalized and close to background. Fluorescent imaging generally suffers from high background and autofluorescene of tissue. We needed a reproducible assay that can show clear differences in the signal intensities to differentiate inflammatory potential of materials. Materials chosen for the approach were inflammatory at varying degrees. The upmost inflammatory response comes from infection. Infection is a major problem and not easy to detect in clinics. Detecting infections at early stages will help in effective treatment. Therefore, bioluminescent immune cells were used that allowed to differentiate inflammatory and non-inflammatory materials and clearly distinguished infections. This is a reliable method to evaluate biocompatibility of materials before introducing them into clinics. Further discussion will be focused on the several strategies used to detect inflammation and their limitations, advantages of bioluminescent imaging over fluorescent imaging, differentiating inflammatory potential of materials using bioluminescent cells and alternative strategies to monitor infections.

7.1 Detection of inflammatory materials by fluorescent imaging

To detect differences in the inflammatory potential of implants, several inflammatory products have been targeted using different approaches enabling their visualization *in vivo*. Macrophages and neutrophils release numerous inflammatory products such as reactive oxygen species, cytokines and chemokines in response to inflammatory biomaterial [70]. Reactive oxygen radicals produced during inflammation were visualized using hydrocyanines [45]. The reduced form of hydrocyanines was weakly fluorescent due to disrupted π conjugation but on oxidation it becomes fluorescent and could be visualized in near infra-red region [45]. The fluorescence could be correlated to the amount of ROS produced in response to inflammatory stimulus. Inflammatory or infected implants could be detected and differentiated from the biocompatible implants after local application of hydrocyanine. The oxidation potential of the hydrocyanines also seemed to be dependent on diffusion through the tissue, which could be the reason for variability of responses in independent experiments. Some degree of ROS activity could be seen for the sham surgery which was comparable to the biocompatible implant suggesting that ROS production was in response to injury and not due to the implant. The systemic administration of the hydrocyanine was unable to reach the inflammation site and showed accumulation in organs which could be due to limited diffusion properties of the compound. Though

the system was able to differentiate the inflammatory potential of the implants but reliability and specificity seemed to be compromised. Chemiluminescent agents such as luminol or L-012 can also be used to detect oxygen radicals [49, 204]. Luminol is a redox sensitive compound that emits blue light upon oxidation and can be visualized by bioluminescent imaging. It is easily distributed and eliminated from the body due to its small size. This makes it a better probe for detection of oxygen radicals [205]. However, the oxidizing agent of the compound is unknown and it reacts with many reactive oxygen radicals released during phagocytic oxidative burst that limits specificity of the compound [205]. It is essential to improve the sensitivity of the existing ROS detecting agents or to develop novel compounds that can reliably detect inflammation associated oxygen radicals.

Inflammatory proteases were also considered as potential target to visualize inflammation. Implant associated inflammatory process involves the accumulation of inflammatory cells at the implantation site and these cells produce degradative enzymes such as proteases to amplify the response [70]. Cathepsins are lysosomal proteases that are released by macrophages in pathological conditions such as rheumatoid arthritis, cancer, bronchial asthma and obesity [206-209]. These proteases have physiological role in apoptosis, protein degradation and antigen presentation. Moreover, the resolution of inflammation involves the apoptosis of inflammatory cells that indicates a major role of cathepsins in innate immune response [178]. To visualize the cathepsin activity in response to inflammatory stimulus, a cathepsin-activatable probe was used. The probe is fluorescent when internalized by the cells and cleaved by cathepsins with in lysosomes. Temporal increase in fluorescence showed the production of cathepsins in response to infected implants. However, the signal was delocalized and fluorescence intensity could not be precisely assigned to a single implant. Cathepsin B and L are cysteine proteases and have their function in inflammation and cholesterol trafficking [210]. The probe was shown to be activated by cathepsin B, L, S and K by the manufacturer suggesting non-specific activation and fluorescence which could be the reason for delocalized signals. Although, in a previous study cathepsin-activatable fluorophore was shown to evaluate the biocompatibility of injected biomaterials but some extent of delocalization of fluorescence was observed which confirms results of this study. In conclusion, this method did not appear to be suitable to distinguish inflammatory potential of different implants.

The approach to monitor cell growth stimulating signals has been used to detect tumors and is also expected to be involved in wound healing process [211]. Autotaxin is lipase that generates a lipid signaling molecule which is responsible for cell motility, viability, proliferation and migration [179]. Implant associated inflammation also involves the migration of inflammatory cells to the inflammation site followed by proliferation of fibroblasts to form a fibrous capsule surrounding the implant. To monitor the autotaxin activity, an analogue of autotaxin substrate lysophosphatidylcholine (LPC) was used. The substrate was conjugated to near infra-red fluorophore that produced fluorescence when

cleaved by autotaxin. The fluorescence intensity indicated amount of autotaxin produced in response to inflammation. Autotaxin associated fluorescence increased with time in response to bacterial components on implants. However, the signals were hardly detected because of the high background. In addition the signal intensity increased even in absence of implants that indicates the unspecific activation of substrate. Therefore, this strategy was unable to determine the extent of inflammation in response to individual implants.

Strategies for visualizing enzymatic activities or presence of reactive molecules using fluorescent probes generally suffer from high background due to autofluorescence of tissue as well as background fluorescence of the probe. Consequently, fluorescent imaging and fluorescent inflammatory reporter molecules were unable to fulfil the purpose of distinguishing inflammatory and biocompatible implants. Given the limitations of these strategies, there is no animal model that can quantify the inflammation in accordance to the clinical relevance

7.2 Bioluminescent imaging versus fluorescent imaging

In vivo optical imaging is extremely useful technique to monitor implant related inflammation or infection because it does not involve animal killing and fate of single implant can be recorded over time. The major advantage of non-invasive optical imaging is that each animal can serve as internal controls thereby, avoiding even subtle differences in the handling and animal to animal variability. It is relatively cheaper and less complex when compared to other imaging modalities such as PET/SPECT and MRI [212, 213]. However, spatial resolution of the images is low and dependent upon the depth of the desired tissue [213].

Optical imaging can detect photons emitted from the tissues by the fluorescent or bioluminescent source. Fluorescent imaging involves the excitation of the fluorescent molecule at desired wavelength to visualize the emitted light from the tissues [214]. Alternatively, bioluminescent light can be detected as a response of a chemical reaction in the presence of luciferase enzymes [215]. Fluorescent imaging unlike bioluminescent imaging has higher background due to autofluorescence from the tissues which limited the visualization of the signal from a single implant. The exponential decrease of light with the increasing depth of the tissue limits its application to superficial imaging [213]. Moreover, the opaque implants quenched the fluorescence emitted and made the detection system dependent upon the opacity of materials. The fluorescent imaging technique is in insensitive and non-specific due to high background signals. In contrast, bioluminescent imaging technique does not require an external light source and has extremely low background. This can enable the visualization of localized inflammatory responses to each implant. Moreover, the precise quantification of the signal can be possible due to high imaging contrast. In addition, this method is well suited for kinetic

analysis as the luciferin substrate for firefly luciferase enzymes has a short half-life of approximately 3 hours [216]. This technique has high signal to noise ratio which made the imaging technique sensitive and specific [217].

Our standards for a detection method were high and we required a precise and accurate method to evaluate inflammatory potential of different biomaterials. Therefore, we used bioluminescent immune cells to visualize local inflammation in response to biomaterials.

7.3 Monitoring inflammation using bioluminescent immune cells

To evaluate inflammatory potential of biomaterials, a reliable test system was needed. Bioluminescent immune cells improved the sensitivity of the detection method for two reasons. Firstly, because of bioluminescent imaging that enabled visualization of localized tissue response and secondly, immune cells have extremely precise ability to sense and respond to inflammatory stimulus. We could clearly differentiate varying degrees of inflammation ranging from highly inflammatory or infected material to biocompatible implants.

To enable the detection of immune cells *in vivo* has always been a big challenge. The labelling of the immune cells can be achieved either by direct labelling using probes that can be internalized by the immune cells or by genetic modification of cells that results in expression of the reporter protein. The former strategy is simple and is used in clinics. However, the efficiency of the technique depends upon the ability of cells to retain the label and can only be used to label terminally differentiated cells. Furthermore, the label can be lost due to its dilution at each mitotic event that disables long term monitoring of cell viability and proliferation [218]. We needed a reliable detection method for extended period of time which could be achieved by exploiting the genetically modified cells. To this end, immune cells were harvested from a transgenic mouse with substantial constitutive luciferase expression under the influence of an inducible Mx-2 promoter [180]. The potential inducers of Mx-2 promoter activity are infection related cytokines, type I and type III interferons [181]. These cytokines have originally been discovered as part of antiviral response but type I interferons are also induced by different bacteria [182, 184]. This way we developed a two component system in which immune cells were luminescent and detectable in vivo and secondly the luminescence could be enhanced after induction of promoter activity during bacterial infections. This genetic design helped in reliable monitoring of the cells for longer period of time. In addition, to visualize immune cells *in vivo* bioluminescent imaging was required which facilitated quantification of signals due to high signal to background ratio and therefore a distinct difference between bacteria coated and non-inflammatory implants was observed.

The transferred bioluminescent immune cells were recruited at the implantation site and could differentiate implants coated with bacterial components from the biocompatible implants. Amongst isolated total bone marrow cells, monocytes and neutrophils, total bone marrow cells showed a larger difference in signals and were able to distinguish infected implants and sterile implants. The larger difference observed might be due to the presence of progenitor cells or other immune cells in total bone marrow fraction which have the ability to proliferate and differentiate in response to inflammatory stimulus.

In conclusion, total bone marrow fraction had the optimal cells to evaluate the inflammatory potential of biomaterials and was further used to investigate the inflammatory potential of different biomaterials.

7.3.1 A definitive ranking of inflammatory potential of biomaterials

We were able to rank different biomaterials according to their inflammatory potential using luminescent labelled immune cells. Biomaterials need testing before their use in clinics. Materials that were chosen for the study were already evaluated for their biocompatibility in other studies. We selected different biomaterials with different degrees of inflammatory potential. This helped us in determining the efficiency and reliability of the detection method.

Poly (lactide-co-glycolic acid) is a biodegradable copolymer of poly glycolic acid (PGA) and poly lactic acid (PLA). The major applications of the polymer are known in fabrication of the devices for orthopedic surgery, tissue engineering and drug delivery [219]. The polymer undergoes degradation by hydrolyzing the ester bond into acidic monomers. The acidic by products create a local low pH environment thereby stimulating inflammatory response and affecting cellular growth and function [220]. Our observation in the test model using bioluminescent immune cells confirms the inflammatory potential of PLGA. In other study, production of reactive oxygen species in response to PLGA was visualized using hydrocyanines and non-invasive imaging [45]. To dampen the inflammatory response to PLGA, several modifications have been done such as incorporation of anti-inflammatory drugs like dexamethasone or by blending PLGA with magnesium hydroxide nanoparticles to neutralize the pH which may improve the cell viability and minimize the inflammatory reactions [221, 222].

On the other hand, biocompatible titanium implants are standard biomaterials and are used in clinics for decades. They have a broader range of applications as dental and orthopedic implants, prosthetic heart valves and protection cases for pacemakers. Titanium receives extensive attention because of its appropriate mechanical performance, great tensile strength, and high resistance to corrosion and most

importantly excellent biocompatibility [223, 224]. Due to its high standards of biocompatibility, titanium was a good negative control in the testing system.

Magnesium is an extremely low weight metal that was first discovered as orthopedic implants. It is biodegradable and biocompatible biomaterial and has the ability to stimulate bone growth and healing. However, the major limitation of magnesium is its low resistant to corrosion that limited its further use in orthopedics. The magnesium based implants degrade rapidly in physiological environment and produce corrosion particles. Interestingly, these wear particles are harmless and are eliminated from the body through urine [225, 226]. Moreover, the gene expression patterns of tissue surrounding magnesium and titanium implant were similar which indicates its biocompatibility *in vivo* [227]. The magnesium implants were monitored in our animal test system and biocompatibility of magnesium was comparable to titanium implants. Our study lies in accordance to other biocompatibility studies on magnesium.

Inflammatory biomaterials were differentiated from the known biocompatible biomaterials by imaging bioluminescent immune cells. The ability of the detection system to evaluate the inflammatory potential of different biomaterials indicated higher sensitivity of the system when compared to other animal test systems where fluorescent inflammatory reporter molecules were used. This bioluminescent imaging strategy allowed reliable visualization and quantification of biomaterial associated inflammation.

7.3.2 Material induced inflammation versus injury

Injury elicits inflammation. To this end, injectable biomaterials were used that stimulate minimum tissue injury and can be used to evaluate material induced inflammation. Injectable biomaterials are widely used in drug delivery and tissue engineering. Here, we were able to rank the inflammation in response to injectable materials using luminescent labelled cells. Materials were chosen according to their bio-degradability in physiological environment.

Polymeric microspheres are one form of injectable materials that are used as controlled drug delivery agents, filler agents to restore tissue volume and embolic particles to occlude vessels of tumors. The controlled shape and size of the microspheres makes them ideal injectable biomaterial. Microspheres in circulation should be biocompatible, perform desired function and have predictable degradation kinetics [228]. They have been tested in animal models to assess their inflammatory potential. Cathepsin activity was observed in response to polystyrene microspheres of size 3 μm that suggests the presence of macrophages and neutrophils that attempt to internalize and degrade the microspheres [54]. In this study we showed the dependency of immune response on the degradability of microspheres. Polystyrene microspheres (1 μm) stimulated chronic inflammatory response due to its

non-degradable characteristics. In contrast, biodegradable PLGA microspheres of similar size showed acute inflammation which could be due to resorption of the implant. PLGA based biomaterials were inflammatory due to its acidic degradation products.

Another injectable material is biodegradable chitosan which is a polysaccharide derived from crab shells. The applications of chitosan in biomedical field are in wound dressing and drug delivery. Chitosan membranes were also proposed as artificial kidney membranes due to their appropriate membrane permeability and high tensile strength but due to its thrombogenic properties it was not put into use. It was initially considered as biocompatible but the absolute inertness of chitosan was questionable because the immunogenicity of chitosan depends upon its source (crab, shrimps and fungus), variability in tertiary structures due to manufacturing processes and degree of contaminants [229]. Moreover, chitosan has been shown as potent activator of NLRP3 inflammasome [230, 231]. In addition, our animal test system was able to monitor the inflammatory cells recruited in response to chitosan.

Traditionally, histology was the detection method to analyze local tissue inflammation in response to implants. The technique required more number of animals to follow the inflammation kinetics and moreover, processing of the tissue sections involves tedious steps such as fixation, embedding and staining. However, we validated our *in vivo* imaging results using this technique. Here in this study, we observed a similar inflammatory response to PLGA and polystyrene implants after histologic analysis.

The detection method developed here allowed rapid and reliable *in vivo* monitoring of implant related inflammation. It permitted analysis of foreign body response to different biomaterials thereby, eliminating the need of expensive and time consuming histological analysis.

7.3.3 Application of implant inflammation model

Biomaterial science is an interdisciplinary field where materials scientists work towards the improvement of physical and chemical properties of the biomaterials, chemists develop novel antibacterial or anti-inflammatory compounds as coatings on biomaterials and biologists screen the biocompatibility and functionality of novel materials and coatings. Here, we developed a screening method to assess the immune response of novel materials or coatings in real time. This method can follow a single implant in vivo and can help in studying the interaction of implants with tissue. Moreover, novel or existing anti-inflammatory drugs can be tested and monitored in real time using bioluminescent cells. In addition, controlled local drug delivery methods have always been an attraction to eliminate implant infections. This model can help in monitoring slow local response of the drug for longer period of time. Immune cells are mostly the targets of anti- inflammatory drugs and

to monitor their effect using bioluminescent cells will allow their visualization during action. Thus, these approaches reveal the clinical benefits of the animal model for implant-related inflammation.

7.4 Implant infections

Detecting implant infections at early stages is clinically important for effective treatment. These infections are mostly resistant to conventional antibiotics and can cause serious complications in the host. To treat these infections, there is a need to monitor them *in vivo*. Here, we used siderophore agents to target bacteria *in vivo*. These siderophores have high iron solubility and are taken up by bacteria under iron limiting conditions. We took an advantage of this natural mechanism of bacteria and conjugated a fluorophore to the siderophore linked agents for non-invasive imaging. Transgenic mice that allow visualization of innate immune response to bacteria were used to confirm the bacterial infection by bioluminescent imaging. Fluorescence of the siderophore agents was co-localized with bioluminescent innate immune response to bacterial infections, thus confirming the specificity of the siderophore compounds to bacteria. This indicates that siderophore agents can target bacteria and can be used as therapeutic carrier to eliminate infections.

Diagnosing and treating bacterial infections on implant is a challenge due to lack of accuracy and specificity of bacteria targeting compounds. Although numerous bacterial targeting strategies have been developed, none could be proven clinically useful. In this study, siderophore based compounds demonstrated high specificity due to their uptake by bacteria. Therefore, siderophore drug complexes have tremendous potential to treat infections. We demonstrated promising preliminary results of the siderophore compounds which need further characterization to show compound uptake by bacteria. Moreover, the efficacy of the antibiotic linked to siderophore compounds needs to be tested *in vitro* and *in vivo*.

7.5 Developmental potential of bone marrow derived neutrophils

We were using isolation procedure based on Ly6G and Ly6C that are specific for neutrophils and monocytes which make up the major population in bone marrow. Even though the cells were not analyzed, subsequently we will call $Ly6G^{+}/Ly6C^{int}$ neutrophils and $Ly6G^{-}/Ly6C^{hi}$ monocytes. This preliminary study was related to our unexpected findings about neutrophils that showed unusual survival time in inflamed tissue. Neutrophils are the main cell types of innate immune system. Neutrophils have a short half-life in circulation of 1.5 hours and 8 hours in mice and humans, respectively. However, the myth of short lived cells is changing and several studies have shown prolonged half-life of neutrophils in circulation under basal conditions which is 12.5 hours and 5.4

days in mice and humans respectively [200]. Inflammatory diseases such as acute respiratory distress syndrome (ARDS), pneumonia, sepsis, rheumatoid arthritis and cystic fibrosis exhibit delayed apoptosis of neutrophils in blood and synovial fluid [232-235]. One of the reasons for delayed apoptosis is increased levels of growth factor GM-CSF in sepsis, burns and acute respiratory syndrome [232]. In our case, the prolonged survival of neutrophils was first thought to be due to dividing monocytes which was present as side population in isolated neutrophils. We ruled out that possibility by sorting pure neutrophils from side population. We observed growth factor induced prolonged survival of neutrophils *in vitro*.

Furthermore, as we know neutrophils are produced in bone marrow from a progenitor cell myeloblast which then differentiates to promeyelocyte that is committed to neutrophil lineage. Eventually, promyelocyte matures to form myelocytes. These three cell types constitute mitotic pool of bone marrow in which cells proliferate. When myelocytes produce metamyelocytes, then they constitute post mitotic pool and can no longer divide [200]. Recently, a study revealed that post mitotic neutrophils can switch the lineage to macrophages in vitro when cultured in presence of appropriate growth factors and cytokines [202]. Another similar research showed that neutrophils express macrophage specific receptors and have the ability to transdifferentiate to macrophages [203]. In support to this, we observed temporal loss of typical phenotype markers of neutrophils when cultured in presence of GM-CSF. This could be due to the change in phenotypic characteristics of cells in presence of growth factor. It is still unclear that these cells were really transdifferentiating to some other cell types or not. However, the phenotypic changes appeared promising to study the possibility in detail. If true, this study will change the paradigm of neutrophil research and we can provide an *in vivo* model to study the neutrophil kinetics in inflammation.

7.5.1 Further characterization of bone marrow immune cells

The preliminary results on the neutrophil survival gave us a different direction on characterization of cells in presence of inflammation. Bioluminescent neutrophils isolated from luciferase expressing mice allow visualization of cells without extra effort of labelling. Moreover, labelling procedures can manipulate neutrophils affecting their kinetics and migration [236]. Bioluminescent neutrophils are ideal genetically labelled cells and can help in studying the phenotype and function of bone marrow cells *in vitro* and in *vivo*. To find out reprogramming ability of neutrophils, we need gene expression analysis of neutrophils and macrophages under the influence of cytokines and growth factors. If hypothesis of transformation is true in our case, then we will be able to introduce a novel model to study dynamics of neutrophils in real time.

8. Conclusion

The major aim of the study was to evaluate inflammatory potential of novel implant materials in vivo. The initial strategy was to detect reactive species of inflammation by fluorescent imaging. Even though with these strategies inflammatory events could be detected but the method resulted in high background and diffused signal distribution. To improve signal to noise ratio and to get more focused signal, bioluminescent labelled cells were used. With this strategy, we were able to distinguish non inflammatory materials from inflammatory materials or injury. Moreover, sterile inflammation from infections could be distinguished. These results are useful for ranking biocompatibility according to the inflammatory potential of implant materials which is essential in developing optimal materials. We could observe immune response of different degrees varying from highly inflammatory bacterial infections to biocompatible biomaterials. In addition, implant materials of different size and texture have different inflammatory responses which could be evaluated and ranked using this method. Early detection of infections would allow their effective treatment. This detection method could have clinical potential in monitoring infections by replacing optical imaging with MRI or PET scan and by scaling up the labelling of human blood cells. As a side finding, immune cells population expressing neutrophil markers showed an unexpected longevity which suggests that it is previously uncharacterized precursor immune cells population that warrants further investigation.

9. Appendix

9.1 List of figures

9.2 List of tables

9.3 List of abbreviations

APC	*Antigen presenting cells*
Ca	*Calcium*
DOTAM	*1,4,7,10-tetraazacyclododecane-1,4,7,10-tetraacetic acid amide*
ECM	*Extracellular matrix*
EPS	*Extracellular polymeric substances*
FAF	*Fibroblast activating factor*
FGF	*Fibroblast growth factor*
GAGs	*Glycosaminoglycan*
G-CSF	*Granulocyte colony stimulating factor*
GM-CSF	*Granulocyte macrophage colony stimulating factor*
HA	*Hydroxyapatite*
hi	*high*
HMGB	*High mobility group box*
HSP	*Heat shock proteins*
IFN	*Interferons*
int	*Intermediate*
IL	*Interleukins*
LPS	*Lipopolysaccharides*
Na	*Sodium*
P	*Phosphorous*
PAA	*Poly (acrylic acid)*
PEG	*Poly (ethylene glycol)*
PGs	*Proteoglycans*
PLGA	*Poly lactic – co – glycolic acid*
PMNs	*Polymorphonuclear leukocytes*
PRRs	*Pattern recognition receptors*
PVA	*Poly (vinyl alcohol)*
RAGE	*Receptor binding advanced glycation end products*
ROS	*Reactive oxygen species*
Si	*Silica*
TH	*T helpers*
TLR	*Toll like receptors*

9.4 References

1. Freedonia, G., *Implantable medical devices to 2014- demand and sales forecast, market share, market size, market leaders.* 2010.
2. Black, J. and G. Hastings, *Handbook of Biomaterial Properties*. 1998: Springer US.
3. Vacanti, C.A., *The history of tissue engineering.* J Cell Mol Med, 2006. **10**(3): p. 569-76.
4. Mason, C. and P. Dunnill, *A brief definition of regenerative medicine.* Regen Med, 2008. **3**(1): p. 1-5.
5. Ratner, B.D., *Biomaterials Science: An Introduction to Materials in Medicine*. 2004: Elsevier Academic Press.
6. Black, M.M., R.v. Noort, and P.J. Drury, *Medical applications of biomaterials.* Physics in Technology, 1982. **13**(2): p. 50.
7. Sanan, A. and S.J. Haines, *Repairing holes in the head: a history of cranioplasty.* Neurosurgery, 1997. **40**(3): p. 588-603.
8. Hansmann, C., *Eine neue Methode der Fixierung der Fragmente bei complicierten Fracturen.* Verh Dtsch Ges Chir, 1886. **15**: p. 134-.
9. Venable, C.S., W.G. Stuck, and A. Beach, *The effects on bone of the presence of the metals; based upon the electrolysis: an experimental study.* Annals of Surgery, 1937. **105**(6): p. 917-938.
10. Luckey, H.A., et al., *Titanium Alloys in Surgical Implants*. 1983: American Society for Testing & Materials.
11. Kolff, W.J., *The artificial kidney and its effect on the development of other artificial organs.* Nat Med, 2002. **8**(10): p. 1063-1065.
12. Apple, D.J. and J. Sims, *Harold Ridley and the invention of the intraocular lens.* Survey of Ophthalmology, 1996. **40**(4): p. 279-292.
13. Hench, L.L., *Bioactive ceramics.* Annals of the New York Academy of Sciences, 1988. **523**: p. 54-71.
14. Hench, L.L. and J. Wilson, *An Introduction to Bioceramics*. 1993: World Scientific.
15. Walid, H., *Drug-eluting stents : Insights into safety and indications.* Annals of Saudi Medicine, 2008.
16. Xynos, I.D., et al., *Gene-expression profiling of human osteoblasts following treatment with the ionic products of Bioglass® 45S5 dissolution.* Journal of Biomedical Materials Research, 2001. **55**(2): p. 151-157.
17. Donaruma, L.G., *Definitions in biomaterials, D. F. Williams, Ed., Elsevier, Amsterdam, 1987, 72 pp.* Journal of Polymer Science Part C: Polymer Letters, 1988. **26**(9): p. 414-414.
18. Williams, D.F., *The Williams Dictionary of Biomaterials*. 1999: Liverpool University Press.
19. Porter, J.A. and J.A. Von Fraunhofer, *Success or failure of dental implants? A literature review with treatment considerations.* General Dentistry, 2005. **53**(6): p. 423-432.
20. Montanaro, L., D. Campoccia, and C.R. Arciola, *Advancements in molecular epidemiology of implant infections and future perspectives.* Biomaterials, 2007. **28**(34): p. 5155-5168.
21. Gorbet, M.B. and M.V. Sefton, *Endotoxin: The uninvited guest.* Biomaterials, 2005. **26**(34): p. 6811-6817.
22. Williams, D.F., *On the mechanisms of biocompatibility.* Biomaterials, 2008. **29**(20): p. 2941-2953.
23. Jones, C.A., et al., *Total Joint Arthroplasties: Current Concepts of Patient Outcomes after Surgery.* Clinics in Geriatric Medicine, 2005. **21**(3): p. 527-541.
24. Bruning, N., *Breast Implants: Everything You Need to Know*. 2002: Hunter House.
25. Vert, M., J. Mauduit, and S. Li, *Biodegradation of PLA/GA polymers: increasing complexity.* Biomaterials, 1994. **15**(15): p. 1209-1213.
26. Shive, M.S. and J.M. Anderson, *Biodegradation and biocompatibility of PLA and PLGA microspheres.* Adv Drug Deliv Rev, 1997. **28**(1): p. 5-24.
27. Williams, D.F., *To engineer is to create: The link between engineering and regeneration.* Trends in Biotechnology, 2006. **24**(1): p. 4-8.

28. Onuki, Y., et al., *A Review of the Biocompatibility of Implantable Devices: Current Challenges to Overcome Foreign Body Response.* Journal of diabetes science and technology (Online), 2008. **2**(6): p. 1003-1015.
29. Ito, A., et al., *Zinc-releasing calcium phosphate for stimulating bone formation.* Materials Science and Engineering: C, 2002. **22**(1): p. 21-25.
30. Webster, T.J., et al., *Osteoblast response to hydroxyapatite doped with divalent and trivalent cations.* Biomaterials, 2004. **25**(11): p. 2111-21.
31. Bennewitz, N.L. and J.E. Babensee, *The effect of the physical form of poly(lactic-co-glycolic acid) carriers on the humoral immune response to co-delivered antigen.* Biomaterials, 2005. **26**(16): p. 2991-2999.
32. Kirkpatrick, C.J., et al., *Current trends in biocompatibility testing.* Proc Inst Mech Eng H, 1998. **212**(2): p. 75-84.
33. Santos, M.H., et al., *Biocompatibility evaluation of hydroxyapatite/collagen nanocomposites doped with Zn+2.* Biomed Mater, 2007. **2**(2): p. 135-41.
34. Brown, S.A., et al., *Cell Culture Test Methods*. 1983: American Society for Testing and Materials.
35. Ciapetti, G., et al., *Application of a combination of neutral red and amido black staining for rapid, reliable cytotoxicity testing of biomaterials.* Biomaterials, 1996. **17**(13): p. 1259-64.
36. Morrison, C., et al., *In vitro biocompatibility testing of polymers for orthopaedic implants using cultured fibroblasts and osteoblasts.* Biomaterials, 1995. **16**(13): p. 987-92.
37. Kretzmer, E.A., et al., *An animal model for cochlear implants.* Arch Otolaryngol Head Neck Surg, 2004. **130**(5): p. 499-508.
38. Pearce, A.I., et al., *Animal models for implant biomaterial research in bone: a review.* Eur Cell Mater, 2007. **13**: p. 1-10.
39. Todescan, R., Jr., R.M. Pilliar, and A.H. Melcher, *A small animal model for investigating endosseous dental implants: effect of graft materials on healing of endosseous, porous-surfaced implants placed in a fresh extraction socket.* Int J Oral Maxillofac Implants, 1987. **2**(4): p. 217-23.
40. Waterston, R.H., et al., *Initial sequencing and comparative analysis of the mouse genome.* Nature, 2002. **420**(6915): p. 520-62.
41. Koschwanez, H.E. and W.M. Reichert, *In vitro, in vivo and post explantation testing of glucose-detecting biosensors: current methods and recommendations.* Biomaterials, 2007. **28**(25): p. 3687-703.
42. Lindner, E., et al., *Ion-selective membranes with low plasticizer content: electroanalytical characterization and biocompatibility studies.* J Biomed Mater Res, 1994. **28**(5): p. 591-601.
43. Marchant, R., et al., *In vivo biocompatibility studies. I. The cage implant system and a biodegradable hydrogel.* J Biomed Mater Res, 1983. **17**(2): p. 301-25.
44. Kao, W.J., et al., *Role for interleukin-4 in foreign-body giant cell formation on a poly(etherurethane urea) in vivo.* J Biomed Mater Res, 1995. **29**(10): p. 1267-75.
45. Selvam, S., et al., *Minimally invasive, longitudinal monitoring of biomaterial-associated inflammation by fluorescence imaging.* Biomaterials, 2011. **32**(31): p. 7785-92.
46. Suri, S., et al., *In vivo fluorescence imaging of biomaterial-associated inflammation and infection in a minimally invasive manner.* J Biomed Mater Res A, 2015. **103**(1): p. 76-83.
47. Liu, W.F., et al., *Real-time in vivo detection of biomaterial-induced reactive oxygen species.* Biomaterials, 2011. **32**(7): p. 1796-1801.
48. Zhou, J., et al., *Noninvasive assessment of localized inflammatory responses.* Free radical biology & medicine, 2012. **52**(1): p. 218-226.
49. Kielland, A., et al., *In vivo imaging of reactive oxygen and nitrogen species in inflammation using the luminescent probe L-012.* Free Radic Biol Med, 2009. **47**(6): p. 760-6.
50. Daiber, A., et al., *Measurement of NAD(P)H oxidase-derived superoxide with the luminol analogue L-012.* Free Radic Biol Med, 2004. **36**(1): p. 101-11.
51. Daiber, A., et al., *Detection of superoxide and peroxynitrite in model systems and mitochondria by the luminol analogue L-012.* Free Radic Res, 2004. **38**(3): p. 259-69.
52. Lee, D., et al., *In vivo imaging of hydrogen peroxide with chemiluminescent nanoparticles.* Nat Mater, 2007. **6**(10): p. 765-9.

53. Lee, D., et al., *Detection of hydrogen peroxide with chemiluminescent micelles.* Int J Nanomedicine, 2008. **3**(4): p. 471-6.
54. Bratlie, K.M., et al., *Rapid Biocompatibility Analysis of Materials via In Vivo Fluorescence Imaging of Mouse Models.* PLoS ONE, 2010. **5**(4): p. e10032.
55. Anderson, J.M., *Biological responses to materials.* Annual Review of Materials Science, 2001. **31**: p. 81-110.
56. Anderson, J.M., *Multinucleated giant cells.* Current Opinion in Hematology, 2000. **7**(1): p. 40-47.
57. Gretzer, C., et al., *The inflammatory cell influx and cytokines changes during transition from acute inflammation to fibrous repair around implanted materials.* Journal of Biomaterials Science, Polymer Edition, 2006. **17**(6): p. 669-687.
58. Luttikhuizen, D.T., M.C. Harmsen, and M.J.A. Van Luyn, *Cellular and molecular dynamics in the foreign body reaction.* Tissue Engineering, 2006. **12**(7): p. 1955-1970.
59. Wilson, C.J., et al., *Mediation of biomaterial-cell interactions by adsorbed proteins: A review.* Tissue Engineering, 2005. **11**(1-2): p. 1-18.
60. Steele, J.G., et al., *Attachment of human bone cells to tissue culture polystyrene and to unmodified polystyrene: the effect of surface chemistry upon initial cell attachment.* J Biomater Sci Polym Ed, 1993. **5**(3): p. 245-57.
61. Howlett, C.R., et al., *Mechanism of initial attachment of cells derived from human bone to commonly used prosthetic materials during cell culture.* Biomaterials, 1994. **15**(3): p. 213-22.
62. Kilpadi, K.L., P.L. Chang, and S.L. Bellis, *Hydroxylapatite binds more serum proteins, purified integrins, and osteoblast precursor cells than titanium or steel.* J Biomed Mater Res, 2001. **57**(2): p. 258-67.
63. Takebe, J., et al., *Anodic oxidation and hydrothermal treatment of titanium results in a surface that causes increased attachment and altered cytoskeletal morphology of rat bone marrow stromal cells in vitro.* Journal of Biomedical Materials Research, 2000. **51**(3): p. 398-407.
64. Lopes, M.A., et al., *Hydrophobicity, surface tension, and zeta potential measurements of glass-reinforced hydroxyapatite composites.* Journal of Biomedical Materials Research, 1999. **45**(4): p. 370-375.
65. Hallab, N.J., et al., *Evaluation of metallic and polymeric biomaterial surface energy and surface roughness characteristics for directed cell adhesion.* Tissue Eng, 2001. **7**(1): p. 55-71.
66. Ponsonnet, L., et al., *Relationship between surface properties (roughness, wettability) of titanium and titanium alloys and cell behaviour.* Materials Science and Engineering: C, 2003. **23**(4): p. 551-560.
67. Steven, M.S. and A.H. Thomas, *The Vroman Effect*, in *Proteins at Interfaces II*. 1995, American Chemical Society. p. 112-128.
68. Keselowsky, B.G., et al., *Role of plasma fibronectin in the foreign body response to biomaterials.* Biomaterials, 2007. **28**(25): p. 3626-3631.
69. McNally, A.K., et al., *Vitronectin is a critical protein adhesion substrate for IL-4-induced foreign body giant cell formation.* Journal of Biomedical Materials Research - Part A, 2008. **86**(2): p. 535-543.
70. Franz, S., et al., *Immune responses to implants – A review of the implications for the design of immunomodulatory biomaterials.* Biomaterials, 2011. **32**(28): p. 6692-6709.
71. Müller, P., *Blood Coagulation and Fibrinolysis*, in *Biochemical Pathways*. 2012, John Wiley & Sons, Inc. p. 357-365.
72. Heemskerk, J.W.M., E.M. Bevers, and T. Lindhout, *Platelet activation and blood coagulation.* Thrombosis and Haemostasis, 2002. **88**(2): p. 186-193.
73. Tang, L., *Mechanisms of fibrinogen domains: Biomaterial interactions.* Journal of Biomaterials Science, Polymer Edition, 1998. **9**(12): p. 1257-1266.
74. Hu, W.J., J.W. Eaton, and L. Tang, *Molecular basis of biomaterial-mediated foreign body reactions.* Blood, 2001. **98**(4): p. 1231-1238.
75. Gorbet, M.B. and M.V. Sefton, *Biomaterial-associated thrombosis: Roles of coagulation factors, complement, platelets and leukocytes.* Biomaterials, 2004. **25**(26): p. 5681-5703.
76. Schmaier, A.H., *Contact activation: A revision.* Thrombosis and Haemostasis, 1997. **78**(1): p. 101-107.

77. Sperling, C., et al., *Blood coagulation on biomaterials requires the combination of distinct activation processes.* Biomaterials, 2009. **30**(27): p. 4447-4456.
78. Fischer, M., C. Sperling, and C. Werner, *Synergistic effect of hydrophobic and anionic surface groups triggers blood coagulation in vitro.* Journal of Materials Science: Materials in Medicine, 2010. **21**(3): p. 931-937.
79. Nilsson, B., et al., *The role of complement in biomaterial-induced inflammation.* Molecular Immunology, 2007. **44**(1-3): p. 82-94.
80. Lhotta, K., et al., *Rapid activation of the complement system by cuprophane depends on complement component C4.* Kidney International, 1998. **53**(4): p. 1044-1051.
81. Hed, J., M. Johansson, and M. Lindroth, *Complement activation according to the alternate pathway by glass and plastic surfaces and its role in neutrophil adhesion.* Immunology Letters, 1984. **8**(6): p. 295-299.
82. Tengvall, P., A. Askendal, and I. Lundström, *Ellipsometric in vitro studies on the activation of complement by human immunoglobulins M and G after adsorption to methylated silicon.* Colloids and Surfaces B: Biointerfaces, 2001. **20**(1): p. 51-62.
83. Andersson, J., et al., *C3 adsorbed to a polymer surface can from an initiating alternative pathway convertase.* Journal of Immunology, 2002. **168**(11): p. 5786-5791.
84. Sarma, J.V. and P.A. Ward, *The complement system.* Cell and Tissue Research, 2011. **343**(1): p. 227-235.
85. Fischer, M., et al., *The ability of surface characteristics of materials to trigger leukocyte tissue factor expression.* Biomaterials, 2010. **31**(9): p. 2498-2507.
86. Anderson, J.M., A. Rodriguez, and D.T. Chang, *Foreign body reaction to biomaterials.* Seminars in Immunology, 2008. **20**(2): p. 86-100.
87. Bianchi, M.E., *DAMPs, PAMPs and alarmins: All we need to know about danger.* Journal of Leukocyte Biology, 2007. **81**(1): p. 1-5.
88. Agresti, A. and M.E. Bianchi, *HMGB proteins and gene expression.* Curr Opin Genet Dev, 2003. **13**(2): p. 170-8.
89. Muller, S., L. Ronfani, and M.E. Bianchi, *Regulated expression and subcellular localization of HMGB1, a chromatin protein with a cytokine function.* J Intern Med, 2004. **255**(3): p. 332-43.
90. Scaffidi, P., T. Misteli, and M.E. Bianchi, *Release of chromatin protein HMGB1 by necrotic cells triggers inflammation.* Nature, 2002. **418**(6894): p. 191-5.
91. Qin, S., et al., *Role of HMGB1 in apoptosis-mediated sepsis lethality.* J Exp Med, 2006. **203**(7): p. 1637-42.
92. Dumitriu, I.E., et al., *HMGB1: guiding immunity from within.* Trends Immunol, 2005. **26**(7): p. 381-7.
93. Yang, D., et al., *High mobility group box-1 protein induces the migration and activation of human dendritic cells and acts as an alarmin.* J Leukoc Biol, 2007. **81**(1): p. 59-66.
94. Dumitriu, I.E., et al., *The secretion of HMGB1 is required for the migration of maturing dendritic cells.* J Leukoc Biol, 2007. **81**(1): p. 84-91.
95. Foell, D., et al., *S100 proteins expressed in phagocytes: a novel group of damage-associated molecular pattern molecules.* J Leukoc Biol, 2007. **81**(1): p. 28-37.
96. Schmitt, E., et al., *Intracellular and extracellular functions of heat shock proteins: repercussions in cancer therapy.* J Leukoc Biol, 2007. **81**(1): p. 15-27.
97. Kobayashi, S.D., et al., *Neutrophils in the innate immune response.* Archivum Immunologiae et Therapiae Experimentalis, 2005. **53**(6): p. 505-517.
98. Nimeri, G., et al., *The influence of plasma proteins and platelets on oxygen radical production and F-actin distribution in neutrophils adhering to polymer surfaces.* Biomaterials, 2002. **23**(8): p. 1785-1795.
99. Labow, R.S., E. Meek, and J.P. Santerre, *Neutrophil-mediated biodegradation of medical implant materials.* Journal of Cellular Physiology, 2001. **186**(1): p. 95-103.
100. Scapini, P., et al., *The neutrophil as a cellular source of chemokines.* Immunological Reviews, 2000. **177**: p. 195-203.
101. Yamashiro, S., et al., *Phenotypic and functional change of cytokine-activated neutrophils: Inflammatory neutrophils are heterogeneous and enhance adaptive immune responses.* Journal of Leukocyte Biology, 2001. **69**(5): p. 698-704.

102. Martinez, F.O., et al., *Macrophage activation and polarization.* Frontiers in Bioscience, 2008. **13**(2): p. 453-461.
103. Mosser, D.M. and J.P. Edwards, *Exploring the full spectrum of macrophage activation.* Nature Reviews Immunology, 2008. **8**(12): p. 958-969.
104. Stein, M., et al., *Interleukin 4 potently enhances murine macrophage mannose receptor activity: A marker of alternative immunologic macrophage activation.* Journal of Experimental Medicine, 1992. **176**(1): p. 287-292.
105. Xia, Z. and J.T. Triffitt, *A review on macrophage responses to biomaterials.* Biomedical Materials, 2006. **1**(1): p. R1-R9.
106. DeFife, K.M., et al., *Interleukin-13 Induces Human Monocyte/Macrophage Fusion and Macrophage Mannose Receptor Expression.* Journal of Immunology, 1997. **158**(7): p. 3385-3390.
107. Kao, W.J., et al., *Role for interleukin-4 in foreign-body giant cell formation on a poly(etherurethane urea) in vivo.* Journal of Biomedical Materials Research, 1995. **29**(10): p. 1267-1275.
108. McNally, A.K. and J.M. Anderson, *Interleukin-4 induces foreign body giant cells from human monocytes/macrophages: Differential lymphokine regulation of macrophage fusion leads to morphological variants of multinucleated giant cells.* American Journal of Pathology, 1995. **147**(5): p. 1487-1499.
109. Xia, Z.D., et al., *Macrophages in degradation of collagen/hydroxylapatite(CHA), beta-tricalcium phosphate ceramics (TCP) artificial bone graft. An in vivo study.* Chinese Medical Journal, 1994. **107**(11): p. 845-849.
110. Christenson, E.M., J.M. Anderson, and A. Hiltner, *Oxidative mechanisms of poly(carbonate urethane) and poly(ether urethane) biodegradation: In vivo and in vitro correlations.* Journal of Biomedical Materials Research - Part A, 2004. **70**(2): p. 245-255.
111. Santerre, J.P., et al., *Understanding the biodegradation of polyurethanes: From classical implants to tissue engineering materials.* Biomaterials, 2005. **26**(35): p. 7457-7470.
112. Zhao, Q.H., et al., *Human plasma α2-macroglobulin promotes in vitro oxidative stress cracking of Pellethane 2363-80A: In vivo and in vitro correlations.* Journal of Biomedical Materials Research, 1993. **27**(3): p. 379-388.
113. Kao, W.J., et al., *Theoretical analysis of in vivo macrophage adhesion and foreign body giant cell formation on polydimethylsiloxane, low density polyethylene, and polyetherurethanes.* Journal of Biomedical Materials Research, 1994. **28**(1): p. 73-79.
114. Broughton, G., 2nd, J.E. Janis, and C.E. Attinger, *The basic science of wound healing.* Plast Reconstr Surg, 2006. **117**(7 Suppl): p. 12s-34s.
115. Eming, S.A., T. Krieg, and J.M. Davidson, *Inflammation in wound repair: Molecular and cellular mechanisms.* Journal of Investigative Dermatology, 2007. **127**(3): p. 514-525.
116. Chu, C.C., J.A. von Fraunhofer, and H.P. Greisler, *Wound Closure Biomaterials and Devices*. 1996: Taylor & Francis.
117. Ratner, B.D., *The Engineering of Biomaterials Exhibiting Recognition and Specificity.* Journal of Molecular Recognition, 1996. **9**(5-6): p. 617-625.
118. Rungsiyakull, C., et al., *Surface morphology optimization for osseointegration of coated implants.* Biomaterials, 2010. **31**(27): p. 7196-7204.
119. Dinnes, D.L.M., et al., *Material surfaces affect the protein expression patterns of human macrophages: A proteomics approach.* Journal of Biomedical Materials Research - Part A, 2007. **80**(4): p. 895-908.
120. Jones, J.A., et al., *Proteomic analysis and quantification of cytokines and chemokines from biomaterial surface-adherent macrophages and foreign body giant cells.* Journal of Biomedical Materials Research - Part A, 2007. **83**(3): p. 585-596.
121. Yim, E.K.F. and K.W. Leong, *Significance of synthetic nanostructures in dictating cellular response.* Nanomedicine: Nanotechnology, Biology, and Medicine, 2005. **1**(1): p. 10-21.
122. Fink, J., et al., *Stimulation of monocytes and macrophages: Possible influence of surface roughness.* Clinical Hemorheology and Microcirculation, 2008. **39**(1-4): p. 205-212.
123. Chen, S., et al., *Characterization of topographical effects on macrophage behavior in a foreign body response model.* Biomaterials, 2010. **31**(13): p. 3479-3491.

124. Hersel, U., C. Dahmen, and H. Kessler, *RGD modified polymers: Biomaterials for stimulated cell adhesion and beyond.* Biomaterials, 2003. **24**(24): p. 4385-4415.
125. Shin, H., S. Jo, and A.G. Mikos, *Biomimetic materials for tissue engineering.* Biomaterials, 2003. **24**(24): p. 4353-4364.
126. Kao, W.J., et al., *Fibronectin modulates macrophage adhesion and FBGC formation: The role of RGD, PHSRN, and PRRARV domains.* Journal of Biomedical Materials Research, 2001. **55**(1): p. 79-88.
127. Kao, W.J. and Y. Liu, *Utilizing biomimetic oligopeptides to probe fibronectin-integrin binding and signaling in regulating macrophage function in vitro and in vivo.* Front Biosci, 2001. **6**: p. D992-9.
128. Franchimont, D., et al., *Glucocorticoids and inflammation revisited: The state of the art - NIH Clinical Staff Conference.* NeuroImmunoModulation, 2002. **10**(5): p. 247-260.
129. Patil, S.D., F. Papadimitrakopoulos, and D.J. Burgess, *Dexamethasone-loaded poly(lactic-co-glycolic) acid microspheres/poly(vinyl alcohol) hydrogel composite coatings for inflammation control.* Diabetes Technology and Therapeutics, 2004. **6**(6): p. 887-897.
130. Patil, S.D., F. Papadmitrakopoulos, and D.J. Burgess, *Concurrent delivery of dexamethasone and VEGF for localized inflammation control and angiogenesis.* Journal of Controlled Release, 2007. **117**(1): p. 68-79.
131. Norton, L.W., et al., *Vascular endothelial growth factor and dexamethasone release from nonfouling sensor coatings affect the foreign body response.* Journal of Biomedical Materials Research - Part A, 2007. **81**(4): p. 858-869.
132. Oshikawa, K., H. Yamasawa, and Y. Sugiyama, *Human lung fibroblasts inhibit macrophage inflammatory protein-1α production by lipopolysaccharide-stimulated macrophages.* Biochemical and Biophysical Research Communications, 2003. **312**(3): p. 650-655.
133. Vancheri, C., et al., *Normal Human Lung Fibroblasts Differently Modulate Interleukin-10 and Interleukin-12 Production by Monocytes.* American Journal of Respiratory Cell and Molecular Biology, 2001. **25**(5): p. 592-599.
134. Chung, A.S. and W.J. Kao, *Fibroblasts regulate monocyte response to ECM-derived matrix: The effects on monocyte adhesion and the production of inflammatory, matrix remodeling, and growth factor proteins.* Journal of Biomedical Materials Research Part A, 2009. **89A**(4): p. 841-853.
135. Scott, J.E., *Extracellular matrix, supramolecular organisation and shape.* Journal of Anatomy, 1995. **187**(2): p. 259-269.
136. Rhodes, J.M. and M. Simons, *The extracellular matrix and blood vessel formation: not just a scaffold.* Journal of Cellular and Molecular Medicine, 2007. **11**(2): p. 176-205.
137. Ottani, V., M. Raspanti, and A. Ruggeri, *Collagen structure and functional implications.* Micron, 2001. **32**(3): p. 251-260.
138. Papagiannopoulos, A., T.A. Waigh, and T.E. Hardingham, *The viscoelasticity of self-assembled proteoglycan combs.* Faraday Discussions, 2008. **139**: p. 337-357.
139. Hoffman, A.S., *Hydrogels for biomedical applications.* Advanced Drug Delivery Reviews, 2002. **54**(1): p. 3-12.
140. Valentin, J.E., et al., *Extracellular matrix bioscaffolds for orthopaedic applications: A comparative histologic study.* Journal of Bone and Joint Surgery - Series A, 2006. **88**(12): p. 2673-2686.
141. Nagai, M., et al., *In vitro Study of Collagen Coating of Titanium Implants for Initial Cell Attachment.* Dental Materials Journal, 2002. **21**(3): p. 250-260.
142. Rammelt, S., et al., *Coating of titanium implants with type-I collagen.* Journal of Orthopaedic Research, 2004. **22**(5): p. 1025-1034.
143. Becker, D., et al., *Proliferation and differentiation of rat calvarial osteoblasts on type I collagen-coated titanium alloy.* Journal of Biomedical Materials Research, 2002. **59**(3): p. 516-527.
144. Nakamura, H.K., et al., *A Role for Proteoglycans in Mineralized Tissue-Titanium Adhesion.* Journal of Dental Research, 2007. **86**(2): p. 147-152.
145. Rammelt, S., et al., *Coating of titanium implants with collagen, RGD peptide and chondroitin sulfate.* Biomaterials, 2006. **27**(32): p. 5561-5571.

146. Rammelt, S., et al., *In vivo effects of coating loaded and unloaded Ti implants with collagen, chondroitin sulfate, and hydroxyapatite in the sheep tibia.* Journal of Orthopaedic Research, 2007. **25**(8): p. 1052-1061.
147. Witt, D.P. and A.D. Lander, *Differential binding of chemokines to glycosaminoglycan subpopulations.* Current Biology, 1994. **4**(5): p. 394-400.
148. Salek-Ardakani, S., et al., *Heparin and heparan sulfate bind interleukin-10 and modulate its activity.* Blood, 2000. **96**(5): p. 1879-1888.
149. Gristina, A.G., *Biomaterial-centered infection: microbial adhesion versus tissue integration.* Science, 1987. **237**(4822): p. 1588-1595.
150. Savage, D.C. and M. Fletcher, *Bacterial Adhesion: Mechanisms and Physiological Significance*. 1985: Springer.
151. Sugarman, B. and E.J. Young, *Infections Associated With Prosthetic Devices.* 1984: CRC Press.
152. Slusher, M.M., et al., *Extended-Wear Lenses, Biofilm, and Bacterial Adhesion.* Archives of Ophthalmology, 1987. **105**(1): p. 110-115.
153. An, Y.H. and R.J. Friedman, *Concise review of mechanisms of bacterial adhesion to biomaterial surfaces.* J Biomed Mater Res, 1998. **43**(3): p. 338-48.
154. Heilmann, C., et al., *Evidence for autolysin-mediated primary attachment of Staphylococcus epidermidis to a polystyrene surface.* Molecular Microbiology, 1997. **24**(5): p. 1013-1024.
155. Foster, S.J., *Molecular characterization and functional analysis of the major autolysin of Staphylococcus aureus 8325/4.* Journal of Bacteriology, 1995. **177**(19): p. 5723-5725.
156. Donaruma, L.G., *Surface and interfacial aspects of biomedical polymers. Joseph D. Andrade, Ed., Plenum, New York, 1985, 479 pp. Price: $69.50.* Journal of Polymer Science Part C: Polymer Letters, 1986. **24**(8): p. 427-428.
157. Laverty, G., S.P. Gorman, and B.F. Gilmore, *2 - Biofilms and implant-associated infections*, in *Biomaterials and Medical Device - Associated Infections*, L. Barnes and I.R. Cooper, Editors. 2015, Woodhead Publishing: Oxford. p. 19-45.
158. Cooper, I.R., *1 - Introduction to biomaterials and medical device-associated infections*, in *Biomaterials and Medical Device - Associated Infections*, L. Barnes and I.R. Cooper, Editors. 2015, Woodhead Publishing: Oxford. p. 3-17.
159. Vilain, S., et al., *DNA as an Adhesin: Bacillus cereus Requires Extracellular DNA To Form Biofilms.* Applied and Environmental Microbiology, 2009. **75**(9): p. 2861-2868.
160. Mann, E.E., et al., *Modulation of eDNA Release and Degradation Affects Staphylococcus aureus Biofilm Maturation.* PLoS ONE, 2009. **4**(6): p. e5822.
161. Harmsen, M., et al., *Role of extracellular DNA during biofilm formation by listeria monocytogenes.* Applied and Environmental Microbiology, 2010. **76**(7): p. 2271-2279.
162. Daniels, R., J. Vanderleyden, and J. Michiels, *Quorum sensing and swarming migration in bacteria.* FEMS Microbiol Rev, 2004. **28**(3): p. 261-89.
163. Donlan, R.M., *Biofilms: microbial life on surfaces.* Emerg Infect Dis, 2002. **8**(9): p. 881-90.
164. Swift, S., et al., *Quorum sensing as a population-density-dependent determinant of bacterial physiology.* Adv Microb Physiol, 2001. **45**: p. 199-270.
165. Rutherford, S.T. and B.L. Bassler, *Bacterial quorum sensing: its role in virulence and possibilities for its control.* Cold Spring Harb Perspect Med, 2012. **2**(11).
166. Parsek, M.R. and E.P. Greenberg, *Sociomicrobiology: the connections between quorum sensing and biofilms.* Trends Microbiol, 2005. **13**(1): p. 27-33.
167. Romeo, T., *Bacterial Biofilms*. 2008: Springer.
168. Islam, M.S., J.P. Richards, and A.K. Ojha, *Targeting drug tolerance in mycobacteria: a perspective from mycobacterial biofilms.* Expert review of anti-infective therapy, 2012. **10**(9): p. 1055-1066.
169. Montanaro, L., et al., *Scenery of Staphylococcus implant infections in orthopedics.* Future Microbiology, 2011. **6**(11): p. 1329-1349.
170. Wilson, S.K. and J.W. Costerton, *Biofilm and Penile Prosthesis Infections in the Era of Coated Implants: A Review.* The Journal of Sexual Medicine, 2012. **9**(1): p. 44-53.
171. Bose, S. and A.K. Ghosh, *4 - Diagnosis of biofilm-associated infections in medical devices*, in *Biomaterials and Medical Device - Associated Infections*, L. Barnes and I.R. Cooper, Editors. 2015, Woodhead Publishing: Oxford. p. 71-82.

172. Praneenararat, T., A.G. Palmer, and H.E. Blackwell, *Chemical methods to interrogate bacterial quorum sensing pathways.* Organic & Biomolecular Chemistry, 2012. **10**(41): p. 8189-8199.
173. Rabin, N., et al., *Tailor-made LasR agonists modulate quorum sensing in Pseudomonas aeruginosa.* Organic & Biomolecular Chemistry, 2013. **11**(41): p. 7155-7163.
174. Mattmann, M.E. and H.E. Blackwell, *Small Molecules That Modulate Quorum Sensing and Control Virulence in Pseudomonas aeruginosa.* The Journal of Organic Chemistry, 2010. **75**(20): p. 6737-6746.
175. Chen, M., Q. Yu, and H. Sun, *Novel strategies for the prevention and treatment of biofilm related infections.* Int J Mol Sci, 2013. **14**(9): p. 18488-501.
176. Rucker, M., et al., *Angiogenic and inflammatory response to biodegradable scaffolds in dorsal skinfold chambers of mice.* Biomaterials, 2006. **27**(29): p. 5027-38.
177. Catelas, I., M.A. Wimmer, and S. Utzschneider, *Polyethylene and metal wear particles: characteristics and biological effects.* Semin Immunopathol, 2011. **33**(3): p. 257-71.
178. Conus, S. and H.U. Simon, *Cathepsins and their involvement in immune responses.* Swiss Med Wkly, 2010. **140**: p. w13042.
179. Park, G.Y., et al., *Autotaxin production of lysophosphatidic acid mediates allergic asthmatic inflammation.* Am J Respir Crit Care Med, 2013. **188**(8): p. 928-40.
180. Pulverer, J.E., et al., *Temporal and Spatial Resolution of Type I and III Interferon Responses In Vivo.* Journal of Virology, 2010. **84**(17): p. 8626-8638.
181. Asano, A., H.K. Jin, and T. Watanabe, *Mouse Mx2 gene: organization, mRNA expression and the role of the interferon-response promoter in its regulation.* Gene, 2003. **306**(0): p. 105-113.
182. Haller, O., P. Staeheli, and G. Kochs, *Interferon-induced Mx proteins in antiviral host defense.* Biochimie, 2007. **89**(6–7): p. 812-818.
183. Mordstein, M., et al., *Interferon-λ Contributes to Innate Immunity of Mice against Influenza A Virus but Not against Hepatotropic Viruses.* PLoS Pathog, 2008. **4**(9): p. e1000151.
184. Decker, T., M. Muller, and S. Stockinger, *The yin and yang of type I interferon activity in bacterial infection.* Nat Rev Immunol, 2005. **5**(9): p. 675-87.
185. Trinchieri, G., *Type I interferon: friend or foe?* The Journal of Experimental Medicine, 2010. **207**(10): p. 2053-2063.
186. Lienenklaus, S., et al., *Novel reporter mouse reveals constitutive and inflammatory expression of IFN-beta in vivo.* J Immunol, 2009. **183**(5): p. 3229-36.
187. Perrakis, A. and W.H. Moolenaar, *Autotaxin: structure-function and signaling.* J Lipid Res, 2014.
188. Fleming, T.J., M.L. Fleming, and T.R. Malek, *Selective expression of Ly-6G on myeloid lineage cells in mouse bone marrow. RB6-8C5 mAb to granulocyte-differentiation antigen (Gr-1) detects members of the Ly-6 family.* J Immunol, 1993. **151**(5): p. 2399-408.
189. Daley, J.M., et al., *Use of Ly6G-specific monoclonal antibody to deplete neutrophils in mice.* J Leukoc Biol, 2008. **83**(1): p. 64-70.
190. Rose, S., A. Misharin, and H. Perlman, *A novel Ly6C/Ly6G-based strategy to analyze the mouse splenic myeloid compartment.* Cytometry. Part A : the journal of the International Society for Analytical Cytology, 2012. **81**(4): p. 343-350.
191. DeLeo, F.R., *Modulation of phagocyte apoptosis by bacterial pathogens.* Apoptosis, 2004. **9**(4): p. 399-413.
192. Ablasser, A., et al., *Nucleic acid driven sterile inflammation.* Clinical Immunology, 2013. **147**(3): p. 207-215.
193. Liu, H., E.B. Slamovich, and T.J. Webster, *Less harmful acidic degradation of poly(lactic-co-glycolic acid) bone tissue engineering scaffolds through titania nanoparticle addition.* International Journal of Nanomedicine, 2006. **1**(4): p. 541-545.
194. Varde, N.K. and D.W. Pack, *Microspheres for controlled release drug delivery.* Expert Opinion on Biological Therapy, 2004. **4**(1): p. 35-51.
195. Jayakumar, R., et al., *Biomaterials based on chitin and chitosan in wound dressing applications.* Biotechnology Advances, 2011. **29**(3): p. 322-337.
196. Patel, M.P., R.R. Patel, and J.K. Patel, *Chitosan mediated targeted drug delivery system: a review.* J Pharm Pharm Sci, 2010. **13**(4): p. 536-57.

197. Sasaki, Y., et al., *Iba1 is an actin-cross-linking protein in macrophages/microglia.* Biochem Biophys Res Commun, 2001. **286**(2): p. 292-7.
198. Guggenbichler, J.P., et al., *Incidence and clinical implication of nosocomial infections associated with implantable biomaterials - catheters, ventilator-associated pneumonia, urinary tract infections.* GMS Krankenhhyg Interdiszip, 2011. **6**(1): p. Doc18.
199. Barrat, F.J., et al., *Nucleic acids of mammalian origin can act as endogenous ligands for Toll-like receptors and may promote systemic lupus erythematosus.* The Journal of Experimental Medicine, 2005. **202**(8): p. 1131-1139.
200. Kolaczkowska, E. and P. Kubes, *Neutrophil recruitment and function in health and inflammation.* Nat Rev Immunol, 2013. **13**(3): p. 159-75.
201. Hamilton, J.A., *GM-CSF in inflammation and autoimmunity.* Trends Immunol, 2002. **23**(8): p. 403-8.
202. Araki, H., et al., *Reprogramming of human postmitotic neutrophils into macrophages by growth factors.* Blood, 2004. **103**(8): p. 2973-80.
203. Sasmono, R.T., et al., *Mouse neutrophilic granulocytes express mRNA encoding the macrophage colony-stimulating factor receptor (CSF-1R) as well as many other macrophage-specific transcripts and can transdifferentiate into macrophages in vitro in response to CSF-1*. J Leukoc Biol, 2007. **82**(1): p. 111-23.
204. Tseng, J.-C. and Andrew L. Kung, *In Vivo Imaging of Inflammatory Phagocytes.* Chemistry & Biology, 2012. **19**(9): p. 1199-1209.
205. Gross, S., et al., *Bioluminescence imaging of myeloperoxidase activity in vivo.* Nature medicine, 2009. **15**(4): p. 455-461.
206. Ikeda, Y., et al., *Cathepsins B and L in synovial fluids from patients with rheumatoid arthritis and the effect of cathepsin B on the activation of pro-urokinase.* J Med Invest, 2000. **47**(1-2): p. 61-75.
207. Joyce, J.A. and D. Hanahan, *Multiple roles for cysteine cathepsins in cancer.* Cell Cycle, 2004. **3**(12): p. 1516-619.
208. Faiz, A., et al., *The Expression and Activity of Cathepsins D, H and K in Asthmatic Airways.* PLoS ONE, 2013. **8**(3): p. e57245.
209. Li, X., et al., *Increased expression of cathepsins and obesity-induced proinflammatory cytokines in lacrimal glands of male NOD mouse.* Invest Ophthalmol Vis Sci, 2010. **51**(10): p. 5019-29.
210. Hannaford, J., H. Guo, and X. Chen, *Involvement of cathepsins B and L in inflammation and cholesterol trafficking protein NPC2 secretion in macrophages.* Obesity (Silver Spring), 2013. **21**(8): p. 1586-95.
211. Madan, D., et al., *Non-Invasive Imaging of Tumors by Monitoring Autotaxin Activity Using an Enzyme-Activated Near-Infrared Fluorogenic Substrate.* PLoS ONE, 2013. **8**(11): p. e79065.
212. Lowik, C.W., et al., *Whole body optical imaging in small animals and its translation to the clinic: intra-operative optical imaging guided surgery.* Eur J Cancer, 2009. **45 Suppl 1**: p. 391-3.
213. Kaijzel, E.L., G. van der Pluijm, and C.W. Lowik, *Whole-body optical imaging in animal models to assess cancer development and progression.* Clin Cancer Res, 2007. **13**(12): p. 3490-7.
214. Becker, A., et al., *Receptor-targeted optical imaging of tumors with near-infrared fluorescent ligands.* Nat Biotechnol, 2001. **19**(4): p. 327-31.
215. Sato, A., B. Klaunberg, and R. Tolwani, *In vivo bioluminescence imaging.* Comp Med, 2004. **54**(6): p. 631-4.
216. Thompson, J.F., L.S. Hayes, and D.B. Lloyd, *Modulation of firefly luciferase stability and impact on studies of gene regulation.* Gene, 1991. **103**(2): p. 171-7.
217. Rais, B., et al., *Animal Test Models for Implant-Associated Inflammation and Infections*, in *Biomedical Technology*, T. Lenarz and P. Wriggers, Editors. 2015, Springer International Publishing. p. 175-187.
218. Youn, H. and K.-J. Hong, *In Vivo Non Invasive Molecular Imaging for Immune Cell Tracking in Small Animals.* Immune Network, 2012. **12**(6): p. 223-229.
219. Makadia, H.K. and S.J. Siegel, *Poly Lactic-co-Glycolic Acid (PLGA) as Biodegradable Controlled Drug Delivery Carrier.* Polymers, 2011. **3**(3): p. 1377-1397.

220. Sung, H.-J., et al., *The effect of scaffold degradation rate on three-dimensional cell growth and angiogenesis.* Biomaterials, 2004. **25**(26): p. 5735-5742.
221. Hickey, T., et al., *Dexamethasone/PLGA microspheres for continuous delivery of an anti-inflammatory drug for implantable medical devices.* Biomaterials, 2002. **23**(7): p. 1649-56.
222. Lee, H., et al., *Fabrication and characteristics of anti-inflammatory magnesium hydroxide incorporated PLGA scaffolds formed with various porogen materials.* Macromolecular Research, 2014. **22**(2): p. 210-218.
223. AFFAIRS, A.C.O.S., *Titanium applications in dentistry.* The Journal of the American Dental Association, 2003. **134**(3): p. 347-349.
224. Jorge, J., et al., *Titanium in Dentistry: Historical Development, State of the Art and Future Perspectives.* The Journal of Indian Prosthodontic Society, 2013. **13**(2): p. 71-77.
225. Staiger, M.P., et al., *Magnesium and its alloys as orthopedic biomaterials: A review.* Biomaterials, 2006. **27**(9): p. 1728-1734.
226. Saris, N.E., et al., *Magnesium. An update on physiological, clinical and analytical aspects.* Clin Chim Acta, 2000. **294**(1-2): p. 1-26.
227. Badar, M., et al., *The formation of an organic coat and the release of corrosion microparticles from metallic magnesium implants.* Acta Biomaterialia, 2013. **9**(7): p. 7580-7589.
228. Saralidze, K., L.H. Koole, and M.L.W. Knetsch, *Polymeric Microspheres for Medical Applications.* Materials, 2010. **3**(6): p. 3537-3564.
229. Rinaudo, M., *Chitin and chitosan: Properties and applications.* Progress in Polymer Science, 2006. **31**(7): p. 603-632.
230. Bueter, C.L., et al., *Chitosan but not chitin activates the inflammasome by a mechanism dependent upon phagocytosis.* J Biol Chem, 2011. **286**(41): p. 35447-55.
231. Bueter, C.L., et al., *Spectrum and mechanisms of inflammasome activation by chitosan.* J Immunol, 2014. **192**(12): p. 5943-51.
232. Ertel, W., et al., *Circulating mediators in serum of injured patients with septic complications inhibit neutrophil apoptosis through up-regulation of protein-tyrosine phosphorylation.* J Trauma, 1998. **44**(5): p. 767-75; discussion 775-6.
233. Matute-Bello, G., et al., *Neutrophil apoptosis in the acute respiratory distress syndrome.* Am J Respir Crit Care Med, 1997. **156**(6): p. 1969-77.
234. Brown, V., et al., *Dysregulated apoptosis and NFkappaB expression in COPD subjects.* Respir Res, 2009. **10**: p. 24.
235. Milot, E. and J.G. Filep, *Regulation of Neutrophil Survival/Apoptosis by Mcl-1.* TheScientificWorldJournal, 2011. **11**: p. 1948-1962.
236. Tak, T., et al., *What's your age again? Determination of human neutrophil half-lives revisited.* J Leukoc Biol, 2013. **94**(4): p. 595-601.

10.Acknowledgements

I would like to sincerely express my gratitude to my supervisor Prof. Dr. Peter P. Müller without whom this thesis would not be possible. I am deeply indebted to him for guidance and support at all times of research and writing of this thesis. I would like to thank my thesis committee member Dr. Hansjörg Hauser for his stimulating suggestions and critical reason of data. I would like to express my appreciation to Dr. Stefan Lienenklaus for his expertise in in vivo optical imaging and also for his insightful suggestions. I would like to thank our collaborator and my thesis committee member Prof. Dr. Peter Behrens for his support in project. I would also like to thank Dr. Mario Köster for providing me transgenic mice to carry out my experiments. I am thankful to Dr. Maria Höxter for performing FACS sorting experiments. I must appreciate Dr. Marina Pils for performing histology and also helping in interpretation of data. I would also like to thank Dr. Mark Brönstrup for a huge support in funding last experiments of my research. I must acknowledge Dr. Haiyu Hu, Dr. Verena Fetz and Kevin Ferreira in synthesis and characterization of siderophore compounds. My appreciation to Dr. Sabine Kirchoff, Dr. Berenike, Daniela Romke and rest of graduate school for providing outstanding support to graduate students. A special thanks to Dr. Upneet Hillebrand, Dr. Sharmila Nair and Dr. Marcin Cebula for helping me in my experimental design and FACS experiments. I must thank Dr. Christoph Lipps for his suggestions and support. I would also like to thank my lab-mate Muhammad Imran Rahim for being supportive at all times. I must thank Danim, Neha, Petra, Tharini, Sripriya, Shiwani and Niharika for being dependable friends.

At the end, I would like to thank my family for their unconditional support and love. My heartfelt thanks goes to Hameeda Khatoon for her selfless love and support. I would also like to thank Faisal Anees for being so supportive and patient with me.

BUSHRA RAIS

Militschstrasse 38, Braunschweig, Germany 38124 | C: +49 (0) 15785279733 | Bushra.Rais@helmholtz-hzi.de

Summary

Research Biologist with five years in laboratory research
Expertise in cell culture and animal experiments.
Accomplished in generating and applying new protocols and technologies.
Versed in organizing, writing and editing detailed reports and research papers.

Highlights

- Animal handling (FELASA B certified)
- In vivo optical imaging
- Sterile surgery in mice
- Cell culture expertise (including BMDMs, neutrophils and conditionally immortalised cells)
- Confocal microscopy
- Flow cytometery
- Quantitative PCR
- Immunohistochemistry
- Nucleic Acids Isolation
- Fluent in English
- Skilled scientific writing
- Data analysis and presentation skills
- Good scientific practice
- Strong communication skills
- Ability to expand collaborations

Experience

PhD — Sep 2012 to Current
Helmholtz Centre for Infection Research - Braunschweig
Designed and conducted experiments to achieve research objectives.
Established novel in vitro and in vivo biological test systems to study the interaction of biomaterials with cells and tissues.
Managed the mouse experiments independently and coordinated the weekly ordering and housing of mice
Identified the advantage of conditionally immortalized cells in the cell-material interface studies

Research Assistant — Dec 2011 to Jun 2012
Kings College London - London
Assisted in qPCR experiments for the running project
Extracted RNA from various organs of the rainbow trout fish
Conducted cloning related experiments
Designed and checked primers
Developed competent cells for transformation experiments

Master's research project — Jan 2011 to Jul 2011
Kings College London - London
Studied the transcriptional profile of a cardiovascular disorder, Deep Venous Thrombosis (DVT)
Gained experience in qPCR and immunohistochemistry.
Analysed and presented the data in simplified text and illustrated graphs

Education

Master of Science, Biomedical and Molecular Sciences Research — 2011
Kings College London - London, United Kingdom
Graduated with merit.

Bachelor of technology, Biotechnology — 2009
Amity University - Lucknow, India
Graduated with distinction
Received 'Gold medal' for being excellent in academics

Publications

Rais B, et al. Animal Test Models for Implant-Associated Inflammation and Infections. Biomedical Technology.74: Springer International Publishing; 2015. p. 175-87.

Rahim M.I., Eifler R., Rais B. and Müller, P.P. Alkalization is responsible for antibacterial effects of corroding magnesium. Journal of Biomedical Materials Research Part A. 2015.

Rais B, et al. Novel strategy to detect implant-related inflammation or infection. *Manuscript in preparation.*

External presentations

Rais B. and Müller P.P., Animal model for monitoring biomaterial associated inflammation or infection. Talk. Annual meeting of the Scandinavian Society for Biomaterials- Latvia. May 6–8th, 2015.

Rais B., Rahim M.I., Guledani A., and Müller P.P., Real time imaging of cells, tissue and bacteria. Talk. Annual Retreat – Helmholtz Centre for Infection Research- Goslar. May 20th-22nd, 2015

Rais B., and Müller P.P., In vivo imaging of biomaterial associated inflammation and infection. Talk. Progress Seminar – Helmholtz Centre for Infection Research- Braunschweig. March 20, 2014

Rais B., Tolle C., Köster M., Hauser H. and Müller P.P., In vivo imaging of biomaterial associated inflammation or infection. Poster. BMT – 48th DGBMT Annual Conference – Hannover. October 8-10th, 2014.

Rais B. and Müller P.P., Quantification of biomaterial associated inflammation and infection. Poster. 7th International PhD symposium- Helmholtz Centre for Infection Research. December 11, 2014

Rais B. and Müller P.P., Development of biological test systems to study interactions of novel implant materials with cells, tissues and bacteria. Poster. 6th International PhD symposium- Helmholtz Centre for Infection Research. December 12, 2013.

Rais B., Rahim M.I. and Müller P.P., In vitro and in vivo biocompatibility testing of medical implants. Poster. International Conference on Biomedical technology - Hannover. November 20th-22nd, 2013.

Rais B. and Müller P.P., In vivo and in vitro evaluation of implant biocompatibility. Poster. Annual Retreat – Helmholtz Centre for Infection Research- Bad Bevensen. June 13th-14th, 2013

References

1. Prof. Dr. Peter P. Müller
Group Leader - Chemical Biology Department
Helmholtz-Zentrum für Infektionsforschung Inhoffenstraße 7
38124 Braunschweig, Germany
Tel.: +49 (0) 531-6181-5070
Fax: +49 (0) 531-6181-5002
Email: Peter.Müller@helmholtz-hzi.de

2. Dr. Hansjörg Hauser
Head of Department
Gene Regulation and Differentiation
Helmholtz-Zentrum für Infektionsforschung Inhoffenstraße 7
38124 Braunschweig, Germany
Tel.: +49 (0) 531-6181-5000
Fax: +49 (0) 531-6181-500
Email: Hansjoerg.Hauser@helmholtz-hzi.de